

Aus der Referenz- und Translationszentrum für kardiale Stammzelltherapien und
Klinik und Poliklinik für Herzchirurgie an der Universitätsmedizin Rostock

Direktor: Prof. Dr. med. habil. Gustav Steinhoff

Magnetische Nanopartikel-basierter Gentransfer: Mechanismen und Klinische Perspektiven

Inauguraldissertation

zur

Erlangung des akademischen Grades
Doktor der Medizinwissenschaften (Dr. rer. hum.)
der Universitätsmedizin Rostock



vorgelegt von

Evgenya Delyagina, geb. am 14.08.1986 in St. Petersburg, Russia
aus Reinach BL, Schweiz

Rostock, August 2016

Gutachter:

1. Gutachter: Prof. Dr. med. Gustav Steinhoff
Klinik und Poliklinik für Herzchirurgie, Universitätsmedizin Rostock
2. Gutachter: Prof. Dr. med. Dr. rer. nat. Brigitte M. Pützer
Institut für Experimentelle Gentherapie und Tumorforschung,
Universitätsmedizin Rostock
3. Gutachter: Prof. Dr. rer. nat. Martin Zenke
Helmholtz-Institut für Biomedizinische Technik,
Universitätsklinikum der RWTH, Aachen

Datum der Einreichung: 08. August 2016

Datum der Verteidigung: 08. März 2017

From the Reference and Translation Center for Cardiac Stem Cell Therapy and
Department of Cardiac Surgery at the University Medicine Rostock

Director: Prof. Dr. med. habil. Gustav Steinhoff

Magnetic Nanoparticle-based Gene Delivery: Mechanisms and Clinical Perspectives

Dissertation

to

obtain the academic degree

Doctor rerum humanarum (Dr. rer. hum.)

at the University Medicine Rostock



submitted by

Evgenya Delyagina, born on 14.08.1986 in St. Petersburg, Russia
from Reinach BL, Switzerland

Rostock, August 2016

Reviewers:

1. Reviewer: Prof. Dr. med. Gustav Steinhoff
Department of Cardiac Surgery, University Medicine Rostock
2. Reviewer: Prof. Dr. med. Dr. rer. nat. Brigitte M. Pützer
Institute of Experimental Gene Therapy and Cancer Research,
University Medicine Rostock
3. Reviewer: Prof. Dr. rer. nat. Martin Zenke
Helmholtz-Institute for Biomedical Engineering, University clinic
RWTH, Aachen

Submission date: August 08, 2016

Defense date: March 08, 2017

Zusammenfassung

Die Fortschritte in der Gentherapie bergen große Hoffnungen für viele Patienten mit seltenen genetischen Krankheiten, Krebsleiden und Herz-Kreislauf-Erkrankungen. Die Sicherheit der gentherapeutischen Ansätze bereitet jedoch weiterhin Schwierigkeiten, was eine schnelle Entwicklung und klinische Anwendungen von Gentherapien limitiert. Virale Vektoren zählen zu den effizientesten Transfermethoden von Nukleinsäuren in Zellen. Aufgrund der erheblichen Nebenwirkungen, welche die Anwendung von Viren verursacht, wurden in der letzten Jahrzehnten die unterschiedlichsten nicht-viralen Methoden entwickelt. Obwohl einige nicht-virale Methoden für den Gentransfer bereits in klinischen Studien (Phase I und II) getestet werden, ist ihre Effizienz geringer im Vergleich zu den viralen Ansätzen. Daher muss es Ziel der Forschung sein, verträgliche und wirksame Systeme für den Gentransfer zu entwickeln um nachhaltig den Erfolg in der Gentherapie zu sichern.

Der Fokus dieser Arbeit lag auf der Weiterentwicklung eines magnetischen Nanopartikel-basierten Systems für den Gentransfer, welches zuvor in unserer Forschungsgruppe entwickelt wurde. Dieser nicht-virale Vektor basiert auf kationischen Polyplexen bestehend aus Plasmid-DNA (pDNA) und Polyethylenimin (PEI), welche kovalent an magnetische Eisenoxid-Nanopartikel (MNP) gebunden werden. Die Vorteile dieses Systems sind: eine vereinfachte Herstellung, hohe Affinität zur Nukleinsäure, relativ hohe Effizienz und Sicherheit, sowie die Möglichkeit den Vektor zielgerichtet mit Hilfe eines externen Magnetfeldes zu lenken. Das Ziel dieser Arbeit war, die pDNA/PEI/MNP Komplexe für die Anwendung in klinisch relevante Zellen (humane mesenchymale Stammzellen, hMSC) zu optimieren. Zusätzlich sollte der intrazelluläre Mechanismus der MNP-basierten Transfektion untersucht, sowie die klinischen Perspektiven von MNP-basierten Gentherapien analysiert werden.

Die Ergebnisse dieser Arbeit haben gezeigt, dass pDNA/PEI/MNP Komplexe eine effiziente und sichere Transfektion von Knochenmark-isolierten hMSC auch ohne Anwendung eines Magnetfeldes leisten können. Um die Unterschiede zwischen den Transfektionsmechanismen von Polyplexen und MNP-basierten Komplexen weiter zu erforschen, wurden umfangreiche Kollokalisationsstudien durchgeführt. Dafür wurden erstmalig alle drei Komponenten des Transfektionssystems (pDNA, PEI und MNP) mit fluoreszierenden Farbstoffen markiert und zu unterschiedlichen Zeitpunkten mittels konfokaler Laser Scanning Mikroskopie visualisiert. Die Analyse von Kollokalisationskoeffizienten zeigte, dass MNP-basierte Vektoren aufgrund eines effizienteren pDNA-Freisetzungsprozesses eine

bessere Transfektionseffizienz im Vergleich zu Polyplexen besitzen. Diese Ergebnisse unterstreichen den Einfluss der Zusammensetzung des Vektors auf den Transfektionsprozess und seine Effizienz. Im Folgenden wurde niedermolekulares PEI (600 Da) genutzt um die Biokompatibilität des Transfektionssystems zu verbessern. Das neue System wurde charakterisiert und in COS-7 Zellen getestet. Obwohl der erstellte Vektor eine höhere Biokompatibilität und Sicherheit versprach, erzielte er nicht vergleichbare Effizienzen im Vergleich zu den Vektoren mit hochmolekularem PEI (25 kDa). Weitere Möglichkeiten die Biokompatibilität und Sicherheit von MNP-basierte Transfektionssysteme zu verbessern wurden in einer Übersicht über die neuesten Strategien in dieser Arbeit zusammengefasst.

Schlussendlich wurde im Rahmen dieser Arbeit eine MNP-basierte nicht-virale Gentransfermethode für klinisch relevante Zellen (i.e. hMSC) entwickelt. In den *in vitro* Studien zum Transfektionsmechanismus konnten die Vorteile eines magnetischen Transfektionsvektors belegt werden. Zusätzlich gibt es eine Vielzahl möglicher Modifikationsstrategien um die Biokompatibilität von MNP-basierten Transfektionskomplexen zu verbessern. Dies ist eine wesentliche Grundlage für weitere Forschungsfortschritte. Dennoch sind für die klinische Entwicklung der Genterapie und deren Translation in die Klinik weitere präklinische Studien erforderlich, wie etwa die Untersuchung der *in vivo* Verteilung der Transfektionskomplexe bzw. der Abbauprodukte.

Summary

The recent progress in gene therapy gave hope to many patients with rare genetic diseases, cancer and cardiovascular disorders. However, the safety aspects of this approach still remain a big concern, which limits rapid development and clinical use of gene therapy based drugs. Although viral vectors provide the most efficient delivery of nucleic acids to cells, serious side effects related to their application have forced the development of nonviral gene delivery methods in the last decades. Some of these nonviral gene delivery methods have already entered phase I-II clinical trials, although their efficacy is still lower than that of viral vectors. Hence, the development of safe and efficient gene delivery systems is the key to the overall success of gene therapy.

Current work was focused on a particular magnetic nanoparticle-based gene delivery system, developed previously by our group. This combined nonviral carrier system consists of polyplexes – plasmid DNA (pDNA), condensed by polyethylenimine (PEI) - which are covalently bound to the iron oxide magnetic nanoparticles (MNP). The beneficial properties of this system include ease of production, high affinity to nucleic acids, relatively high efficiency and safety as well as potential for targeted delivery due to magnetic compounds. This work aimed to optimize pDNA/PEI/MNP complexes for application in clinically relevant cells (human mesenchymal stem cells (hMSC)), to gain insights about the intracellular mechanism of MNP-mediated transfection and to evaluate the clinical perspectives of MNP-based gene therapy.

The results of the current work showed that pDNA/PEI/MNP complexes can efficiently and safely transfect bone marrow derived hMSC even without application of a magnetic field. To further study the differences in transfection mechanisms between polyplexes and MNP-based complexes, extensive colocalization studies were performed. To this end, for the first time, all three components of the transfection system (pDNA, PEI and MNP) were selectively labelled with fluorescent dyes and visualized by confocal laser scanning microscopy at different time points. The analysis of colocalization coefficients demonstrated that the MNP-based carrier provided better transfection efficiency due to more efficient release of pDNA in comparison to polyplexes alone. This finding emphasized a strong influence of the carrier composition on transfection processes and the efficacy. Next, aiming to increase the biocompatibility of the studied transfection system, PEI with low molecular weight (600 Da) was used. The system was characterized and tested in COS-7 cells. While the designed system

was rather safe, it could not outperform the original composition with high molecular weight PEI (25 kDa). Therefore, an overview of the recent strategies for improvement of biocompatibility properties and safety profile of MNP-based transfection systems complemented this work.

In conclusion, this work introduced a MNP-based nonviral gene delivery approach that could be of use for clinically relevant cells (i.e. hMSC). The *in vitro* mechanism studies explained the beneficial properties of the proposed carrier design. The variety of modification strategies to improve the biocompatibility of this system provides a firm basis for further research progress. Nevertheless, thorough preclinical studies, including investigations on the *in vivo* biodistribution of transfection systems and their components will be essential for further clinical development and translation.

Table of Contents

Zusammenfassung.....	I
Summary	III
1 Introduction.....	1
1.1 From genetic modifications in bacteria to gene therapy in humans.....	1
1.1.1 Genetic engineering	1
1.1.2 Gene therapy: history and clinical progress	1
1.2 Gene therapy methods	3
1.3 Viral gene delivery: methods and clinical applications.....	4
1.4 Nonviral gene delivery: methods and clinical applications.....	6
1.4.1 Physical methods for gene delivery	7
1.4.2 Chemical methods for gene delivery.....	8
1.5 Magnetic targeting in gene delivery	15
1.6 Aim of the study	20
2 Materials and Methods.....	21
2.1 Materials.....	21
2.1.1 Cell culture media and supplements	21
2.1.2 Labelling and staining reagents.....	21
2.1.3 Conjugated antibodies.....	21
2.1.4 Chemicals and different assays	22
2.1.5 Other reagents	22
2.2 Cell culture	22
2.2.1 COS-7 culture	22
2.2.2 hMSC isolation and culture.....	23
2.3 Plasmids.....	23
2.4 Biotinylation of PEI.....	24
2.5 Filtration of MNP	24
2.5.1 Determination of iron concentration in filtered MNP.....	24
2.6 Preparation of transfection complexes	26
2.6.1 pDNA/PEI and pDNA/PEI/MNP ($MW_{(PEI)} = 25$ kDa).....	26
2.6.2 pDNA/PEI600 and pDNA/PEI600/MNP ($MW_{(PEI)} = 600$ Da).....	26
2.7 Gel electrophoresis	27
2.8 Particle size and Zeta potential measurement	27

2.9	Transfection experiments	27
2.9.1	Transfection with pDNA/PEI600 or pDNA/PEI600/MNP complexes (MW _(PEI) =600 Da)	27
2.9.2	Transfection with pDNA/PEI or pDNA/PEI/MNP complexes (MW _(PEI) = 25 kDa)	27
2.10	Luciferase reporter gene assay	28
2.11	BCA protein assay	28
2.12	EGFP expression assay	28
2.13	Determination of cell viability.....	29
2.14	Characterization of hMSC with and without transfection.....	29
2.14.1	Immunophenotyping of hMSC	29
2.14.2	Functional differentiation assay for hMSC	30
2.15	Fluorescent labelling of transfection complexes	30
2.16	Microscopy.....	32
2.16.1	Superresolution structured illumination microscopy (SR-SIM)	32
2.16.2	Confocal laser scanning microscopy (CLSM).....	33
2.16.3	Colocalization studies	34
2.17	Statistical analysis	35
3	Results.....	36
3.1	Transfection in hMSC	36
3.1.1	Characterization of transfection complexes (MW _(PEI) = 25 kDa)	36
3.1.2	Optimization of transfection conditions with pDNA/PEI/MNP complexes (MW _(PEI) = 25 kDa) in hMSC	37
3.1.3	pEGFP transfection	37
3.1.4	Characterization of hMSC.....	38
3.1.5	Monitoring of transfection efficiency in hMSC over time.....	40
3.2	Mechanism of MNP-mediated transfection.....	41
3.2.1	Characterization and visualization of fluorescently labelled transfection complexes	41
3.2.2	Intracellular localization of transfection complexes 24 h after transfection	43
3.2.3	Monitoring of pDNA release from transfection complexes in hMSC	46
3.3	Transfection with LMW PEI-based magnetic complexes (MW _(PEI) = 600 Da)	48
3.3.1	Characterization of pDNA/PEI600 transfection complexes	48
3.3.2	Optimization of transfection conditions with pDNA/PEI600/MNP complexes in COS-7 cell line.....	49
4	Discussion	51

4.1	Transfection in hMSC	52
4.1.1	Characterization of transfection complexes ($MW_{(PEI)} = 25$ kDa)	52
4.1.2	Optimization of transfection in hMSC	52
4.1.3	Monitoring of transfection overtime	53
4.2	Mechanism of MNP-mediated transfection.....	53
4.2.1	Insights the mechanism of transfection.....	53
4.2.2	Visualization of transfection complexes	55
4.2.3	Intracellular localization of transfection complexes	57
4.2.4	Monitoring of pDNA release from transfection complexes.....	58
4.3	Transfection with LMW PEI-based magnetic complexes.....	59
4.4	Future perspectives of MNP-based gene delivery.....	60
4.4.1	Modifications of the MNP-based carrier.....	62
4.4.2	Modifications of genetic material	63
5	Conclusion	66
6	Bibliography.....	67
7	Appendix	i
	List of abbreviations.....	i
	List of figures	v
	List of tables	vi
	Acknowledgement.....	vii
	Curriculum Vitae.....	ix
	Publication List	xi
	Conference Presentation List	xii

1 Introduction

1.1 From genetic modifications in bacteria to gene therapy in humans

1.1.1 Genetic engineering

Everyday, various kinds of **genetic modifications** (also termed **genetic engineering**) are easily performed in every research lab all over the world. Many experiments, i.e. bacteria transformation, transduction, transfection, gene knockout, reporter gene expression, together with genetically engineered animal models became a routine, although deoxyribonucleic acid (DNA) has become a topic of intense research since less than 70 years ago. The aim of genetic engineering is to modify the genome of an organism by artificial means. The first discoveries in bacterial genetics by F. Griffith [2], J. Alloway [3, 4], O. Avery [4], N. Zinder [5], E. Tatum and J. Lederberg (Nobel Prize winners in 1958) [6], including the work of J. Watson and F. Crick on a DNA structure in 1953 [7] (Nobel Prize winners in 1962) evoked a great interest in this field [8]. Already in 1976, H. Boyer and R. Swanson founded the first genetic engineering company Genentech. Following the breakthrough of H. Boyer and S. Cohen in recombinant DNA technology [9], the company focused on the production of human hormones using genetically engineered bacteria (somatostatin, insulin, growth hormone) [10].

Nowadays, genetic engineering is widely used in industrial production of medicines (e.g. hormones, vaccines, monoclonal antibodies), basic research and agriculture. Gene therapy is one of the most important and challenging fields, where genetic modifications play a key role.

1.1.2 Gene therapy: history and clinical progress

Gene therapy is an experimental technique, aiming to cure or treat the disease by introduction or alteration of genetic material within a cell or organism. The gene therapy of reproductive or germline cells is defined as germline gene therapy. The main risk of germline gene therapy is that it can change the genetic make-up of the patient and can be passed onto offspring of the patient. Therefore, due to unresolved ethical issues regarding human germline gene therapy, no approved applications of this form of treatment exist [11]. All further discussion about gene therapy in this work will focus on somatic gene therapy, which affects gene expression of the cells that will be corrective to the organism, but not inherited.

The first understanding that genetic modifications could serve for the treatment of genetic disorders appeared in late 1960s, when it became apparent that viruses might be of use for gene

delivery. In 1968, S. Rogers and P. Pfuderer showed “proof-of-principle” of virus-mediated gene transfer using a tobacco mosaic virus [12]. However, the new findings raised many concerns. M. Fox and J. Littlefield in their editorial, published in *Science* in 1971, discussed the hazards and limitations of viral approach for gene therapy. They emphasized the safety issues of viral vectors (mutagenesis and tumorigenesis), and doubted their efficiency (the inability of a small population of genetically modified patient cells to completely cure the disease) [13]. Yet, since 45 years, a great progress in gene therapy field has been made, though the main concerns remain the same.

The first clinical trials, aiming to evaluate the safety of gene therapy were carried out in 1990s. S. Rosenberg, for instance, performed clinical trials on patients with metastatic melanoma [14]. M. Blaese and C. Bordignon were independently working on adenosine deaminase (ADA) deficiency [15, 16]. M. Cavazzano-Calvo reported restored immunity in patients with X-linked severe immunodeficiency after the application of hematopoietic cells, transduced with a retroviral vector [17]. Although, the results were not always as good as expected, gene therapy in general experienced a boom until the death of Jesse Gelsinger in 1999 [8, 18]. The trial of M. Batshaw and J. Wilson in 1999 included the worst case of unsuccessful gene therapy, where for the first time the side effect was directly related to the viral vector [19]. The study aimed to evaluate the safety of adenovirus, carrying recombinant complementary DNA (cDNA), in patients with ornithine transcarbamylase deficiency. Due to severe immune response, that caused a multiorgan failure, the 18-years old patient died 4 days after the treatment. This tragedy raised up such issues as non-compliance with the study protocol and underreporting of adverse events, which led to the reduction of efforts and resources, invested in gene therapy in the next years [1].

The shift of research focus towards development of novel vectors for gene therapy, combining low immunogenicity with efficient delivery, led to a number of successful studies, reported in the last decade. For instance, a positive dynamic was observed in the treatment of malignant brain tumors, lipoprotein lipase (LPL) deficiency, Parkinson’s disease, severe heart failure, Leber’s congenital amaurosis, β -thalassemia, haemophilia B, Wiskott-Aldrich syndrome and severe combined immunodeficiencies (SCID) [1]. Finally, in 2012 the first approved gene therapy drug appeared on the market. After a long and tortuous approval process Glybera[®] (alipogene tiparvovec) was recommended by the European Medicines Agency (EMA) for the treatment of adults with LPL deficiency – a rare monogenic disease. The active substance of Glybera[®] is a modified adeno-associated virus (AAV), engineered to express the LPL gene in the muscle tissue [20]. Another gene therapy approach has been just recently

(April, 2016) recommended by the Committee for Medicinal Products for Human Use (the authority of the EMA) for marketing authorisation. Strimvelis™ is a medicinal product, developed by Italian researchers and GlaxoSmithKline Trading Services (Ireland) for the treatment of a very rare indication - ADA–SCID in children. It includes autologous CD34+ cells transduced with a retroviral vector encoding for the human ADA cDNA sequence [20, 21]. However, the regulatory process, which led to the approval of Glybera®, included several reapplications and reexaminations of the drug, thus highlighting the prolonged and challenging regulatory pathway of gene therapy products in the European Union (EU) [22, 23].

To date, over 2350 clinical trials involving genetic modifications are approved, ongoing or completed in 36 countries all over the world. Although initially gene therapy was thought to treat genetic diseases, most of the reported clinical trials were dedicated to cancer treatment (64.4%) [24]. The reasons for that are scientific advances in selective tumor targeting by genetic vectors, that can be reached by a number of methods [25]. However, of more than 6000 inherited diseases known to date, very few can be treated by supplying a missing or defective gene product exogenously. For many other monogenic diseases, gene therapy might be the most successful approach. To date, only 235 clinical trials address their treatment to monogenic diseases (10%) [24]. The key to successful development of effective and safe gene therapy products is an appropriate selection and optimization of gene delivery methods.

1.2 Gene therapy methods

Gene therapy can be performed directly (*in vivo*) or indirectly (*ex vivo*). The first approach comprises **direct** delivery of the gene of interest to the target organs or tissues in the organism (e.g. via systemic or local injection). The **indirect** approach or cell-based gene therapy includes two steps: gene delivery to the cells, previously isolated from patient or donor, and further transplantation of transfected/transduced cells to the target site [26]. Both, *in vivo* and *ex vivo* applications have their advantages and drawbacks. Thus, the outcome and side effects of direct gene therapy depend on the administration way. The success of cell-based gene therapy is strongly related to the type of selected cells and their migration and proliferation properties. Moreover, the selection of the appropriate method for gene delivery is a very crucial step in both cases. It very much defines efficacy, selectivity and safety of the therapy. Kaestner et al. have recently discussed the technical aspects of mostly used gene delivery methods [27]. They also proposed a guideline for selecting a method of gene transfer in eukaryotic cells both, *in vitro* and *in vivo*. The authors admit, that the general recommendation is difficult, but their

guideline might help the researchers, seeking the optimal gene delivery method for their experiments and support them in developing novel transfection techniques in placing their method correctly in the context of applications [27].

The overview of the methods, utilized for gene delivery in clinical trials is shown in Figure 1.1. Different types of viruses represent the major part of them (67%), while nonviral methods are used just in 22% of reported clinical trials [24].

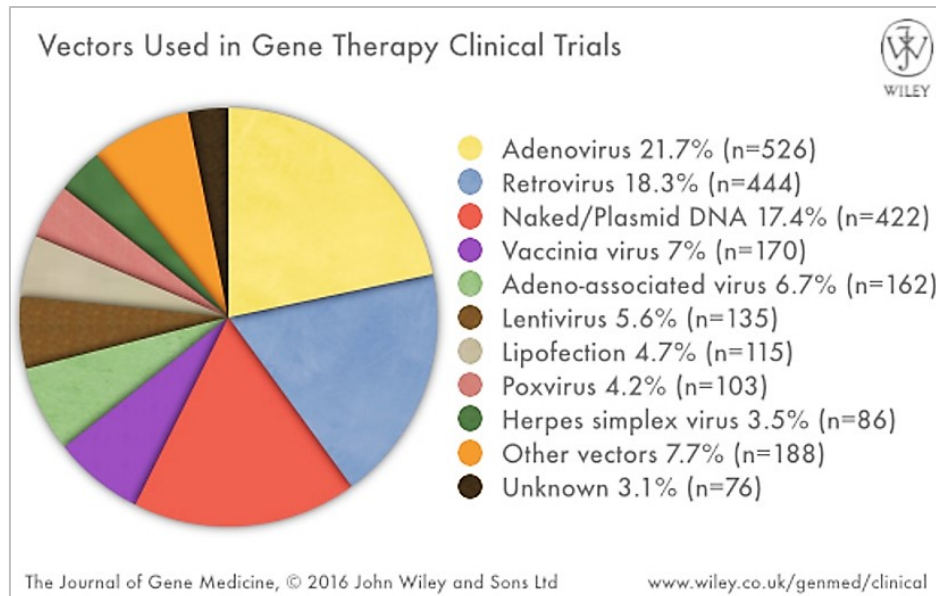


Figure 1.1: Overview of the methods, utilized in gene therapy clinical trials worldwide.
Retrieved from <http://www.abedia.com/wiley/> [24].

The next sections of this chapter will thoroughly describe the advantages and limitations of both, viral and nonviral methods, focusing on their current or potential clinical applications.

1.3 Viral gene delivery: methods and clinical applications

Virus-mediated gene delivery was initially a method of choice for gene therapy due to high efficiency. Viruses are perfect gene delivery systems created by nature. Once scientists had realized that, they tried to use the natural viral properties for the goals of medicine. A comprehensive review on viral gene delivery and its clinical outlook has been recently published by Kotterman et al. [1]. Table 1.1 summarizes several application examples of viral vectors, used in gene therapy in the last decade.

Adenoviruses represent 21.7% of all gene delivery methods used in clinical trials (Fig. 1.1), as they provide a very high transduction efficiency *in vivo*. However, they were shown to be highly immunogenic and provide only a short-term transgene expression [68].

Table 1.1: Viral vectors most recently used in gene therapy clinical trials worldwide (Phase I/II) and their clinical applications (years 2005-2015). The data are taken and modified from [1].

Virus	Indications	Approach	Reference
Retrovirus (murine leukemia)	ADA-SCID	<i>Ex vivo</i>	[28]
Lentivirus (self-inactivating)	β -thalassemia	<i>Ex vivo</i>	[29]
	Leukodystrophy		[30, 31]
	Wiskott-Aldrich Syndrom		[32]
	Leukemia		[33-35]
Adenovirus	Vaccines against HIV, malaria, tuberculosis, influenza	<i>In vivo</i>	[36-41]
	Coronary artery disease		[42]
	Cancer therapy (glioma, B-cell lymphoma)		[43, 44]
Adeno-associated virus	Heamophilia B	<i>In vivo</i>	[45, 46]
	Rheumatoid arthritis		[47]
	Cystic fibrosis		[48]
	Lipoprotein lipase deficiency		[49-51]
	Leber's congenital amaurosis		[52-54]
	Choroideremia		[55]
	Muscular dystrophy		[56, 57]
	Severe heart failure		[58]
	α -1-Antitrypsin deficiency		[59, 60]
	Parkinson's disease		[61-63]
Herpes simplex virus	Malignant melanoma	<i>In vivo</i> (intratumoral)	[64]
Vaccinia virus	Liver cancer, metastatic tumors	<i>In vivo</i> (intratumoral)	[65-67]

Therefore, adenoviral vectors are now widely used in therapies requiring initiation of immune response (cancer treatment) and as a platform for developing vaccines. Due to their short-term expression adenoviruses have also a potential for applications where new formation of biologic structures is required (e.g. angiogenesis) [1].

Retroviruses and **lentiviruses** represent another big group of viral vectors utilized in the clinic (23.9%). Both of them are integrating into the host genome and have been successfully used in clinical trials involving *ex vivo* hematopoietic gene delivery. However, retrovirus-mediated gene delivery is related to insertional mutagenesis, challenging its safety. In order to

decrease these risks, self-inactivating lentiviruses were developed and applied in T-cell therapy of leukemia, hematopoietic stem cell therapy of β -thalassemia, etc. [1, 29, 35].

In parallel, the development of **adeno-associated viruses** (AAV) in the last decade, which represent just 6.7% of viral vectors in clinical trials, led to an increasing number of successful studies worldwide, including Glybera® approval. Recently, AAV were widely used for the treatment of different monogenic diseases (Table 1.1), showing a strong safety profile, persistent gene expression and therapeutic benefits [1].

However, safety of viruses remains the major concern for clinicians. The main risks include insertional mutagenesis (also called genotoxicity), oncogenesis and immunogenesis. Moreover, the production of virus-based delivery systems requires high costs and is not always feasible at high titers. The capacity to load the required amount of transgenic material is also limited for most viruses. Although a big progress in understanding the transduction mechanisms has been made, and novel viral vectors are nowadays more selective and significantly safer than those, developed 20 years ago, many researches are seeking for an “ideal” gene delivery method among the nonviral strategies.

1.4 Nonviral gene delivery: methods and clinical applications

Aiming to minimize the side effects of gene therapy with no loss in efficiency, various nonviral methods were developed and investigated in the last decades. The reviews of Al-Dosari et al. [69], Wang et al. [70], Schlenk et al. [71] and Jin et al. [72] comprehensively describe the recent progresses on nonviral systems for gene delivery. Table 1.2 shows nonviral carriers, recently evaluated or currently involved in clinical trials.

Table 1.2: Nonviral vectors, most recently used in gene therapy clinical trials worldwide (Phase I/II/III) and their clinical applications (years 2005-2015).

Nonviral agent	Indications	Approach	Reference
Naked DNA	Cancer therapy	<i>In vivo</i>	[24, 73]
	Cardiovascular diseases		
	Critical limb ischemia		
Electroporation	Metastatic melanoma	<i>In vivo</i>	[74, 75]
Hydrodynamic gene transfer	Liver cirrhosis with thrombocytopenia	<i>In vivo</i>	[24, 76]
	GNE - myopathy		

Nonviral agent	Indications	Approach	Reference
Cationic lipids	Advanced metastatic melanoma	<i>In vivo</i>	[77, 78]
	Cystic fibrosis		[79]

All nonviral transfection methods can be divided into two groups: physical and chemical methods.

1.4.1 Physical methods for gene delivery

Physical methods are using naked nucleic acids, which are mechanistically delivered to the cell via microinjection, gene gun, electroporation, sonoporation, optical transfection and hydrodynamic gene transfer. These methods might be aggressive for cells as they involve physical damage of the cell membrane, even though it is not a permanent state. Moreover, naked nucleic acids, delivered into the cytosol, undergo a high risk to be destroyed by nucleases. Therefore the level of transgene expression is usually low and the effect is short-term [69, 70]. However, the physical approach is easy to use as it does not require any complex biological structures or chemicals to be produced, and does not lead to an immune response of the organism. Moreover, the delivered gene can be easily “tuned” by standard recombinant DNA techniques [80].

Microinjection is a direct ejection of genetic material into the nucleus of the target cell under observation. This method of gene transfer must be trained in advance and is useful when only a limited number of cells should undergo genetic modification [27]. Microinjections have been widely used in preparation of transgenic animals, *in vitro* fertilization and studies of primary cells and ribonucleic acid (RNA) interference [81]. However, this technology cannot be scaled up for direct *in vivo* applications and is not able to transfect the necessary amount of cells for indirect gene therapy approach. Compared with other physical methods for gene delivery, microinjection is the least feasible for clinical use.

Gene gun technique (or ballistic gene delivery) includes heavy metal particles, carrying DNA on their surface, which are delivered to the cells by a pressurized inert gas [82]. Already in the middle of 90’s this technology was applied for immunomodulation therapy in melanoma patients [83, 84]. **Naked DNA** has entered the clinical trials in 2000. It was used as a vector for intramuscular delivery of growth factors in limb ischemia patients [85, 86]. Up to now, naked plasmid DNA (pDNA) alone has been used as a vector in 422 clinical trials worldwide (17.4% of all gene delivery methods), mainly focused on cancer therapy and cardiovascular diseases [24].

The first clinical trials involving *in vivo* **electroporation** were carried out in 2005 aiming to investigate the safety and efficacy of interleukin – encoding pDNA delivery in treatment of metastatic melanoma [74, 75]. Electroporation requires at least two electrodes, connected to a power supply, that enclose a target tissue (*in vivo*) or cell suspension (*in vitro*). The electrical impulses lead to the temporary formation of pores in the cell membrane, thus enabling DNA to enter the cell [82]. A similar principle of nucleic acid delivery via transiently formed pores is utilized by **sonoporation** and **optical transfection** methods, by the means of ultrasound or laser light stimulation, respectively. In combination with DNA-loaded microbubbles sonoporation technology has been shown to provide efficient gene transfer *in vitro* and *in vivo* [87]. Optical transfection with femtosecond laser was able to provide safe, selective and localized gene delivery in mammalian cells [88].

Hydrodynamic gene transfer employs a rapid intravenous injection of a large volume of pDNA solution, which allows the entry of DNA through the pores in capillary endothelium. This method has been broadly applied aiming to deliver DNA, RNA, proteins or synthetic compounds in various tissues [82]. For instance, in 2008 this method was used in clinical trials of hydrodynamic delivery of thrombopoietin to the liver of cirrhotic patients with thrombocytopenia [76]. A phase I clinical trial for the initial evaluation of safety and efficacy of hydrodynamic transfer of a gene encoding the enzyme for the biosynthesis of sialic acid (Glucosamine [UDP-N-acetyl]-2-epimerase/N-acetylmannosamine kinase, or GNE gene) into a limb vein of patients with GNE – myopathy has been initiated in 2013 [24].

To date, physical gene delivery methods are mostly applied in the production of DNA – vaccines for cancer therapy, which are involved in several Phase I-II clinical trials [24]. Various phase II clinical trials involving naked pDNA, encoding growth factor genes for the gene therapy of cardiovascular diseases are also underway [24]. After successful safety studies, a hepatocyte growth factor encoding plasmid (intramuscular injections) has entered the Phase III clinical trials of critical limb ischemia [73, 89].

1.4.2 Chemical methods for gene delivery

Chemical methods for gene delivery include gene delivery using cationic lipids, cationic polymers and dendrimers, synthetic peptides, inorganic nanoparticles, and combined vectors. Here, the transported nucleic acid is condensed by the carrier and therefore protected from intracellular degradation, which is of advantage in comparison to physical methods. Additionally, the synthetic origin of the above listed nonviral carriers allows chemical

modifications for the adjustment of chemical and physical properties of the delivery system [71].

Whereas viruses have already actively entered the clinical research, nonviral carriers just start their journey from bench to bedside. However, many chemical transfection agents were already commercialized (Table 1.3). A large amount of published articles reporting the development of novel nonviral systems and their pre-clinical investigations indicate a great potential of this approach.

Table 1.3: Examples of chemical carriers for transfection, currently available on the market.

Transfection agent	Company	Country
Cationic lipids		
Lipofectin [®] , Cellfectin [®] , Optifect [™] , DMRIE-C Transfection Reagent, Lipofectamine [®] family	Thermo Fischer Scientific	Waltham, MA, USA
FuGENE [®] , TransFast [™]	Promega	Madison, WI, USA
Attractene, Effectine, HiPerFect TransMessenger	QIAGEN	Venlo, Netherlands
Escort [™]	Sigma-Aldrich	St. Louis, MO, USA
DreamFect [™] , Lullaby siRNA	OZ Biosciences	Marseille, France
GenePORTER [®] , PerFectin [™]	Genlantis	San Diego, CA, USA
TurboFectin 8.0 [™]	OriGene	Rockville, MD, USA
Cationic polymers		
X-tremeGENE [™]	Sigma-Aldrich	St. Louis, MO, USA
jetPEI [®] , jetPRIME [®]	Polyplus-transfection [®]	Illkirch, France
TransIT-X2 [®] Dynamic Delivery System	Mirus Bio [®] LLC	Madison, WI, USA
Xfect Transfection reagent	Clontech Laboratories, Inc.	Mountain View, CA, USA
Magnetic nanoparticles		
Magnetofectamine [™] , PolyMag, LipoMag, CombiMag, NeuroMag, SilenceMag	OZ Biosciences	Marseille, France
nTMag, nTMag Plus	nanoTherics Ltd	Newcastle under Lyme, UK

1.4.2.1 Cationic lipids

To date, **cationic lipids** represent the most successful group of nonviral carriers in terms of clinical applications. To date, many efficient cationic lipid-based transfection reagents were commercialized (Table 1.3).

In general, lipid-based transfection reagents are composed of cationic lipids (e.g. N-[1-(2,3-dioleoyloxy)propyl]-N,N,N-trimethylammonium chloride (DOTMA), N-[1-(2,3-dioleoyloxy)propyl]-N,N,N-trimethylammonium chloride (DOTAP), 1,2-dimyristyloxypropyl-3-dimethyl-hydroxy ethyl ammonium bromide (DMRIE), etc.) mixed with helper (or neutral) lipids (e.g. dioleolylphosphatidylethanolamine (DOPE)) or cholesterol. Cationic lipids are characterized by a hydrophobic tail, a positively charged hydrophilic head group (usually consisting of quaternary ammonium salts) and a linker. These mixtures are able to condense negatively charged nucleic acids, forming positively charged (at physiological pH) liposomes or micelles – lipoplexes. The lipoplexes can easily enter the cell via endocytosis and further process the delivered nucleic acid [90, 91]. The variety of lipid-based transfection reagents nowadays allows scientists to select the optimal reagent for their experiments. Thus, lipid-based transfection systems have been explicitly optimized for the delivery of pDNA, RNA, small interfering (siRNA), microRNA (miRNA) or oligonucleotides. Transfection protocols have been adjusted for different cell types, including suspension and adherent cell cultures, as well as primary and “difficult-to-transfect” cells [92]. The main advantages of cationic lipids as transfection reagents include good biocompatibility, low immunogenicity, high load of delivered nucleic acids and ease in use and preparation [72]. Moreover, various possible chemical modifications of the lipid structure may allow gaining biodegradable properties and improving transfection efficiency, stability and safety of the lipid-based gene delivery systems.

Cationic lipids have entered the clinical trials already in 1993, when Nabel et al. performed the first direct gene delivery study in humans. They used DMRIE/DOPE for the direct intratumoral delivery of a gene, encoding foreign major histocompatibility complex class 1 (MHC 1) protein (human leukocyte antigen serotype B7 (HLA-B7) gene), in HLA-B7-negative patients with stage IV melanoma. The study showed the feasibility, safety, and therapeutic potential of direct lipid-based gene transfer [93, 94]. Further, the lipoplexes consisting of DMRIE/DOPE and genes for MHC 1 protein (HLA-B7 and beta-2-microglobulin) have undergone phase I, II and III clinical trials as Allovectin-7 or later, Allovectin[®] (a registered trademark of Vical Inc., San Diego, California, USA). Despite the promising phase II study results [77, 78], the company had to discontinue the phase III clinical trials, as Allovectin[®] failed to show an improvement compared with chemotherapy at primary and secondary efficacy endpoints [95]. Another indication, where cationic lipids reached the clinical application is cystic fibrosis. Since the middle 90s’ several research groups have independently performed phase I and II clinical trials, where cDNA, encoding a cystic fibrosis transmembrane

regulator gene (CFTR), was delivered by cationic lipids into nasal epithelium of patients [79, 96-101]. These studies reported that the treatment was safe, but the transgene expression levels were not high enough in order to achieve a therapeutic effect [99, 101]. According to the Gene Therapy Clinical Trials Database, a number of similar clinical trials involving CFTR gene has been initiated in the last 5 years, though no data on the outcomes of these studies are available yet [24].

Despite the recent progress, cationic lipid-based transfection reagents still possess several limitations. These include low stability in the bloodstream, low specificity and cytotoxicity related to the cationic nature of the head group [72, 102]. It has also been shown that cationic lipids and pDNA have a synergism in causing cytotoxicity, thus formation of lipoplexes can lead to cell death via apoptosis *in vitro* [103] and even activate an immune response *in vivo* [104]. Therefore, cationic lipids to date remain the method of choice for transfection in experimental settings, and require further improvement of safety and efficacy to proceed in the clinic.

1.4.2.2 Cationic polymers and dendrimers

Cationic polymers represent another big group of chemical methods for transfection. They include various polyamines and their numerous derivatives. Poly(L-lysine) (PLL), polyethylenimine (PEI), and chitosan are the mostly used and investigated cationic polymers for gene delivery (Fig. 1.2).

Numerous reviews and book chapters address their issues to the variety of cationic polymers used nowadays for gene delivery. This group of polymers gained the attention of researches due to its physical and chemical properties, that make cationic polymers a promising tool for gene delivery. Cationic polymers are characterized by their high positive charge (usually provided by numerous aminogroups). Via electrostatic interactions with negatively charged phosphate groups they easily condense nucleic acids and form stable complexes – so called “polyplexes”. Due to a strong positive surface charge, polyplexes attach to the cell membrane and enter the cell via endocytotic pathway, followed by endosomal escape and the release of nucleic acid in the cytosol [105].

Initially, lipopolyamines and polyamidoamines were tested as gene delivery agents in the 90s’ [106-108]. **PLL** was also among the “pioneers” in polymer-based gene delivery. Due to its peptide structure, the polymer is biodegradable, which makes it an attractive tool for *in vivo* applications.

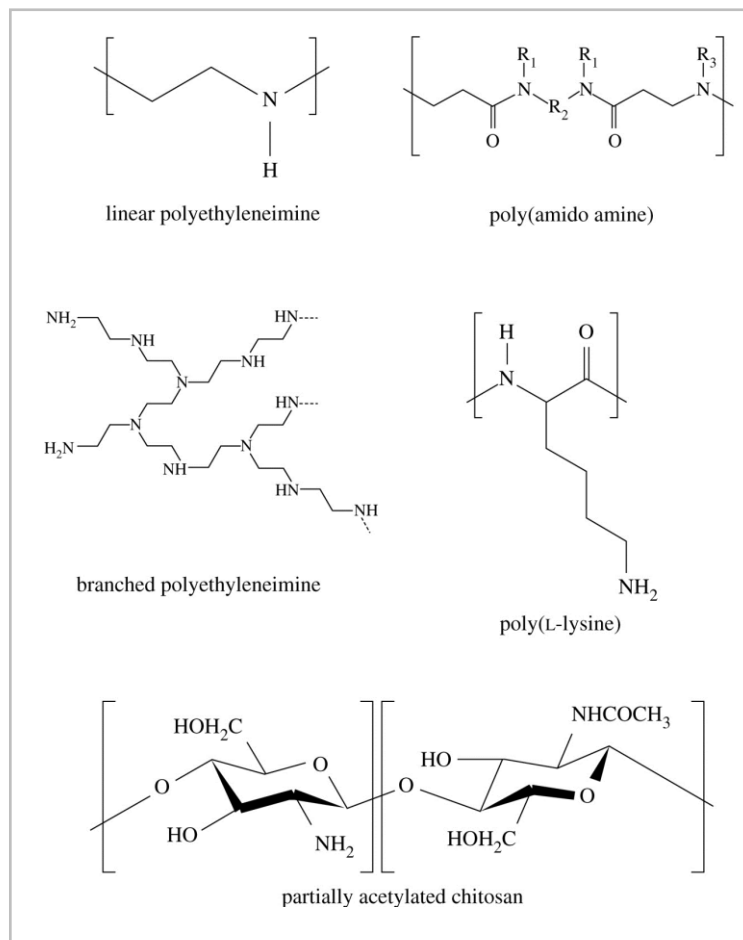


Figure 1.2: Chemical structures of cationic polymers and dendrimers mostly used as gene delivery carriers. Retrieved and modified from <http://rsif.royalsocietypublishing.org/> [105].

However, the toxicity of PLL does not allow to use it for efficient and safe gene delivery [109].

PEI, that later became “a gold standard” for nonviral gene delivery, for the first time was used by Boussif et al. in 1995 [110]. An extensive review on the recent progress in the development of PEI-based gene delivery systems has been published by Wang et al. [111]. PEI has a very high density of amines, as its structure combines primary, secondary and tertiary aminogroups (Fig. 1.2). This feature plays a key role in the efficient delivery of nucleic acids with PEI. Due to the following properties, PEI has remained in the focus as the most promising gene delivery agent in the last decades [111]:

- Efficient condensation of nucleic acids of different size;
- Enhancement of cellular uptake of polyplexes due to their positive charge;
- Protection of delivered nucleic acids from enzymatic degradation;

- Exceptional buffering capacity under acidic pH, which facilitate the endosomal escape of polyplexes due to the “proton sponge effect”¹ [112].

Although PEI alone has demonstrated a high transfection efficiency *in vitro* and *in vivo*, viral gene delivery remains the most effective approach [113]. Moreover, PEI applications are limited due to high cytotoxicity and low biocompatibility of the polymer. PEI was shown to cause membrane damage due to strong electrostatic interactions and apoptosis due to mitochondrial alterations in clinically relevant human cell lines [114, 115]. Therefore, in order to reduce toxicity and improve transfection efficiency, much research has been recently devoted to the development of novel carriers on the basis of PEI or other cationic polymers. PEI with molecular weights (MW) from 600 to 2000 Da, for example, demonstrated much lower cytotoxicity as PEI with MW of 25 kDa used initially. However, these **low-molecular weight** (LMW) polymers alone did not provide the desired transfection efficiency [116].

Naturally-derived cationic polymers, including **chitosan**, has also been shown to have a strong affinity to DNA, providing good transfection rates and low cytotoxicity [117]. Moreover, they are biodegradable and biocompatible, thus possess a great potential as *in vivo* gene delivery vectors. In order to improve their transfection efficiency and specificity, many chemical modifications have been performed and described elsewhere [117].

Dendrimers are spherical, highly branched three dimensional polymers, characterized by high density of amines at the periphery of the macromolecule [118]. The most widely used dendrimers for transfection approaches are poly(amidoamines), or PAMAM, which have already been commercialized as Polyfect[®] and Superfect[®] by QIAGEN (Venlo, Netherlands). Despite many *in vitro* and *in vivo* studies of these agents, their clinical translation is not feasible due to low transfection efficiency [109].

In the last decade numerous strategies for the **modifications** of cationic polymers and dendrimers were performed and characterized in terms of toxicity and transfection efficiency both, *in vitro* and *in vivo*. For instance, coating of cationic polymers with hydrophilic polyethylene glycol (PEG) can improve their pharmacokinetics and stability in the bloodstream by hindering interaction with serum proteins [119]. Modification of polymers with hydrophobic (alkanes, fatty acids, phospholipids) moieties improve condensation of nucleic acids and their intracellular trafficking, and reduce cytotoxicity of the carrier. Additionally, the

¹ The hypothesis of “proton sponge effect” has recently been argued as no changes in lysosomal pH, related to the polyplexes, were observed. Thus, the amount of PEI, DNA or polyplexes, escaping the endosomes/lysosomes must be low, but enough for efficient transfection.

selectivity and targeting of cationic polymers – derivatives can be reached by adding of stimuli responsive groups and targeting ligands [120]. The variety of polymer-based nanocarriers, in general, can be characterized by efficient gene transfection, low cytotoxicity, capability to co-deliver nucleic acids and chemotherapy drugs, ease of modification with targeting molecules, and good responsiveness to external stimuli [105].

Despite the promising findings and rapid development of cationic polymer-based transfection systems, none of them has been applied for gene therapy in humans yet.

1.4.2.3 Synthetic peptides

The application of **synthetic peptides**, e.g. cell penetrating peptides (CPPs), for gene delivery is currently rapidly growing. These cationic or amphipathic peptides are able to condense nucleic acids, enter the cells without toxic effects and carry the cargo into live cells, although the mechanisms of their internalization are not clear, yet [121, 122]. CPPs have been mostly used **in combination** with viral or nonviral vectors, aiming to overcome the barriers for gene delivery [121].

1.4.2.4 Inorganic nanoparticles

Inorganic nanoparticles (InNP) for gene delivery represent a big group of nanosized structures of inorganic origin (normally ≤ 100 nm in diameter), which are able to transfer various genetic materials into the cell. They include gold, silica, iron oxide nanoparticles, quantum dots, carbon derivatives (e.g. carbon nanotubes) and calcium phosphate nanoparticles [123]. InNP possess several features that make them attractive for research and development of the carriers for gene transfer:

- Easy preparation;
- Wide availability;
- High functionality;
- Biocompatibility and biodegradability (e.g. silica and calcium phosphate nanoparticles);
- Ability for broad characterization and different modifications;
- Ability for controlled release of delivered nucleic acids (e.g. silica, gold and carbon nanostructures);
- Ability to be monitored and guided *in vivo* (e.g. quantum dots and iron oxides).

Due to the above listed properties and the variety of InNP, many advanced strategies for the delivery of nucleic acids have been developed and investigated in the recent years. These

strategies have been recently described by Voronina et al. in a comprehensive review, covering this topic [123].

Interestingly, the most successful InNP-based transfection systems were produced as **combined vectors**, containing different chemical carriers in order to merge their benefits. For example, gold and silica nanoparticles as well as carbon nanotubes were combined with cationic polymers; calcium phosphate nanoparticles were combined with cationic lipids and targeting moieties [123]. Iron oxide nanoparticles were combined with viral agents, cationic lipids and cationic polymers [124].

Gene delivery systems, based on **iron oxide nanoparticles** require an extensional attention due to their broad application as transfection agents. Due to magnetic properties, they enable magnetic targeting – one of the most advanced and broadly studied technologies in gene delivery, which will be discussed in the next section of this chapter.

1.5 Magnetic targeting in gene delivery

At first, magnetic targeting was applied for site-specific delivery of drugs in cancer chemotherapy in the 1970s. For that purpose cytotoxic drug - loaded magnetic nanoparticles were guided to the target site by an external magnetic field [125, 126]. Several studies, performed in the following 30 years, showed that this approach was able to provide a local treatment with minimized side effects, and therefore attracted attention in other application fields, e.g. gene delivery.

Since the first application of magnetic nanoparticles (MNP) in gene delivery in 2001 [127], they have been widely applied in combination with viruses, cationic polymers and cationic lipids [124].

Christian Plank with colleagues at the Technical University of Munich were the pioneers in the field of magnetically - targeted gene delivery. For the first time their strategy, called magnetofection, was reported in 2002 by Scherer et al. They associated different gene delivery carriers (viruses, cationic lipids, cationic polymers) with superparamagnetic iron oxide nanoparticles (9-11 nm) and further attracted them by magnetic field gradients to the target cells [128]. This approach was later commercialized as Magnetofection™ (OZ Biosciences, Marseille, France) and was adjusted for transfection of various cell types, including primary and hard-to-transfect cells [129]. The group of J. Dobson has later proposed an application of oscillating magnetic fields aiming to improve transfection efficiency of magnetofection by additional lateral motions of MNP-based transfection reagents [130, 131]. This approach has also been commercialized under the name of Magnefect™ (NanoTherics Ltd, Newcastle under

Lyme, UK) [132]. The technique has recently been used by Subramanian et al. for delivery of enhanced green fluorescent protein plasmid (pEGFP) into human prenatal cardiac progenitor cells and adult cardiomyocytes *in vitro*. In comparison to static magnetofection, cationic lipid reagents and electroporation, oscillating magnet-assisted transfection with NeuroMag (nanoTherics, Keele, UK) in this work showed higher efficiency and maintained high cell viability [133]. Similar studies have also been performed to successfully transfect human mesenchymal stem cells and human osteosarcoma fibroblasts with no effect on cell viability and cell functions [134, 135].

Since the reports of Plank's and Dobson's groups, magnetic targeting has become a powerful technique to improve efficiency and to decrease side effects of gene delivery *in vitro* and *in vivo*. An extensive overview of viral and nonviral magnetic targeting strategies, developed recently and successfully used in gene delivery can be found in different reports [124, 136, 137].

Most research groups utilize MNP with a magnetite (Fe_3O_4) core, as they are easy to produce and are well studied due to their wide applications in bioimaging [138]. Several MNP with an iron oxide core have already been approved by the Food and Drug Administration (FDA) for application in magnetic resonance imaging (MRI) (i.e. Resovist[®], Feridex IV[®], FeroHeme[®]), and therefore are well studied regarding their metabolism, pharmacokinetics and safety profile [139, 140]. It has been demonstrated that the iron oxide core of these MNP is broken down into other forms of iron and afterwards incorporated into haemoglobin in newly formed erythrocytes. Moreover, no MNP – related toxicity was observed [140]. Importantly, MNP used for gene delivery are mostly paramagnetic or superparamagnetic, which allows them to remain non magnetic in the absence of a magnetic field. Therefore, the main advantages of these MNP include easy resuspension, slow sedimentation and uniform distribution in the suspension media [141].

To create a magnetic transfection system, various nucleic acid carriers or nucleic acids alone are attached to the MNP - core using molecular linkers or physical interactions, as shown in Figure 1.3. Depending on the final assembly, the diameter of the whole system may vary from 100 to 500 nm. Applying an external static or oscillating magnetic field, MNP-based gene delivery systems can be controlled and manipulated both, *in vivo* and *in vitro*. The benefits of such an approach *in vivo* arise from the local targeting on a tissue scale [124]. The recent study of Muthana et al. proved that a standard clinical MRI scanner is able to provide a real-time image – guided targeting of magnetically labelled cells to the desired tissues in the organism

[142]. *In vitro*, magnetic targeting improves sedimentation of the carriers on the cell membrane, thus enhancing the efficiency of gene delivery [143].

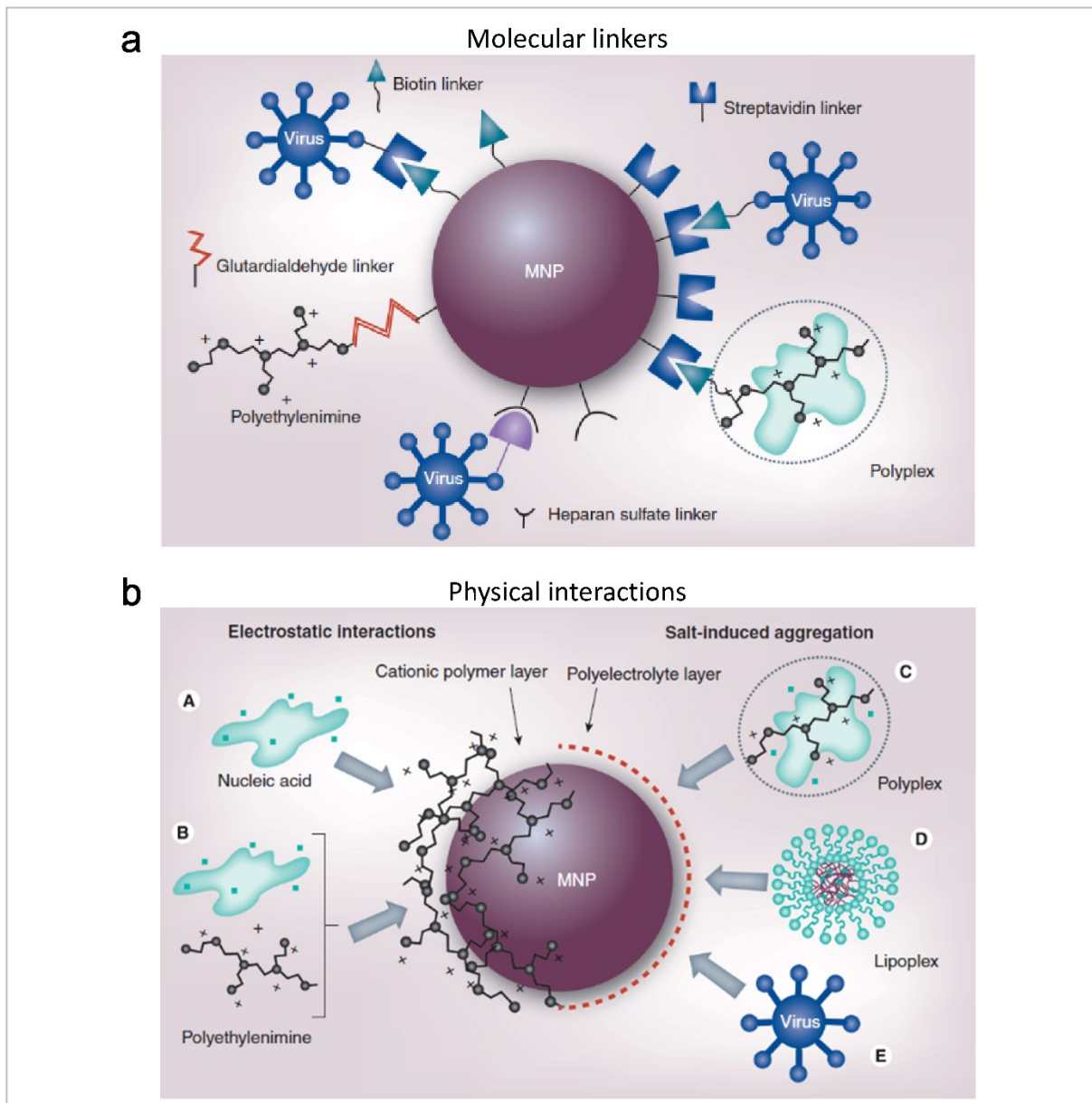


Figure 1.3: Different strategies used for the construction of MNP-based gene carriers, by means of molecular linkers (a) or physical interactions (b). Retrieved from <http://www.futuremedicine.com/> [124].

Magnetofection™ has been successfully applied in a wide range of cell lines, hard-to-transfect and primary cells. It was adapted to all types of nucleic acids (pDNA, siRNA, double-stranded RNA (dsRNA), small hairpin RNA (shRNA), messenger RNA (mRNA), oligodeoxynucleotides), non-viral transfection reagents and viruses [129, 136]. The majority of iron oxide MNP, used for Magnetofection™ are coated with a cationic polymer (most often

PEI), which allows an association of genetic material or transfection agent by salt – induced colloidal aggregation.

Li et al. in 2008 described a similar design of a MNP-based transfection system, consisting of iron oxide nanoparticles, PEI and pDNA [144]. In contrast to complexes for Magnetofection™, pDNA in this system was firstly condensed by biotinylated PEI (forming “polyplexes”), and afterwards attached to streptavidin - coated MNP by biotin – streptavidin interactions (forming “magnetic polyplexes”) (Fig. 1.4). This system provided successful

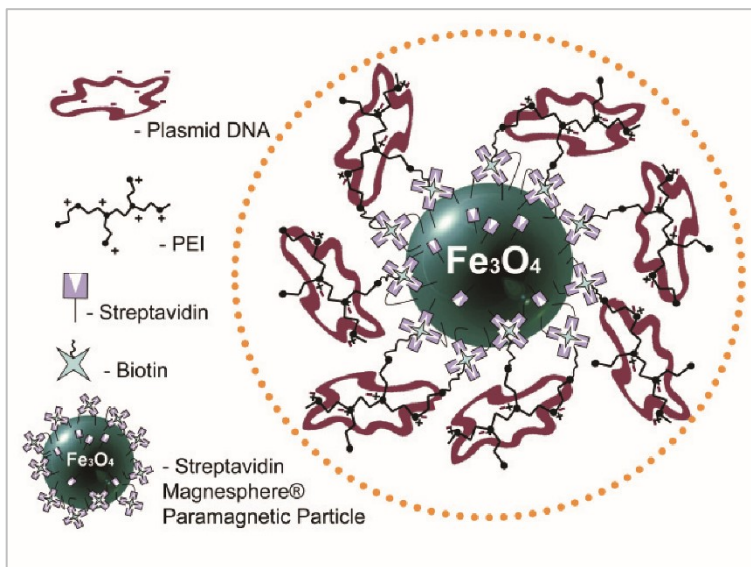


Figure 1.4: Schematic structure of pDNA/PEI/MNP transfection complex. The system includes a paramagnetic streptavidin – coated iron oxide nanoparticle in the core and pDNA/PEI complexes (polyplexes), attached via streptavidin – biotin interactions to the surface.

nonviral gene delivery to three different cell lines (COS-7, HEK 293 and NIH 3T3) and primary endothelial cells (HUVEC) in the presence of an external magnetic field. Moreover, the pilot *in vivo* study in mice showed that after a systemic injection in the tail vein magnetic polyplexes were able to induce a localized thoracic expression of both, reporter and therapeutic genes under guidance of a magnetic field [144].

The study of Chertok et al. in 2010 has demonstrated the potential of PEI – modified iron oxide MNP to be magnetically guided to brain tumors after intra-carotid injection in rats. However, no drug/gene delivery experiments were performed in order to evaluate the efficiency of the investigated carrier [145].

In 2012, streptavidin – coated MNP were used for viral gene delivery by Zhang et al. Their work demonstrated the feasibility of magnetically guided therapeutic delivery of vascular endothelial growth factor (VEGF) gene to the infarcted heart of rats by means of a viral approach. That study focused on a MNP-based adenoviral vector and addressed certain safety concerns due to observed immunogenicity [146].

To date none of the MNP-based gene delivery systems has been applied in the clinic and researchers are still attempting to improve this approach. Therefore, the work presented in this thesis was performed to address the mechanisms of MNP-based gene delivery and its perspectives in terms of clinical applications.

1.6 Aim of the study

Despite the progress in the gene therapy field, this approach remains experimental. Although it showed promising outcomes in treatment of inherited disorders and several cancer conditions, the safety and efficacy of the methods are under strong consideration. Viral vectors were broadly used and investigated as gene delivery carriers due to the high transduction efficiency. However, the risks related to that therapy have only allowed its applications for the treatment of conditions, which have no other cures. Therefore, a wide range of nonviral methods for gene delivery has gained an attention of the researchers. Nevertheless, only few of them have reached the clinical trials (i.e. naked DNA and cationic lipids).

In the last decades, many groups have reported various gene carriers, based on magnetic nanoparticles and/or cationic polymers. Some of them were commercialized and demonstrated good performance in laboratory use. The advantages of those systems include high affinity to nucleic acids, high efficiency, good safety, selectivity and potential for targeted delivery due to magnetic compounds.

The work presented here was dedicated to a gene delivery system, where pDNA was condensed by cationic polymer (PEI) and afterwards covalently bound to iron oxide magnetic nanoparticles. For the first time, this carrier was reported by Li et al. in 2008. Afterwards, the quality of the complexes was improved and transfection protocol was re-optimized in COS-7 cells. These data were published by our group in 2014. The current study was intended to further investigate this nonviral magnetic transfection system and discuss its potential for clinical applications.

The particular aims were set as follows:

1. To test the performance of the transfection system in clinically relevant cells (i.e. human mesenchymal stem cells (hMSC));
2. To study the mechanism of transfection with pDNA/PEI/MNP complexes with focus on intracellular localization and process of pDNA release;
3. To perform pilot tests of magnetic polyplexes, including LMW PEI, aiming to improve the safety of this transfection system;
4. To evaluate the potential of the transfection system for clinical applications, referring to the current progress of gene delivery methods and discuss the future perspectives of MNP-based transfection.

2 Materials and Methods

2.1 Materials

2.1.1 Cell culture media and supplements

Dulbecco's Modified Eagle Medium (DMEM) with 4.5 g/l glucose, 3.7 g/l sodium hydrogen carbonate and L-glutamine, phosphate-buffered saline (PBS) and Roswell Park Memorial Institute (RPMI) 1640 were purchased from PAN Biotech GmbH (Aidenbach, Germany). Mesenchymal Stem Cell Growth Medium (MSCGM) and were purchased from Lonza (Walkersville, MD, USA). Recovery™ Cell Culture Freezing medium (CCFM) was obtained from Gibco (Carlsbad, CA, USA). Minimum Essential Medium alpha (αMEM) was obtained from Life Technologies. Trypsin, Ethylenediaminetetraacetic acid (EDTA), penicillin and streptomycin were procured from PAA (Coelbe, Germany). Fetal bovine serum (FBS) was obtained from HyClone (Logan, UT, USA). Bovine serum albumin (BSA) was obtained from Sigma-Aldrich (St. Louis, MO, USA).

2.1.2 Labelling and staining reagents

Label IT® Tracker™ Intracellular Nucleic Acid Localization Kit was purchased from Mirus (Madison, WI, USA). FluoReporter® Oregon Green® 488 Protein Labeling Kit was obtained from Molecular Probes (Eugene, OR, USA). Atto 565 dye was provided by ATTO-TEC GmbH (Siegen, Germany). 4',6-diamidino-2-phenylindole (DAPI) was purchased from Invitrogen (Carlsbad, CA, USA). FluorSave™ Reagent was obtained from Merck Millipore (Darmstadt, Germany). Alexa Fluor 488 donkey anti-goat Immunoglobulin G (IgG) and Alexa Fluor 488 donkey anti-mouse IgG secondary antibodies and Near-IR LIVE/DEAD® Fixable Dead Cell Stain Kit were purchased from Molecular Probes by Life Technologies (Eugene, OR, USA).

2.1.3 Conjugated antibodies

CD29-APC, CD44-PerCP-Cy5.5, CD45-V500, CD73-PE, CD117-PE-Cy7 antihuman conjugated antibodies were obtained from BD Bioscience (Heidelberg, Germany). CD105-AlexaFluor 488 antihuman conjugated antibodies were obtained from AbD Serotec (Kidlington, UK).

2.1.4 Chemicals and different assays

Branched PEI (MW = 25 kDa), LMW PEI (MW = 600 Da), 3-(4,5-Dimethylthiazol-2-yl)-2,5-diphenyltetrazolium bromide (MTT) and paraformaldehyde (PFA) were obtained from Sigma-Aldrich (St. Louis, MO, USA). Sulfo-NHS-LC-Biotin linker and BCA Protein Assay Kit were obtained from Pierce (Rockford, IL, USA). Streptavidin MagneSphere® Paramagnetic Particles, Reporter Lysis Buffer and Bright Glo Luciferase Reporter Assay were purchased from Promega (Madison, WI, USA). Human Mesenchymal Stem Cell Functional Identification Kit was purchased from R&D Systems (Minneapolis, MN, USA). Plasmid DNA Purification Kit was obtained from Macherey-Nagel (Düren, Germany).

2.1.5 Other reagents

6x DNA Loading Dye and GeneRuler™ 1 kb DNA Ladder were purchased from Thermo Fisher Scientific Baltics UAB (Vilnius, Lithuania). Agarose was obtained from Biozym Scientific GmbH, Hessisch Oldendorf, Germany. Boric acid, NaCl, dimethyl sulfoxide (DMSO) and trisaminomethane (Tris) were obtained from Carl Roth (Karlsruhe, Germany).

2.2 Cell culture

2.2.1 COS-7 culture

African green monkey kidney fibroblast-like cell line (COS-7) was purchased from American Type Culture Collection (Manassas, VA, USA). The complete growth medium for COS-7 cell culture included a base medium (DMEM with 4.5 g/l glucose, 3.7 g/l sodium hydrogen carbonate and L-glutamine), which was supplemented with 10% FBS, 100 U/ml penicillin and 100 µg/ml streptomycin. Cells were seeded in 75 cm² flasks and maintained at 37°C in a humidified 5% CO₂ incubator. The culture medium was renewed 2-3 times per week. At a confluency of 80 - 90% cells were subcultured. For that, old medium was removed, cell layer was rinsed with PBS and Trypsin/EDTA solution (0.25% (w/v) trypsin and 0.53 mM EDTA) was added. After incubation at 37°C for 3-4 min, a cell culture medium was added to stop the reaction. Cell suspension was aspirated and transferred to a 50 ml tube for further centrifugation (300g, 10 min). Afterwards, the supernatant was discarded, the cell pellet was resuspended in fresh cell culture medium and seeded in the new flasks. The subculturing of COS-7 cells was performed at a ratio of 1:4 or 1:8.

2.2.2 hMSC isolation and culture

hMSC were derived from human bone marrow following the procedure, previously described by Gäbel et al. [147]. Sternal aspirates for this study were obtained from patients during coronary artery bypass grafting at the Department of Cardiac Surgery (University of Rostock). All bone marrow donors gave the informed written consent to use their samples for experimental purposes. Mononuclear cells (MNC) were isolated by density gradient centrifugation (445 g, 35 min) of bone marrow aspirates in Leucosep® tubes (Greiner Bio-One GmbH, Solingen, Germany) with 15 ml of RPMI medium. Afterwards the interphase of MNC was collected and seeded in 175 cm² flasks for further selection by plastic adherence in MSCGM, supplemented with 100 U/ml penicillin and 100 µg/ml streptomycin. The culture was maintained at 37°C in a humidified 5% CO₂ incubator. The medium was renewed every 2-3 days. After cell colonies reached 70-80% confluency, hMSC were subsequently passaged or kept frozen in liquid nitrogen for long-term storage. The subculturing was performed at a ratio of 1:2 as described above for COS-7 cells. For freezing, a Recovery™ CCFM and Nunc® CryoTubes® (Sigma-Aldrich, St. Louis, MO, USA) were used. hMSCs of passage 3 were used in all experiments.

2.3 Plasmids

pEGFP-N3 plasmid, encoding EGFP under control of the cytomegalovirus (CMV) - promoter was obtained from Clontech (Palo Alto, CA, USA). pcDNA3.1-Luc plasmid encoding firefly luciferase under CMV - promoter in pcDNA 3.1 vector (Invitrogen, Carlsbad, CA, USA) was a kind gift of Dr. Wenzhong Li (University of Rostock, Germany).

For amplification, the plasmids were transformed in *Escherichia coli* DH5α-strain (Invitrogen, Carlsbad, CA, USA). Isolation and purification of both plasmids were performed using Plasmid DNA Purification Kit according to the manufacturer's protocol. The concentration and purity of obtained pDNA were checked by measuring their absorbance at 260 and 280 nm. Plasmids with 260/280 absorbance ratio of ~1.8 were considered as suitable for further experiments. Plasmids were stored in 5mM Tris/HCl (pH 8.5) buffer in aliquots at -20°C.

2.4 Biotinylation of PEI

Both, PEI (MW = 25 kDa) and PEI600 (MW=600 Da) were biotinylated using a Sulfo-NHS-LC-Biotin linker (Fig. 2.1) and kindly provided by Dr. Wenzhong Li (University of Rostock, Germany). Both types of biotinylated PEI were stored at amine concentrations of 7.5 mM at 4°C.

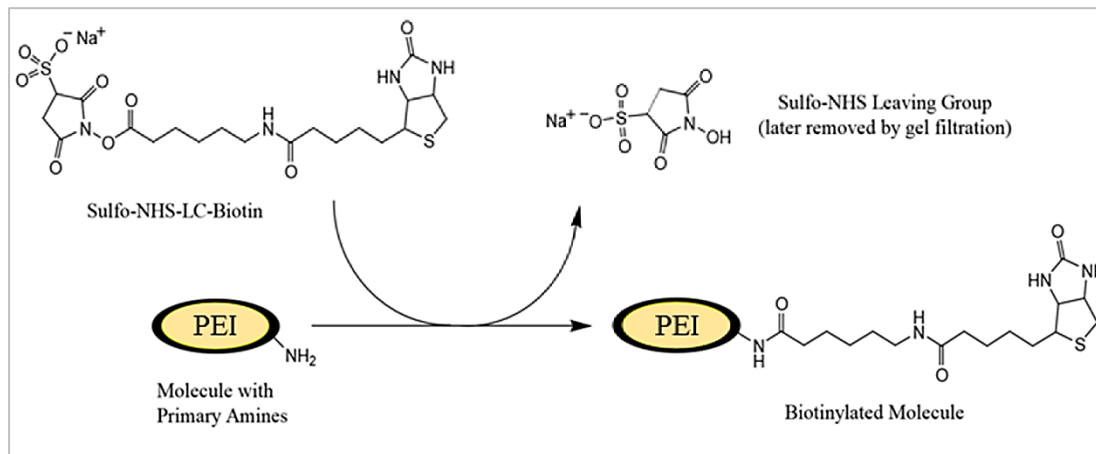


Figure 2.1: The principle of biotinylation of PEI using Sulfo-NHS-LC-Biotin linker. (Adapted from Thermo Fischer Scientific Inc., EZ-Link™ Sulfo-NHS-LC-Biotinylation Kit, Instructions, 2012)

2.5 Filtration of MNP

At first, Streptavidin MagneSphere® Paramagnetic Particles were sonicated for 15 min at room temperature (RT). In order to exclude aggregates and particles bigger than 450 nm, they were additionally filtered through a Millex-HV filter with a 0.45 μm pore size hydrophilic polyvinylidene difluoride (PVDF) membrane (Millipore, Tullagreen, Ireland) using a syringe. After filtration the iron concentration was measured as described below in section 2.5.1. The obtained suspension of MNP was stored in MNP buffer (PBS buffer containing 1mg/ml BSA), in aliquots at 4°C.

2.5.1 Determination of iron concentration in filtered MNP

For the determination of iron concentration, ultraviolet-visible (UV-VIS) spectrophotometry was used. The method was adopted from Rad et al., who reported that the described technique is sensitive and reproducible for determination of dissolved iron at a minimum concentration of 3 $\mu\text{g/ml}$. At first, the peak absorbance values for iron standard

(5 µg/ml in water), blank solution (20 µl MNP Buffer in 980 µl water) and MNP sample (20 µl MNP in 980 µl water) were obtained (Fig.2.2a).

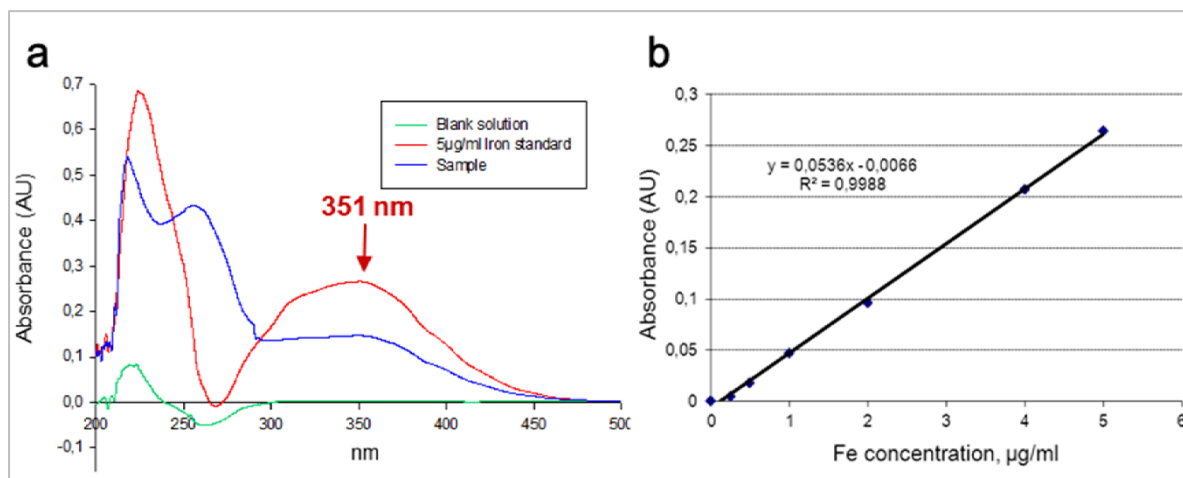
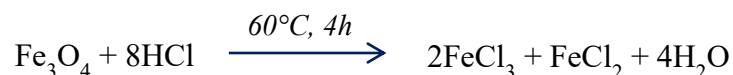


Figure 2.2: Determination of iron concentration. Absorbance curves of blank solution (green), iron standard (red) and MNP sample (blue) (a); calibration curve for determination of iron concentration (b).

Therefore, the samples in open glass tubes were incubated at 110°C overnight in order to evaporate the liquid. Afterwards, 1 ml of hydrochloric acid (5 M) was added, tubes were capped and samples were further incubated at 60°C for 4 h. Following this incubation, the temperature of the samples was normalized to RT, samples were transferred to the 1.5 ml cuvettes and the absorbance profile of 200 – 500 nm wavelengths was obtained using a spectrophotometer. The peak absorbance value for the iron standard was 351 nm. The colored products are most likely to be obtained from the chemical reaction provided below:



In the next step, the absorbance values of different iron standard dilutions (from 0 to 5 µg/ml) at a wavelength of 351 nm were measured against blank solution in order to generate a calibration curve (Fig. 2.2b). The method showed a significant correlation between iron concentration and absorbance ($R^2 > 0.99$) and was further applied for the determination of the iron content in MNP samples.

2.6 Preparation of transfection complexes

2.6.1 pDNA/PEI and pDNA/PEI/MNP ($MW_{(PEI)} = 25 \text{ kDa}$)

For preparation of both, pDNA/PEI and pDNA/PEI/MNP transfection complexes, pDNA and PEI solutions were first mixed at different molar ratios of PEI nitrogen to pDNA phosphate (NP ratios). pDNA and PEI were diluted in equal volumes of glucose solution in water (5%), well mixed and incubated for 30 min at RT. Plasmid DNA solution was always diluted to a concentration of 50 ng/ μl . The required volumes of PEI solutions were calculated depending on NP ratio and required amount of pDNA, using the following equation:

$$NP = \frac{C(PEI) * V(PEI)}{3 * m(pDNA)}$$

where:

NP – NP ratio (refers to the number of nitrogen of PEI per pDNA phosphate);

$C(PEI)$ – concentration of amine nitrogen in PEI, mM;

$V(PEI)$ – volume of PEI to be used, μl ;

3 nmol of phosphate in 1 μg of pDNA;

$m(pDNA)$ – mass of pDNA to be used, μg .

For preparation of pDNA/PEI/MNP complexes with final iron concentration from 0.5 to 6 $\mu\text{g}/\text{ml}$, the appropriate amount of filtered MNP was added to pDNA/PEI complexes and incubated for 30 min at RT. pDNA/PEI and pDNA/PEI/MNP complexes were freshly prepared every time prior to transfection experiments.

2.6.2 pDNA/PEI600 and pDNA/PEI600/MNP ($MW_{(PEI)} = 600 \text{ Da}$)

Preparation of pDNA/PEI600 complexes was performed in a similar manner, as described above for pDNA/PEI. Plasmid DNA solution was always diluted to a concentration of 30 ng/ μl for proper formation of pDNA/PEI600 complex.

For the preparation of pDNA/PEI600/MNP transfection complexes, the required amount of MNP (from 2 to 16 μl) was added to pDNA/PEI600 mixture, well mixed and further incubated for 30 min at RT. In the part of work, referring to PEI600, Streptavidin MagneSphere® Paramagnetic Particles with an average effective hydrodynamic diameter of 200 nm and iron content of 1 $\mu\text{g}/\mu\text{l}$ (as to the information, provided by the supplier) were used without filtration.

2.7 Gel electrophoresis

For gel electrophoresis, pDNA/PEI complexes (with pEGFP-N3 plasmid) at different NP ratios were prepared in the same way, as for transfection experiments (see Section 2.6). 10 μ l of each sample were mixed with 2 μ l of 6x Loading Dye and further loaded on 1% agarose gel, containing 6 μ l of Ethidium Bromide, in TBE Buffer (Tris-borate-EDTA, pH=8.0) for 30 min at 120 v. GeneRuler™ 1 kb DNA Ladder was used as a reference. Afterwards the gel was analyzed using a ChemiDoc XRS System (BioRad Laboratories GmbH, Munich, Germany).

2.8 Particle size and Zeta potential measurement

The mean hydrodynamic diameter of both, filtered MNP and transfection complexes, was determined using Dynamic Light Scattering (DLS) technique with a Brookhaven 90Plus Nanoparticle Size Analyzer (Brookhaven Instruments, New York, NY). Surface charge was evaluated using Zeta Potential, which was measured by ZetaPALS Analyzer (Brookhaven Instruments) utilizing a Phase Analysis Light Scattering (PALS) method. For all measurements, transfection complexes were prepared in the same way, as described above (see Section 2.6).

2.9 Transfection experiments

2.9.1 Transfection with pDNA/PEI600 or pDNA/PEI600/MNP complexes

($MW_{(PEI)}=600$ Da)

For transfection experiments with PEI600, COS-7 cells (20 000 cells per well) were seeded in 48-well plates shortly before transfection. Afterwards, freshly prepared pDNA/PEI600 or pDNA/PEI600/MNP complexes (see Section 2.6.2) were added to the cells and gently mixed. The cell culture medium was replaced with the fresh one 48 h after transfection. Luciferase Reporter Gene Assays were performed after 72 h as described below (see Section 00).

2.9.2 Transfection with pDNA/PEI or pDNA/PEI/MNP complexes ($MW_{(PEI)} = 25$ kDa)

For transfection experiments with pDNA/PEI or pDNA/PEI/MNP complexes hMSC were seeded in different multiwell plates depending on the assay 24 h before transfection (Table 2.1).

Table 2.1: Cell seeding numbers for Luciferase Reporter Gene Assay, EGFP expression assay and laser scanning microscopy.

Assay	Plate format	Cell number/well
Luciferase reporter gene assay	96-well plate	5 000
EGFP expression assay	12-well plate	30 000
Laser scanning microscopy	24-well plate	15 000 (on coverslips)

At the day of transfection pDNA/PEI and pDNA/PEI/MNP complexes were prepared as described above (see Section 2.6.1) and added to the cells dropwise. Four hours after transfection hMSC were washed with PBS, medium was replaced with the fresh one, and cells were further incubated until the desired time point.

2.10 Luciferase reporter gene assay

For luciferase reporter gene assays, cells were transfected with pcDNA3.1-Luc plasmid, encoding firefly luciferase gene following the described protocol. For analysis cells were washed and lysed with Reporter Lysis Buffer at -80°C for 30 min. 10 μl of obtained cell lysate were mixed with Bright Glo Luciferase substrate (100 μl) and luminescence was immediately measured using Infinite 200 microplate reader (Tecan Trading AG, Maennedorf, Switzerland). Relative light units (RLU) were normalized against protein concentration determined by bicinchoninic acid (BCA) protein assay, which was performed in parallel.

2.11 BCA protein assay

For the determination of protein concentration BCA Protein Assay Kit was used. Briefly, 25 μl of cell lysate were mixed with 200 μl of BCA Working solution according to the manufacturer's protocol and incubated at 37°C for 30 min. Afterwards, the absorbance of the samples was measured at 550 nm wavelength by Bio-Rad Model 680 microplate reader (Bio Rad Laboratories GmbH, Munich, Germany). The protein concentration was finally calculated using a standard curve, which was prepared according the manufacturer's protocol.

2.12 EGFP expression assay

For EGFP expression assays, cells were transfected with pEGFP-N3 plasmid as described above (see Sections 2.6 and 2.9). EGFP expression was at first observed under a fluorescent microscope Axiovert 40 CFL (Carl Zeiss, Goettingen, Germany). The images were acquired with ZEN 2010 Blue Software (Carl Zeiss, Jena, Germany). Afterwards cells were trypsinized,

washed with PBS and stained with DAPI for exclusion of dead cells. Subsequent quantitative analysis of transfection efficiency was performed using BD™ FACS LSR II flow cytometer (BD Biosciences, San Jose, CA). The data were acquired and analyzed using BD FACSDiva™ software (BD Biosciences).

2.13 Determination of cell viability

The viability of the cells was determined by measuring their metabolic activity using MTT reagent. For that cells were seeded in 96-well plate with 150 µl medium per well and transfected according to the described protocol (see Section 2.9). After 24 hours of incubation 15 µl of MTT solution (5 mg/ml in PBS) was added to the cells and further incubated for 4 hours at 37°C, 5% CO₂. After spent medium was removed, purple formazan crystals were dissolved in 100 µl DMSO. Optical density (OD) of the obtained solution was determined by Bio-Rad Model 680 microplate reader (Bio Rad Laboratories GmbH, Munich, Germany) at 550 nm wavelength with reference to 655 nm. Cell viability was calculated and normalized to control using the following formula:

$$\text{Cell viability} = \frac{(OD_{550} - OD_{655})_{\text{sample}}}{(OD_{550} - OD_{655})_{\text{control}}} * 100\%$$

where:

OD₅₅₀ – optical density at 550 nm wavelength;

OD₆₅₅ – optical density at 655 nm wavelength.

Cells treated with 5% glucose solution only (volume equal to transfection complexes) were used as control.

2.14 Characterization of hMSC with and without transfection

2.14.1 Immunophenotyping of hMSC

Immunophenotyping of hMSC was performed 24 h after transfection with pcDNA3.1-Luc plasmid, performed by pDNA/PEI or pDNA/PEI/MNP complexes in 12-well plates as described above (see Section 2.9). For that cells were trypsinized and thoroughly washed with PBS. Afterwards tubes with cells were kept on ice and surface antigens of hMSC were labelled with the following anti-human conjugated antibodies: CD29-APC, CD44-PerCP-Cy5.5, CD45-V500, CD73-PE, CD117-PE-Cy7 and CD105-AlexaFluor 488. For that hMSCs were resuspended in MACS® buffer (EDTA (2mM)/BSA (0.5%) in PBS), counted and divided for

following labelling. The required volume of antibodies was added and cells were incubated at 4°C for 10 min. In the next step cells were gently washed with PBS and transferred to BD Falcon® 5 ml round-bottom tubes (BD Biosciences, San Jose, CA) for the following measurement. In order to determine unspecific binding and autofluorescence levels, mouse isotype antibodies were used as negative controls. Unstained cells served for the determination of cell population. Near-IR LIVE/DEAD® Fixable Dead Cell Stain Kit was used for the exclusion of dead cells in each sample according to the manufacturer's protocol. Data were acquired using BD™ FACS LSR II flow cytometer and analyzed with BD FACSDiva™ software (BD Biosciences, San Jose, CA).

2.14.2 Functional differentiation assay for hMSC

Functional differentiation assay was performed using Human Mesenchymal Stem Cell Functional Identification Kit after transfection of hMSC with pDNA/PEI or pDNA/PEI/MNP complexes. For that cells were transfected with pcDNA3.1-Luc plasmid in 24-well plates on glass coverslips as described in Section 2.9.2 of the current chapter. Cells, which did not undergo transfection were used as a control. 24 h after transfection culture medium was replaced with α MEM Basal Medium, containing Adipogenic or Osteogenic Supplement in order to induce adipogenesis or osteogenesis, respectively. All required media supplements were included in the kit. The assay was performed following manufacturer's protocol for 21 days. Afterwards the specific markers for adipocytes and osteocytes (fatty acid binding protein-4 (FABP-4) and osteocalcin respectively) were stained with Goat Anti-Mouse FABP4 and Goat Anti-Human Osteocalcin Antigen-affinity Purified Polyclonal Antibodies available from the kit. In order to perform further visualization of the cells, following fluorophore-conjugated secondary antibodies were used: Alexa Fluor 488 donkey anti-goat IgG and Alexa Fluor 488 donkey anti-mouse IgG for FABP4 and osteocalcin staining, respectively. Cell nuclei were counterstained with DAPI and coverslips were mounted cell side down onto a drop of FluorSave™ Reagent on microscopic slides. Differentiation capacity was confirmed by confocal laser scanning microscopy (CLSM) using ELYRA PS.1 LSM 780 (Carl Zeiss, Jena, Germany) system and ZEN 2010D software (Carl Zeiss, Goettingen, Germany).

2.15 Fluorescent labelling of transfection complexes

The compounds of transfection complexes (pDNA, PEI and MNP) were separately labelled with different fluorophores as described below. The fluorescent dyes were carefully selected

according to their excitation and emission spectra in order to provide a maximum of intensity for each channel and avoid the overlap of detected signals (Fig. 2.3).

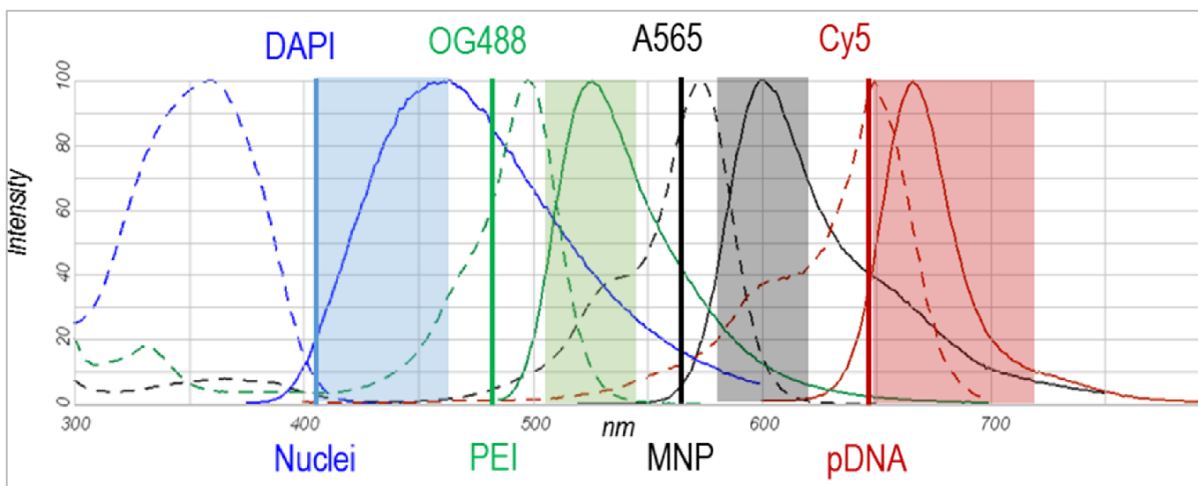


Figure 2.3: Set up for fluorescent labelling of transfection complexes. Labelled components (below) and corresponding dyes (up) with their excitation (dash lines) and emission spectra (bold lines). The colored areas roughly represent parts of spectra detected during the image acquisition.

pDNA (pcDNA3.1-Luc) was labelled with CyTM 5 dye using Label IT[®] TrackerTM Intracellular Nucleic Acid Localization Kit according to the manufacturer's protocol. Labelled pDNA was purified via ethanol precipitation in order to remove the unbound dye. The degree of labelling (DOL) was determined immediately after labelling according to the manufacturer's protocol and was 5.35 pmol of dye per 1 μ g of pDNA. Final pDNA-Cy5 solution was divided in aliquots and stored at -20°C, protected from light.

For labelling of PEI with Oregon Green 488 (OG488) dye, the FluoReporter[®] Oregon Green[®] 488 Protein Labeling Kit was used. The whole procedure was performed according to the manufacturer's protocol. At first, PEI solution was mixed with 1 M sodium bicarbonate solution. Afterwards, the reactive dye stock solution (10 mg/ml in DMSO) was added, and sample was continually mixed for 1 h (RT, protected from light). Purification of PEI-OG488 solution was performed via centrifugation on a spin column available from the kit (1100 g, 5 min). DOL was determined according to the manufacturer's protocol, and was 0.037 moles of dye per 1 mol of PEI. PEI-OG488 solution was stored at 4°C in the dark.

MNP were labelled with biotin-conjugated Atto 565 dye (A565) during the pDNA/PEI/MNP complex formation. For that, the required volume of A565 dye stock solution (200 ng/ μ l in DMSO) was directly added to pDNA/PEI complexes shortly after adding of MNP

(w/w ratio of A565 to MNP was 1 to 1000). Next, complexes were incubated for 30 min at RT according to the protocol of pDNA/PEI/MNP complex formation, described above.

Effective diameter and surface charge of labelled transfection complexes were determined as described above (see section 2.8).

2.16 Microscopy

Super-resolution structured illumination microscopy, confocal microscopy and colocalization studies were performed using the LSM 780 ELYRA PS.1 system.

The samples were prepared as follows: hMSC were seeded in 24-well plates on glass coverslips (0.13 – 0.16 mm thickness) and transfected with labelled transfection complexes as described in section 2.9. For all microscopic observations transfection was performed according to the optimized protocol conditions, that were NP ratio of 2.5, 3 $\mu\text{g}/\text{cm}^2$ pDNA (6 μg pDNA per well) and 1 $\mu\text{g}/\text{ml}$ of iron concentration within the pDNA/PEI/MNP complexes. At a required time point after transfection (2, 6, 12, 18, 24 or 48 hours) samples were thoroughly washed with 1M NaCl in order to remove transfection complexes which did not enter the cell and stayed at the cell surface. Next, cells were additionally washed with PBS and fixed with PFA (4% solution in PBS) for 20 min at RT. Cell nuclei were stained with 250 nM DAPI solution. After final triple washing with PBS, coverslips were carefully mounted (avoiding additional pressure) with antifade reagent (FluorSave™ Reagent) on a microscopic slide.

2.16.1 Superresolution structured illumination microscopy (SR-SIM)

In order to visualize the labelled transfection complexes without a cell environment, pDNA-Cy5/PEI-OG488/MNP-A565 complexes were prepared as described above (see section 2.15). Afterwards, a drop of freshly prepared complexes was added to the microscopic slide, dried out in the dark and covered with coverslip using a FluorSave™ Reagent. The samples were further observed using a 63x Plan Apochromat® objective (numerical aperture (NA) = 1.4) with Immersol™ 518F immersion oil (Carl Zeiss, Oberkochen, Germany). For SR-SIM a special set of lasers and electron multiplying charge coupled device (EM-CCD) camera in a SIM mode of ZEN 2010D software were used. OG488, A565 and Cy5 were subsequently excited with 488 nm, 561 nm and 642 nm SIM - laser lines respectively. The number of SIM – grating rotations used for each image acquisition was maximum possible and reached 5. The

essential image processing was performed using a structured illumination module of the ZEN 2010D software.

2.16.2 Confocal laser scanning microscopy (CLSM)

In this work, CLSM was employed for the following experiments: functional differentiation of hMSC, localization of transfection complexes, photobleaching experiments and colocalization studies.

Table 2.2 contains the characteristics of fluorochromes, used in this work. It also includes description of laser lines, utilized for the excitation, and main beam splitters, which separated the emissions from the excitation light. Emission was recorded using photomultiplier detectors after careful adjustment of emission bands, avoiding spectral overlap. All images of multiple stainings were acquired in a channel mode. Thus the imaging parameters (gain and offset, the pinhole size, the filters and dichroics, the laser source) were defined for every track that served for the detection of one specific signal. The tracks were scanned sequentially.

Table 2.2: List of fluorochromes and laser lines (incl. main beam splitters (MBS) used for their excitation.

Fluorochrom	$E_{X_{max}}$, nm	$E_{m_{max}}$, nm	Laser line	MBS
DAPI	358	461	Diode 405 nm	405
Oregon Green 488	501	526	Argon 458/488/514 nm	488/561/633
Alexa Fluor 488	490	525	Argon 458/488/514 nm	488/561
Atto 565	563	592	He/Ne 561 nm	488/561/633
Cyan-5	649	666	He/Ne 633 nm	488/561/633

To determine nuclear localisation of the transfection complexes, z-series images were acquired with 0.3 μm interval.

In all experiments aiming to visualize transfection complexes, a 63x Plan Apochromat[®] oil immersion objective was used. In experiments of functional differentiation of hMSCs, a 40x Plan Neofluar (NA = 1.3) oil immersion and 20x Plan Apochromat[®] (NA = 0.8) dry objectives were used.

Photobleaching experiments were performed using the bleaching tool of ZEN 2010D software at three selected regions of interest. Cy5, A565 and OG488 were bleached in independent experiments for 3 min with 633 nm, 561nm and 488 nm laser lines respectively, at high laser power.

2.16.3 Colocalization studies

Prior to colocalization studies, in order to correct chromatic aberrations a channel alignment procedure was performed. For that, a MultiSpeck™ Multispectral Fluorescence Microscopy Standard (Invitrogen, Carlsbad, CA) was used. For colocalization studies the imaging parameters (gain, offset and laser power) were first adjusted using negative controls in order to subtract autofluorescence of the cells. After adjustment the settings were kept constant throughout all further experiments. Cells, transfected with unlabelled transfection complexes and further subjected to the same staining procedures as analysed samples were used as a negative control. In each sample 20 healthy looking hMSC were randomly selected and analysed for colocalization of Cy5 and OG488, Cy5 and A565, OG488 and A565 signals. For every analysed cell simultaneously with multichannel acquisition a transmission illumination image was obtained (using the laser light of one channel and transmission photomultiplier) in order to define the cell border, the background area and to adjust the threshold for every channel. Scatter diagrams of colocalization of pDNA-Cy5/PEI-OG488, pDNA-Cy5/MNP-A565 and PEI-OG488/MNP-A565 signals were obtained at 2, 6, 12, 18 and 24 h after transfection. Manders' colocalization coefficients (C_{coef}) were calculated using colocalization module of ZEN 2010D software. These coefficients represent relative fluorescence of colocalized pixels as compared to the total fluorescence detected in one channel above threshold. Their values are independent of fluorescence intensity and demonstrate contribution of one channel to the colocalized pixels [148]. In this study the C_{coef} were calculated according to the formulas below.

To determine how many pDNA-Cy5 pixels were colocalized with PEI-OG488 pixels:

$$C_{coef}(\text{pDNA to PEI}) = \frac{\sum_i(\text{pDNA})\text{pixels, coloc with PEI}}{\sum_i(\text{pDNA})\text{pixels, total}}$$

To determine how many PEI-OG488 pixels were colocalized with MNP-A565 pixels:

$$C_{coef}(\text{PEI to MNP}) = \frac{\sum_i(\text{PEI})\text{pixels, coloc with MNP}}{\sum_i(\text{PEI})\text{pixels, total}}$$

To determine how many pDNA-Cy5 pixels were colocalized with MNP-A565:

$$Ccoef(\text{pDNA to MNP}) = \frac{\sum_i(\text{pDNA})\text{pixels, coloc with MNP}}{\sum_i(\text{pDNA})\text{pixels, total}}$$

2.17 Statistical analysis

Mann-Whitney test was used for analysis of differences in EGFP expression of hMSC from different patients. Statistical analysis in all other experiments was performed using Student's t-test. Particle size values are presented as mean \pm standard deviation (SD). All other values are presented as mean \pm standard error of the mean (SEM). Values with $p \leq 0.05$ were considered to be significantly different.

3 Results

3.1 Transfection in hMSC

3.1.1 Characterization of transfection complexes ($MW_{(PEI)} = 25$ kDa)

In order to confirm the formation of pDNA/PEI complexes at low NP ratios we have analysed them by gel electrophoresis (Fig. 3.1). At NP ratios of 0.25, 0.5 and 0.75 the pDNA band was clearly visible and did not differ from the sample with pDNA alone. At NP ratio of 1 the band was hardly detectable and disappeared completely at NP 1.5, indicating complete retardation of pDNA by pDNA/PEI complexes.

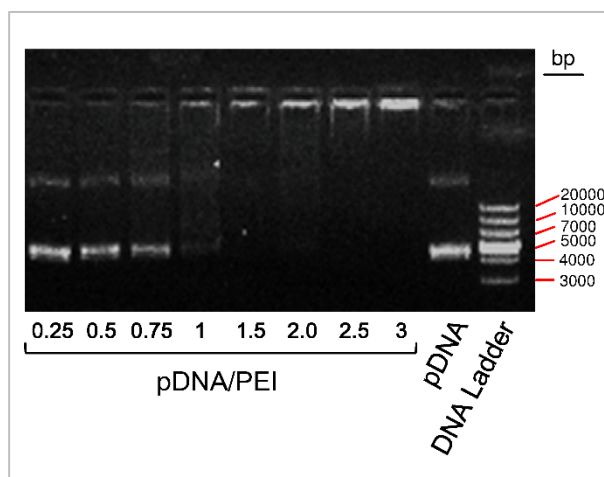


Figure 3.1: Gel electrophoresis of pDNA/PEI transfection complexes at different NP ratios (from 0.25 to 3.0) in comparison to pDNA alone.

According to the results obtained previously for COS-7 cells, the optimal NP ratio for effective transfection was 2.5 [149, 150]. Therefore, transfection complexes at NP ratio of 2.5 were further characterized by effective diameter and surface charge in this work. For that MNP alone, pDNA/PEI and pDNA/PEI/MNP (1 $\mu\text{g}/\text{ml}$ iron) complexes were analyzed by DLS and PALS (Table 3.1). The effective diameter of MNP alone was 168.6 ± 10.25 nm. The surface charge of MNP alone was negative (-29.17 ± 0.98 mV). pDNA/PEI and pDNA/PEI/MNP complexes were positively charged ($+21.6 \pm 2.41$ mV and $+26.8 \pm 1.56$ mV, respectively). Size distributions were 78.39 ± 3.07 nm for pDNA/PEI complexes and from 112.1 ± 6.84 nm for pDNA/PEI/MNP.

Table 3.1 Particle size and surface charge of magnetic nanoparticles alone and transfection complexes (NP ratio 2.5, 1 µg/ml iron) determined by DLS and PALS, respectively. Data represent the mean ± SD (n=10) [149].

	Particle size, nm	Zeta potential, mV
MNP	168.6 ± 10.25	-29.17 ± 0.98
pDNA/PEI	78.39 ± 3.07	+21.6 ± 2.41
pDNA/PEI/MNP	112.1 ± 6.84	+26.8 ± 1.56

3.1.2 Optimization of transfection conditions with pDNA/PEI/MNP complexes

(MW_(PEI) = 25 kDa) in hMSC

For the optimization of transfection conditions in hMSC different pDNA amounts (from 1 to 6 µg/cm²) were tested (Fig. 3.2a). A significant difference in reporter gene expression between pDNA/PEI- and pDNA/PEI/MNP-mediated transfection was first observed at a pDNA concentration of 3 µg/cm². Transfection efficiency with magnetic polyplexes was higher than those of polyplexes. Although transfection rates raised further with the increase of pDNA dosage, cell viability decreased (Fig. 3.2b). Therefore, 3 µg/cm² of pDNA, NP ratio 2.5 and 1 µg/ml of iron content were considered to be the optimal conditions for hMSC transfection with pDNA/PEI/MNP complexes. This composition was used in all further experiments.

3.1.3 pEGFP transfection

Transfection with pEGFP was performed in order to confirm the above obtained data (Figs. 3.2 c, d). The diagram in Figure 3.2c represents results of FACS analyses of pEGFP-transfected cells. Magnetic polyplexes were able to reach up to 22% of transfection efficiency in living cells, whereas 3% of living cells were positive after pDNA/PEI-mediated transfection. Transfection efficiency in cells from different patients varied dramatically, however mean values between the carriers were still different: 1.6% for pDNA/PEI vs. 9.7% for pDNA/PEI/MNP. The representative fluorescence microscopy images of pDNA/PEI and pDNA/PEI/MNP-mediated transfection are shown in Figure 3.2d, confirming the better performance of magnetic polyplexes.

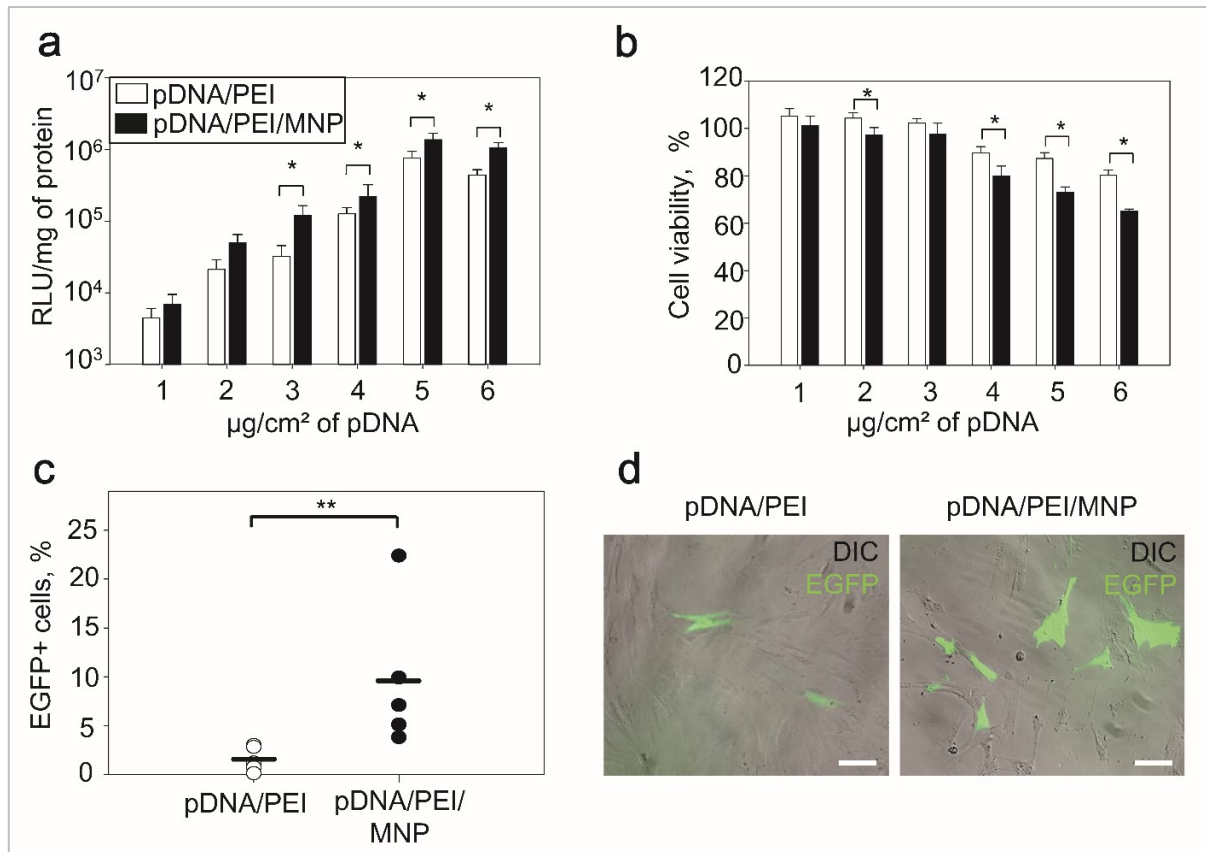


Figure 3.2: Optimization of transfection conditions with pDNA/PEI/MNP complexes in comparison to pDNA/PEI complexes ($MW_{(PEI)} = 25$ kDa) in hMSC. (a,b) Transfection complexes were prepared with varied pDNA amounts (from 1 to 6 $\mu\text{g}/\text{cm}^2$), while other parameters were kept constant (NP ratio 2.5 and 1 $\mu\text{g}/\text{ml}$ of iron). The cells were transfected according to the protocol. 24 h after transfection, a luciferase reporter gene assay and MTT – assay were performed in order to evaluate transfection efficiency (a) and cell viability (b) respectively. Results are representative of 3 independent experiments, each involved 8 replicates ($n=8$). The values are shown as mean \pm SEM. Asterisks represent a significant difference in transfection efficiency ($*p \leq 0.05$) as compared to pDNA/PEI complexes. (c) Transfection efficiency of magnetic polyplexes in comparison to polyplexes (3 $\mu\text{g}/\text{cm}^2$ of pDNA, NP ratio 2.5, 1 $\mu\text{g}/\text{ml}$ of iron) was assessed in hMSC isolated from different patients by flow cytometry 24 h after transfection with pEGFP. The average number of EGFP – expressing cells detected after pDNA/PEI or pDNA/PEI/MNP transfection, relative to the whole cell population was plotted ($n=5$). The bars represent the mean values. Asterisks represent a significant difference, as determined by Mann-Whitney test ($**p \leq 0.01$). (d) Representative fluorescence microscopy images of EGFP expressing hMSC 24 h after transfection with pDNA/PEI or pDNA/PEI/MNP complexes (3 $\mu\text{g}/\text{cm}^2$ of pDNA, NP ratio 2.5, 1 $\mu\text{g}/\text{ml}$ of iron). Scale bars = 10 μm . Adapted from [149].

3.1.4 Characterization of hMSC

Characterization of bone marrow hMSC was initially performed at passage 3 after the isolation procedure. For that, cell morphology, as well as differentiation capacity and surface marker expression were checked. At passage 3 hMSC had a typical spindle shape and maintained their morphology during subsequent passages. Flow cytometry analysis revealed

that cells expressed surface markers, typical for mesenchymal stem cell populations: CD29, CD44, CD73 and CD105, and were negative for hematopoietic surface markers: CD45 and CD117 (Table 3.2).

Table 3.2 Characterization of hMSC. Expression of typical surface markers was evaluated by flow cytometry before and 24 h after transfection with pDNA/PEI or pDNA/PEI/MNP complexes (3 $\mu\text{g}/\text{cm}^2$ of pDNA, NP=2.5, 1 $\mu\text{g}/\text{ml}$ iron). Data represent the mean \pm SD (n=3) [149].

	Surface marker, %					
	CD 29	CD 44	CD 45	CD 73	CD 105	CD 117
No transfection	99.8 \pm 0.1	99.8 \pm 0.1	0.0 \pm 0.0	99.6 \pm 0.1	98.4 \pm 0.5	0.0 \pm 0.0
pDNA/PEI	99.5 \pm 0.2	99.7 \pm 0.1	0.0 \pm 0.0	97.4 \pm 1.9	97.4 \pm 0.4	0.0 \pm 0.0
pDNA/PEI/MNP	98.9 \pm 0.5	99.6 \pm 0.2	0.0 \pm 0.0	99.3 \pm 0.2	96.7 \pm 0.4	0.0 \pm 0.0

Differentiation capacity analysis demonstrated that derived hMSC did differentiate into adipocytes and osteocytes when cultured in adipogenic and osteogenic media, respectively (Fig. 3.3a, d).

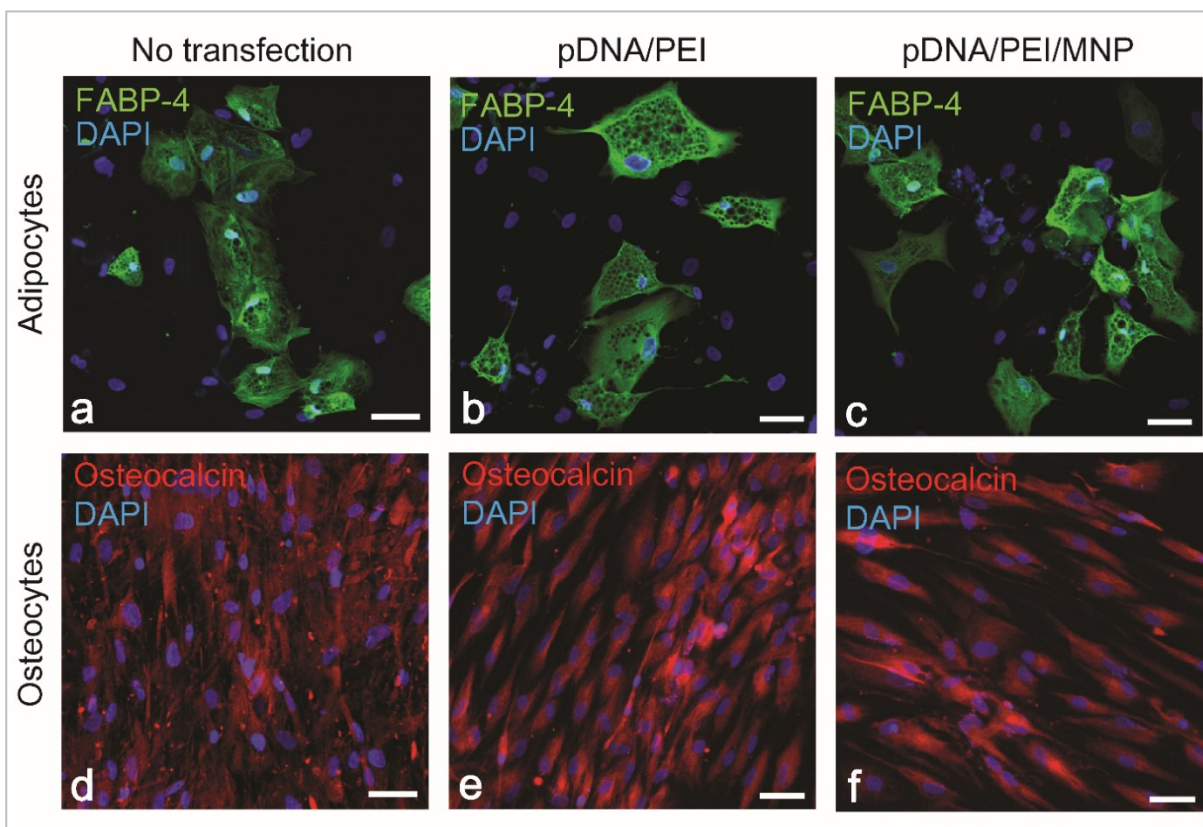


Figure 3.3: Characterization of hMSC. Differentiation capacity towards adipocytes and osteocytes without transfection (a, d) and after transfection with pDNA/PEI (b, e) or pDNA/PEI/MNP (c, f) complexes (3 $\mu\text{g}/\text{cm}^2$ of pDNA, NP ratio 2.5, 1 $\mu\text{g}/\text{ml}$ of iron). The assay was started 24 h after transfection and was analysed after 21 days by immunohistochemistry. Scale bars = 50 μm . Adapted from [149].

Similar characterization of hMSC was performed after their transfection with pDNA/PEI or pDNA/PEI/MNP complexes with the aim to check the well-being of the cells (Fig. 3.3b,c,e,f). Cell morphology did not change compared to untransfected cells. The analysis of immunophenotype after transfection with either polyplexes or magnetic polyplexes did not reveal any significant changes in expression of characteristic hMSC surface markers (Table 3.2). Furthermore transfected hMSC were able to differentiate into adipocytes and osteocytes in the same manner as untransfected cells (Fig. 3.3).

3.1.5 Monitoring of transfection efficiency in hMSC over time

Transfection efficiency in hMSC was monitored at 2, 6, 12, 18, 24 and 48 h time points after transfection with pDNA/PEI or pDNA/PEI/MNP complexes. In these experiments a luciferase reporter gene assay was used. The data are presented in Figure 3.4. The level of reporter gene expression remarkably increased already at the 12 h time point and raised slightly over time for both, polyplexes- and magnetic polyplexes-mediated transfection.

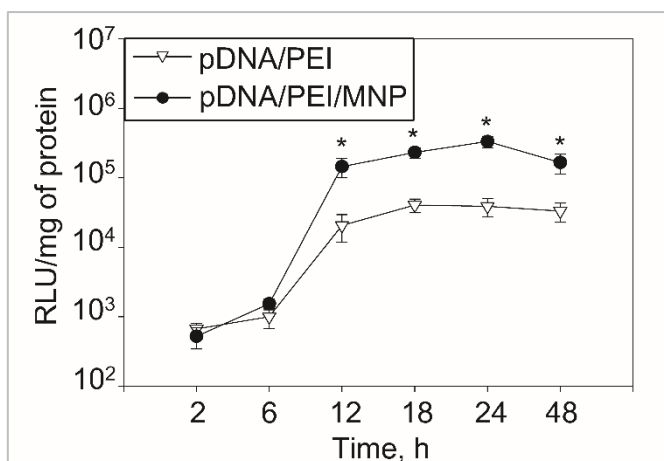


Figure 3.4: Monitoring of transfection efficiency in hMSC over time. Transfection efficiency at different time points (from 2 to 48 h) was evaluated by luciferase reporter gene assay after transfection with pDNA/PEI or pDNA/PEI/MNP complexes (3 $\mu\text{g}/\text{cm}^2$ of pDNA, NP ratio 2.5, 1 $\mu\text{g}/\text{ml}$ of iron). Results are representative of 3 independent experiments, each involved 8 replicates ($n=8$). The values are shown as mean \pm SEM. Asterisks represent a significant difference in transfection efficiency ($*p \leq 0.005$) as compared to pDNA/PEI complexes at each time point. Adapted from [149].

A maximum of transfection efficiency was observed 24 h after transfection in both cases. Reporter gene expression levels in hMSC after pDNA/PEI/MNP-mediated transfection were significantly higher than those after pDNA/PEI – mediated transfection at 12, 18, 24 and 48 h time points after transfection (Fig. 3.4).

3.2 Mechanism of MNP-mediated transfection

3.2.1 Characterization and visualization of fluorescently labelled transfection complexes

Fluorescently labelled transfection complexes were previously optimized and characterized by our group regarding their **transfection efficiency** and **cytotoxicity** in the COS-7 cell line. These data were described elsewhere [149, 150].

In this study luciferase reporter gene assays after transfection with three-color labelled complexes (pDNA-Cy5/PEI-OG488/MNP-A565) or single-labelled complexes were performed in hMSC (Fig. 3.5a). Importantly, no significant differences in transfection efficiency in comparison to unlabelled pDNA/PEI/MNP complexes were observed. Moreover, no influence of fluorescent labelling on cytotoxicity of transfection complexes was detected in all four compositions (Fig 3.5a).

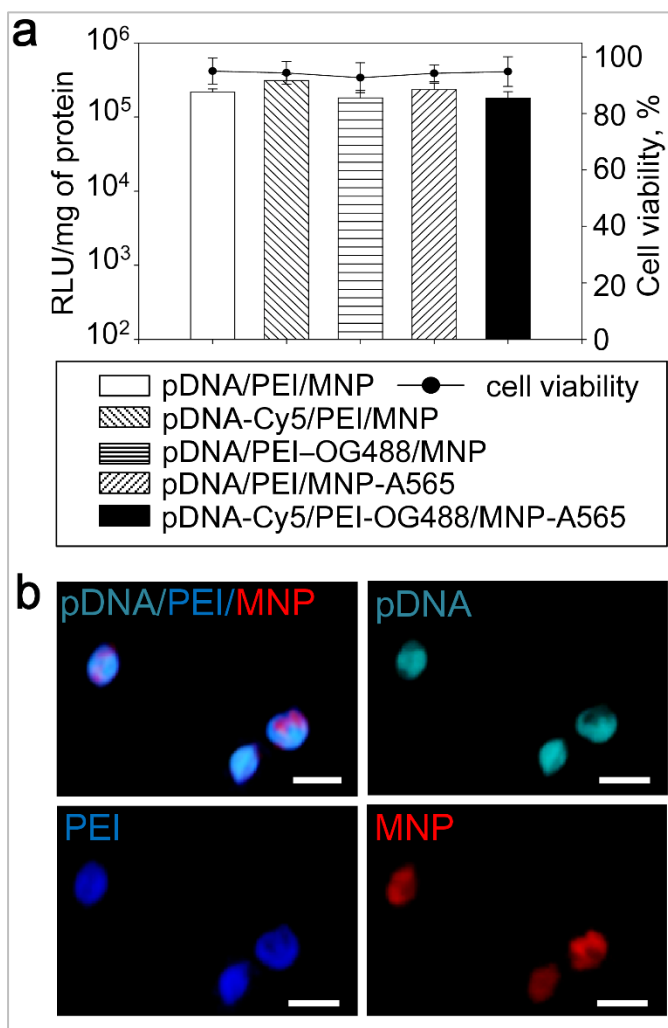


Figure 3.5: Characterization and visualization of fluorescently labelled transfection complexes. (a) Influence of single-labelling or three-color labelling of magnetic polyplexes on transfection efficiency (luciferase reporter gene assay) and cell viability (MTT - assay) was evaluated in hMSC 24 h after transfection (3 $\mu\text{g}/\text{cm}^2$ of pDNA, NP ratio 2.5, 1 $\mu\text{g}/\text{ml}$ of iron). Results are representative of 3 independent experiments, each involved 8 replicates ($n=8$). Data are shown as mean \pm SEM. No significant differences in transfection efficiency and cell viability were detected compared with unlabelled complexes. **(b)** SIM – microscopy images (single channels and merged) of three-color labelled magnetic transfection complexes in the absence of cells. pDNA was labelled with Cy5 dye (cyan), MNP were labelled with A565 dye (red), PEI was labelled with OG488 dye (blue). Scale bars = 0.5 μm . Adapted from [149].

Figure 3.5b shows a SIM-image of labelled pDNA/PEI/MNP complexes in the absence of cells. The complexes had a spherical shape, their size ranged from 300 to 500 nm. Signal intensities in all three channels provided appropriate signal-to-noise ratio. According to the acquisition, pDNA, PEI and MNP were visually colocalized.

Particle size and surface charge of labelled magnetic polyplexes were determined using DLS and PALS techniques. The parameters for single-labelled and three-color labelled complexes were obtained and compared with each other (Table 3.3). Transfection complexes with single labelling of pDNA, as well as complexes with single labelling of MNP did not differ in size and surface charge from unlabelled complexes. Single labelling of PEI led to a slight increase in effective diameter and slight decrease in Zeta potential of magnetic polyplexes, as compared to unlabelled ones. The same effect was observed for three-color labelled transfection complexes. Therefore, an effective diameter of pDNA-Cy5/PEI-OG488/MNP-A565 complexes was between 207.73 and 231.35 nm, the surface charge was $+22.79 \pm 0.76$ mV.

Table 3.3. Particle size and surface charge of single-labelled and three-color labelled magnetic transfection complexes (NP ratio 2.5, 1 μ g/ml iron) determined by DLS and PALS, respectively. Data represent the mean \pm SD (n=10) [149].

	Particle size, nm	Zeta potential, mV
pDNA-Cy5/PEI/MNP	116.27 ± 10.48	$+27.39 \pm 2.48$
pDNA/PEI-OG488/MNP	208.2 ± 19.65	$+17.56 \pm 3.66$
pDNA/PEI/MNP-A565	118.17 ± 5.15	$+29.0 \pm 2.59$
pDNA-Cy5/PEI-OG488/MNP-A565	219.54 ± 11.81	$+22.79 \pm 0.76$

The **photobleaching experiments** were previously performed by our group and are described in detail elsewhere [149, 150]. These results are summarized in Figure 3.6. In the course of bleaching with 633 nm laser, an intensity of Cy5 reduced significantly until the signal was not detectable anymore, whereas intensities of A565 and OG488 signals remained unchanged (Fig. 3.6a, d). Photobleaching with 561 nm laser at high power led to a decrease in fluorescence intensity of A565, while no increase in fluorescence intensities of OG488 and Cy5 occurred (Fig. 3.6b). In a similar manner, photobleaching with 488 nm laser line caused a time-dependent decrease in signal intensity of OG488 and no intensity changes of A565 and Cy5 (Fig. 3.6c).

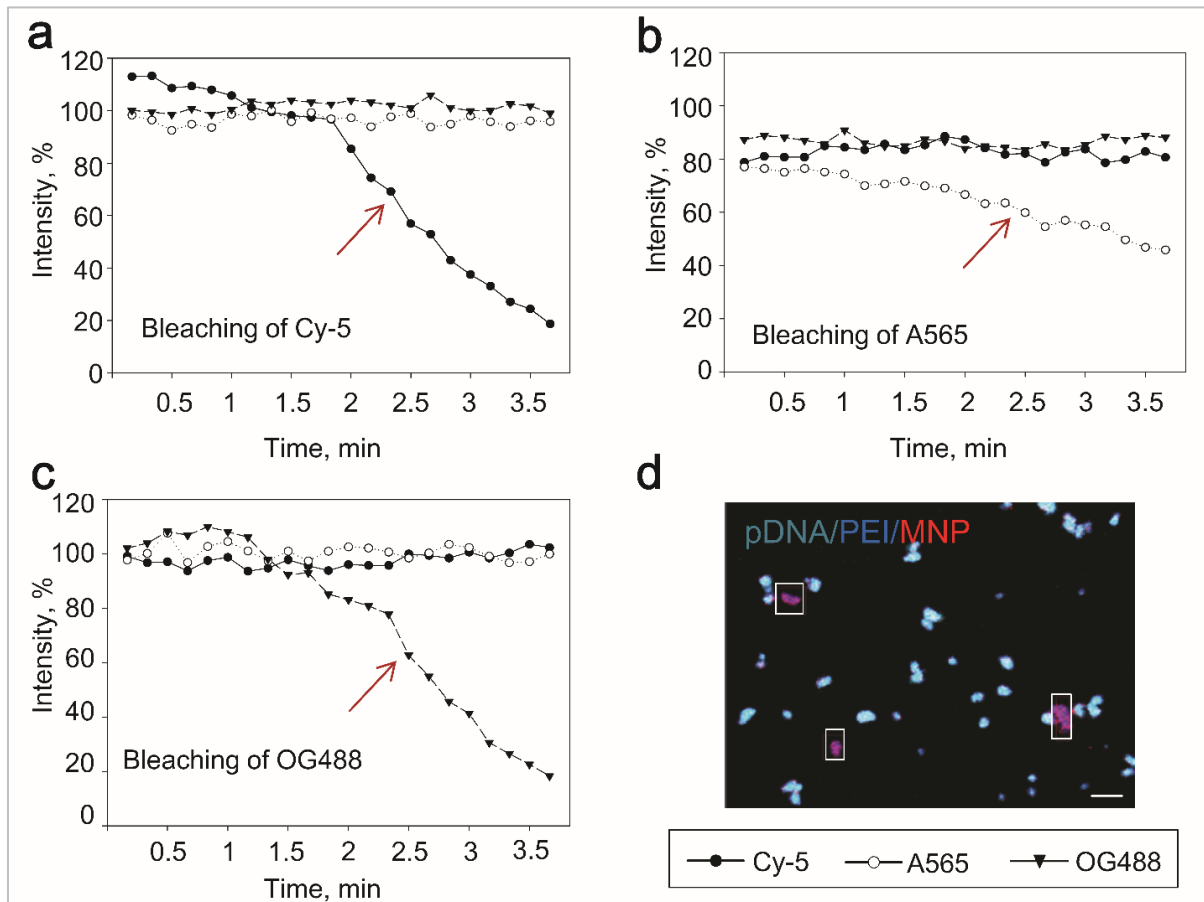


Figure 3.6: Photobleaching experiments. Three-color labelled magnetic transfection complexes (NP ratio 2.5, 1 $\mu\text{g/ml}$ iron) in the absence of cells were fixed on microscopic slides and visualized by laser scanning microscopy. pDNA was labelled with Cy5 dye (cyan), MNP were labelled with A565 dye (red), PEI was labelled with OG488 dye (blue). The fluorophores Cy5, A565 and OG488 were bleached in independent experiments for 3 min with 633 nm (a,d), 561nm (b) and 488 nm (c) laser lines respectively, at high laser power. The plots represent changes in fluorescent intensities over time. (d) Representative image of Cy5 photobleaching experiment. Scale bar = 1 μm . Adapted from [149, 150].

3.2.2 Intracellular localization of transfection complexes 24 h after transfection

Intracellular localization of transfection complexes was observed by CLSM of transfected hMSC. For that a z-series of images were acquired and analysed (Fig. 3.7 and 3.8).

At a 24 h time point after pDNA/PEI-mediated transfection, both, pDNA and PEI signals (visually colocalized) were found in the nuclei of hMSC (Figs. 3.7a and 3.8 b, b'). On the contrary, 24 h after pDNA/PEI/MNP-mediated transfection, no events were observed directly in the cell nuclei (Figs. 3.7b and 3.8 a, a').

A thorough z-stack analysis discovered three well distinguishable types of events in the perinuclear/nuclear region of hMSC (Fig. 3.8a''): condensed pDNA/PEI/MNP complexes (1); groups of PEI-OG488 signals visually colocalized with MNP-565 signals and surrounded by

diffused signal of DNA-Cy5 colocalized with DAPI (2); single DNA-Cy5 signals inside the nucleus (3).

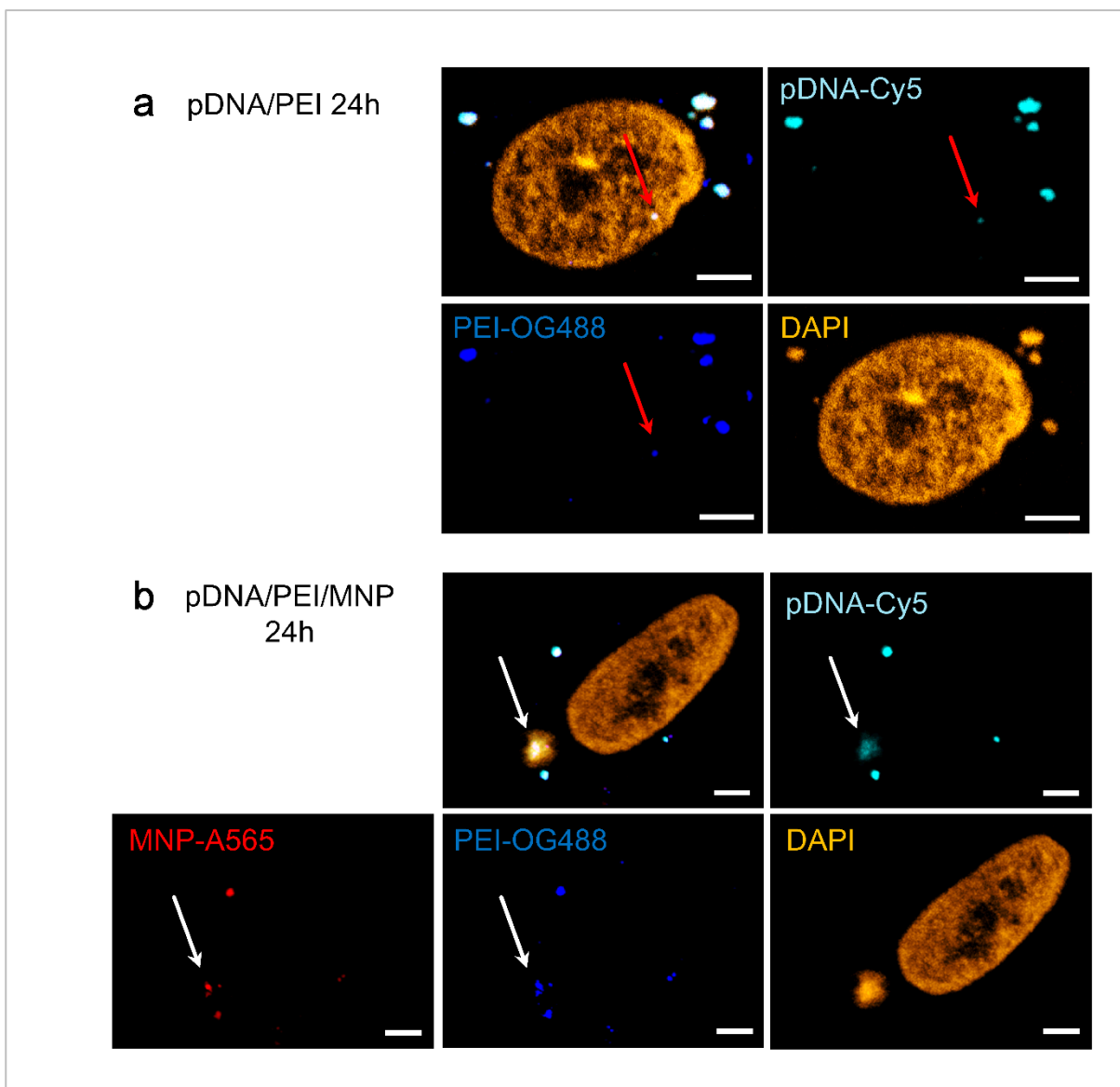


Figure 3.7: Intracellular localization of transfection complexes in hMSC 24 h after transfection. hMSC were transfected with fluorescently labelled pDNA/PEI or pDNA/PEI/MNP complexes ($3 \mu\text{g}/\text{cm}^2$ of pDNA, NP ratio 2.5, $1 \mu\text{g}/\text{ml}$ of iron) and visualized by CLSM 24 h after transfection. pDNA was labelled with Cy5 dye (cyan), MNP were labelled with A565 dye (red), PEI was labelled with OG488 dye (blue), nuclei were stained with DAPI (orange). Merged and single channel – confocal microscopy images of cells transfected with pDNA/PEI (**a**) or pDNA/PEI/MNP (**b**) complexes. Red arrows indicate intranuclear localization of pDNA/PEI complexes. White arrows indicate possible pDNA release event in the perinuclear region. Scale bars = $5 \mu\text{m}$. Taken from [149].

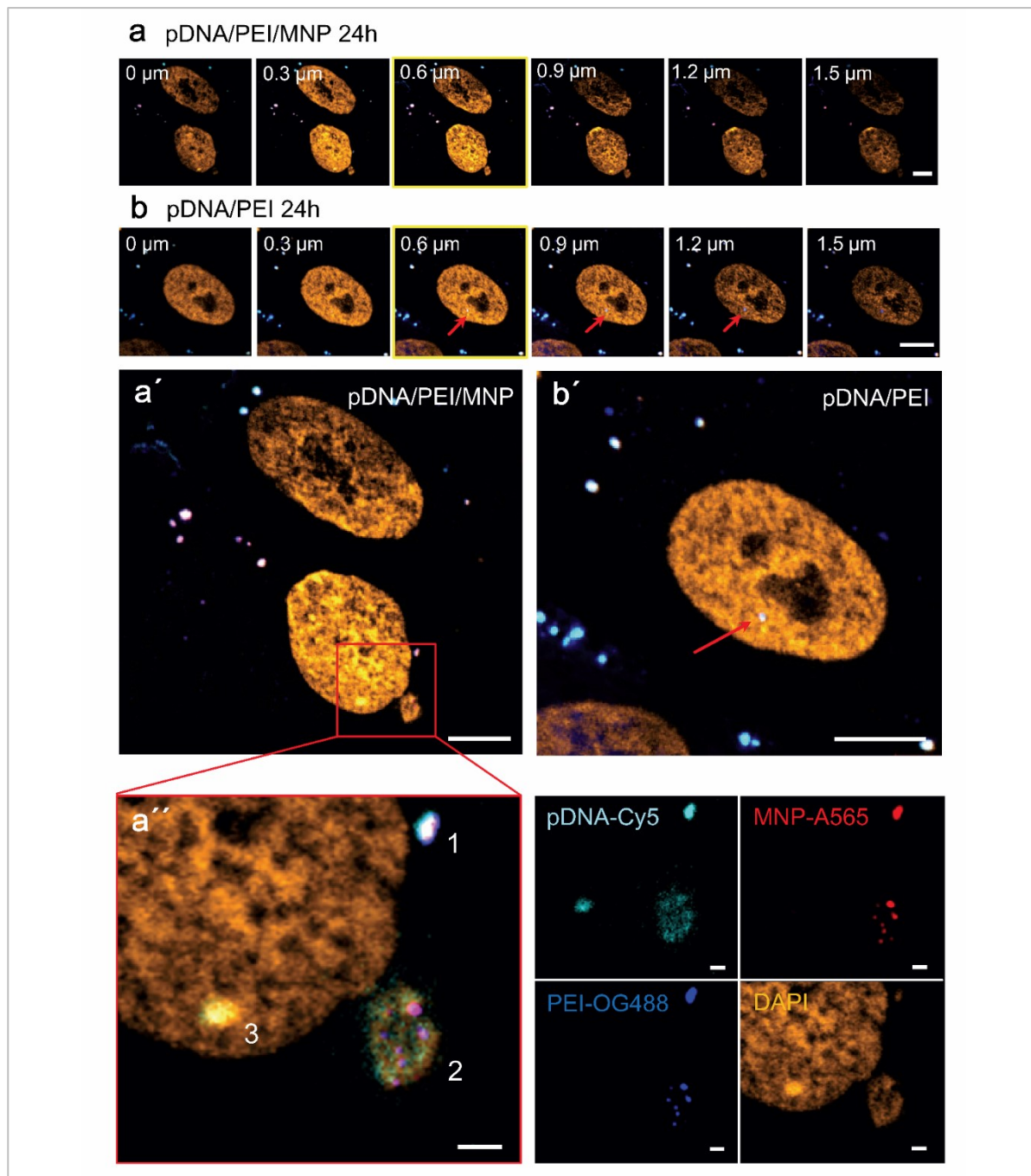


Figure 3.8: Intracellular localization of transfection complexes in hMSC 24 h after transfection, including possible pDNA release events. hMSC were transfected with fluorescently labelled pDNA/PEI or pDNA/PEI/MNP complexes ($3 \mu\text{g}/\text{cm}^2$ of pDNA, NP ratio 2.5, $1 \mu\text{g}/\text{ml}$ of iron) and visualized by CLSM 24 h after transfection. pDNA was labelled with Cy5 dye (cyan), MNP were labelled with A565 dye (red), PEI was labelled with OG488 dye (blue), nuclei were stained with DAPI (orange). Representative z-series of hMSC 24 h after transfection with pDNA/PEI/MNP (**a**) or pDNA/PEI (**b**) complexes. Magnified images of $0.6 \mu\text{m}$ – optical sections of cells transfected with pDNA/PEI/MNP (**a'**) or pDNA/PEI (**b'**). Red arrows indicate intranuclear localization of polyplexes. (**a''**) Magnified area of interest and single channel images show three events, possibly related to pDNA release process: **(1)** condensed pDNA/PEI/MNP complexes, **(2)** release of pDNA, **(3)** nuclear localization of pDNA. Scale bars = $2 \mu\text{m}$. Adapted from [149].

3.2.3 Monitoring of pDNA release from transfection complexes in hMSC

Monitoring of pDNA release from transfection complexes was performed using colocalization studies in hMSC, transfected with labelled pDNA/PEI or pDNA/PEI/MNP complexes. Figures 3.9c and d show representative scatter diagrams, obtained in the course of colocalization studies to calculate C_{coef} . Thus, Figure 3.9c demonstrates the changes in colocalization of pDNA and PEI signals within pDNA/PEI or pDNA/PEI/MNP complexes with the time (at 2, 12 and 24 h time points).

Obviously, the population of colocalized pixels in both cases reduces in size, as signals start to spread along the axes. However, this process is more evident in magnetic polyplexes, than in pDNA/PEI complexes. Figure 3.9d represents colocalization diagrams of PEI and MNP signals within the pDNA/PEI/MNP complexes. Here, the population of colocalized pixels did not change significantly over time. The results of detailed colocalization analysis at 2, 6, 12, 18 and 24 h after transfection are shown in Figures 3.9a and b. C_{coef} for pDNA-Cy5 and PEI-OG488 in samples with pDNA/PEI - or pDNA/PEI/MNP – transfected cells are presented in Figure 3.9a. At 2 h time point significantly more pDNA-Cy5 signals were colocalized with PEI-OG488 signals in magnetic polyplexes compared to pDNA/PEI complexes. Over time, in both cases C_{coef} decreased, signaling a loss of pDNA within transfection complexes. However, at later time points pDNA-PEI colocalization values in pDNA/PEI/MNP – transfected hMSC were significantly lower, than those in pDNA/PEI – transfected cells. Furthermore, 6 h after transfection a significant decrease of pDNA, colocalized with PEI, was observed in the case of magnetic polyplexes. All in all the mean value of C_{coef} dropped from 0.91 to 0.38 in 24 h (58.3% loss), whereas C_{coef} for pDNA within pDNA/PEI complexes reduced its mean value from 0.82 to 0.60 in the same timeframe (26.8% of loss). Additionally we analyzed the loss of pDNA in magnetic polyplexes in relation to MNP-A565 signal (C_{coef} of pDNA to MNP). These data are shown in Figure 3.9b.

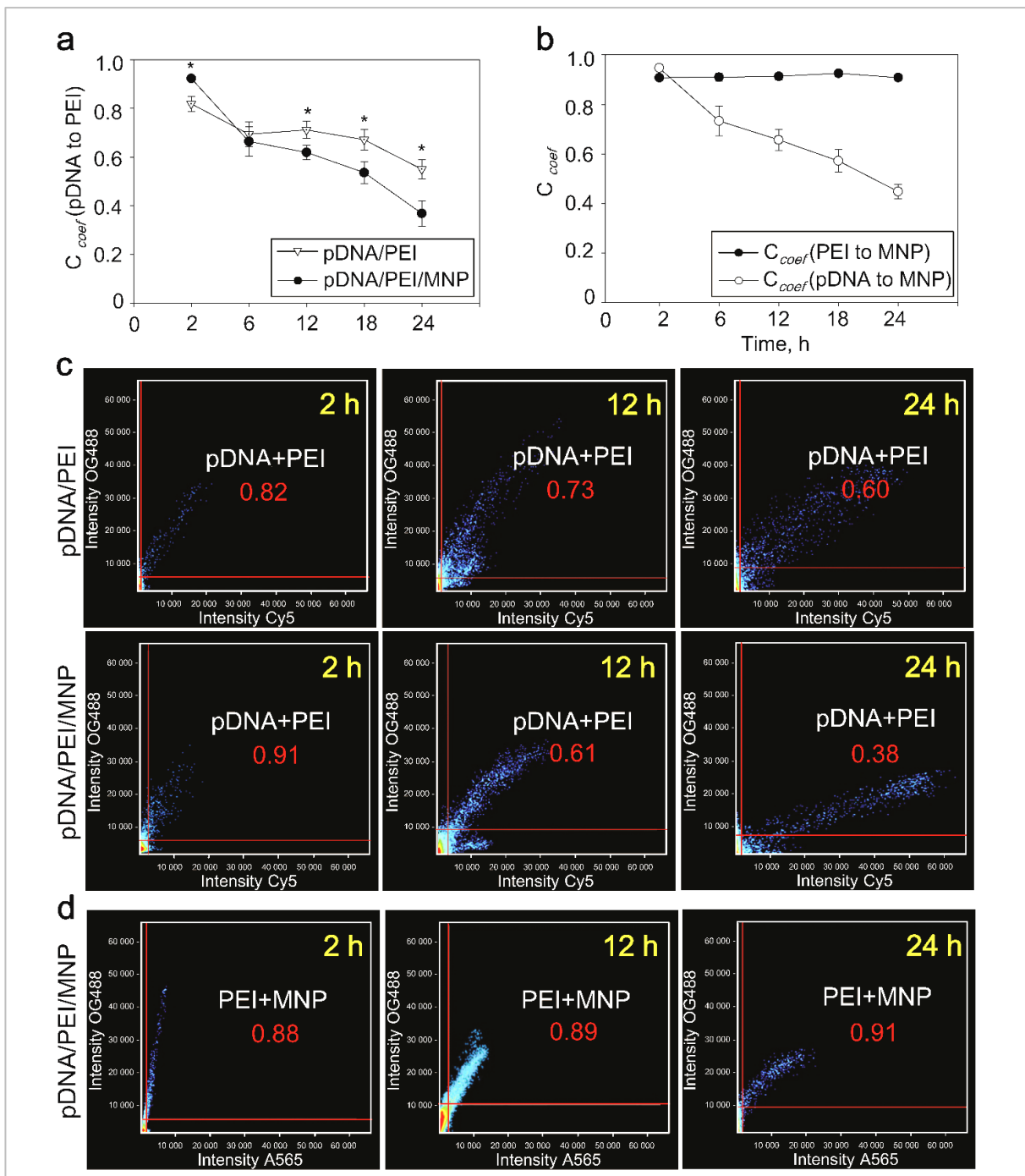


Figure 3.9: Monitoring of pDNA release from transfection complexes in hMSC. hMSC were transfected with fluorescently labelled pDNA/PEI or pDNA/PEI/MNP complexes ($3 \mu\text{g}/\text{cm}^2$ of pDNA, NP ratio 2.5, $1 \mu\text{g}/\text{ml}$ of iron), visualized by CLSM at different time points after transfection (2, 6, 12, 18, 24 h) and analysed for colocalization of Cy5 and OG488, Cy5 and A565, OG488 and A565 signals. Cells, transfected with unlabelled complexes were used as a negative control. pDNA was labelled with Cy5 dye (cyan), MNP were labelled with A565 dye (red), PEI was labelled with OG488 dye (blue), nuclei were stained with DAPI (orange). **(a)** Changing of C_{coef} of pDNA and PEI signals over time in hMSC, transfected with pDNA/PEI or pDNA/PEI/MNP complexes. **(b)** C_{coef} of PEI and MNP signals in comparison with C_{coef} of pDNA and MNP signals over time in hMSC, transfected with pDNA/PEI/MNP complexes. Data are shown as mean \pm SEM ($n = 20$). Representative scatter diagrams of colocalization experiments for **(c)** pDNA and PEI signals or **(d)** PEI and MNP signals in transfected hMSC at different time points. Red numbers indicate the values of **(c)** C_{coef} (pDNA to PEI) and **(d)** C_{coef} (PEI to MNP). Adapted from [149].

The changes in C_{coef} had a similar dynamic as colocalization of pDNA to PEI within pDNA/PEI/MNP complexes. The mean value dropped from 0.95 to 0.45 (47.4 % loss). Moreover, in a similar manner we investigated the colocalization behavior of MNP-A565 and PEI-OG488 signals over time (Fig. 3.9b). At the first time point (2 h) both signals were strongly colocalized. Over time the mean values of C_{coef} did not change significantly.

3.3 Transfection with LMW PEI-based magnetic complexes

(MW_(PEI)= 600 Da)

3.3.1 Characterization of pDNA/PEI600 transfection complexes

pDNA/PEI600 complexes were characterized by effective diameter and surface charge using the same techniques as for transfection complexes with high-molecular weight PEI. The results are presented in Figure 3.10. Detected by DLS, the effective diameter was maximal at NP ratio of 5 and significantly decreased at higher NP ratios. The size of complexes with NP ratios of 40 – 140 remained in range from 160 to 230 nm (Fig. 3.10a).

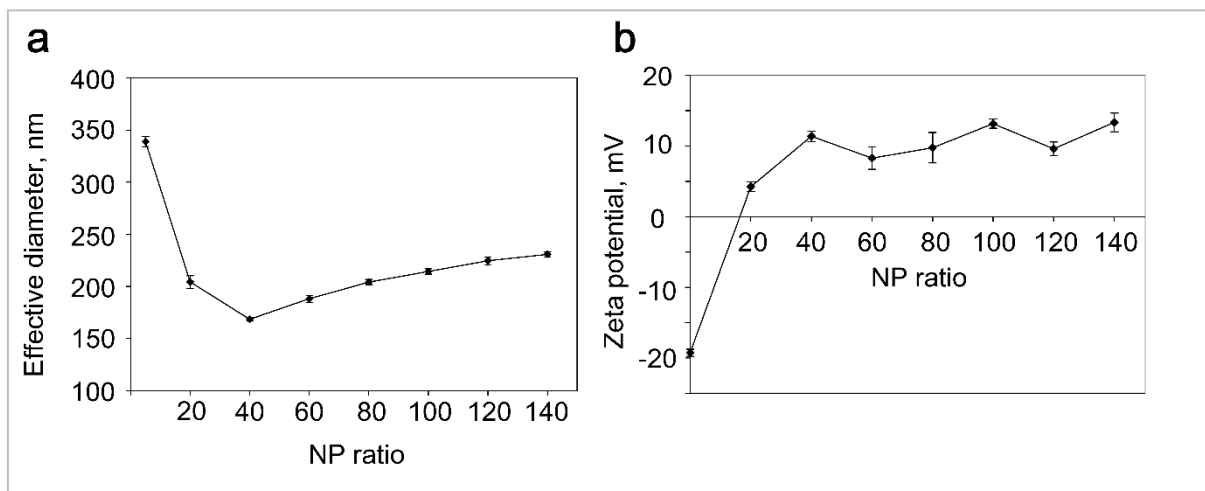


Figure 3.10: Characterization of pDNA/PEI600 transfection complexes. Particle size (a) and surface charge (b) of pDNA/PEI600 transfection complexes prepared at different NP ratios (from 20 to 140) were determined by DLS and PALS, respectively. Data represent the mean \pm SEM (n=10). Adapted from [151].

Zeta potential data, obtained by PALS, confirmed the correlation between NP ratio and effective diameter of transfection complexes, described above. pDNA alone had a negative surface charge (-20 mV) that turned to positive when PEI 600 was added at NP ratio of 20. At NP ratios of 40 – 140 the Zeta potential ranged from +9 mV to +15 mV, indicating the balance between positively charged PEI600 and negatively charged pDNA (Fig. 3.10b).

3.3.2 Optimization of transfection conditions with pDNA/PEI600/MNP complexes in COS-7 cell line

For the optimization of transfection conditions with pDNA/PEI600/MNP complexes (NP ratio, MNP amount), luciferase reporter gene assays and MTT cytotoxicity assays were used (Fig. 3.11). Figure 3.11a demonstrates transfection efficiencies of pDNA/PEI600 complexes at NP ratios of 40 – 140. The highest value of reporter gene expression was observed at NP ratio of 100 ($1.6 \cdot 10^5$ RLU/mg of protein). Therefore it has been chosen for further optimization of MNP amounts, which is shown in Figure 3.11b.

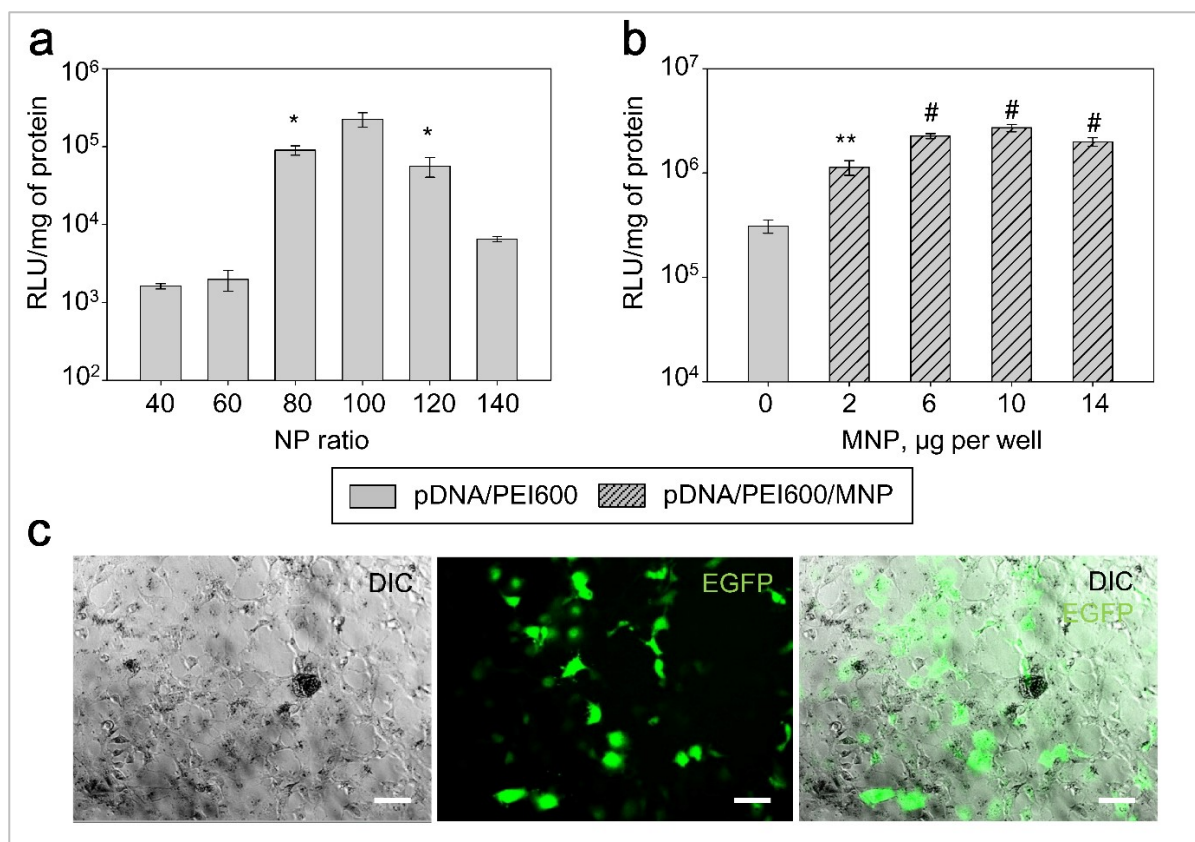


Figure 3.11: Optimization of transfection conditions with PEI600-containing complexes in COS-7 cells. The cells were transfected with (a) pDNA/PEI600 complexes (NP ratios from 40 to 140, 3 µg pDNA/well) or with (b) pDNA/PEI600/MNP complexes (NP ratio 100, 3 µg pDNA/well, 0 – 14 µg of MNP per well). 72 h after transfection, a luciferase reporter gene assay was performed in order to evaluate transfection efficiency. Results are representative of 3 independent experiments, each involved 8 replicates (n=8). The values are shown as mean \pm SEM. Asterisks represent a significant difference in transfection efficiencies (* $p \leq 0.05$, ** $p \leq 0.005$, # $p \leq 0.0005$) as compared to pDNA/PEI600 complexes at NP ratio 100. (c) Representative fluorescence microscopy images (single channels and merged) of EGFP expressing COS-7 cells 72 h after transfection with pDNA/PEI600/MNP complexes (3 µg pDNA/well, NP ratio 100, 10 µg MNP per well). Scale bars = 50 µm.

Interestingly, transfection efficiency increased significantly (4-fold) compared with pDNA/PEI600 complexes even when small amounts of MNP were used (2 µg of iron per well).

However, the highest gene expression level was detected when 10 μg of MNP per well were used. In the latter case, 9-10 fold enhancement was observed, and reporter gene expression reached $2.7 \cdot 10^6$ RLU/mg of protein. Nevertheless, higher amounts of MNP led to a significant decrease in transfection efficiency. All in all the transfection rates of pDNA/PEI600/MNP complexes were lower than those of pDNA/PEI ($MW_{(\text{PEI})} = 25$ kDa) complexes. Thus, NP ratio of 100 and 10 mg of MNP per well were selected as optimal conditions for pDNA/PEI600/MNP transfection.

Afterwards cytotoxicity of PEI600-mediated transfection was checked via MTT - assay and compared with pDNA/PEI ($MW_{(\text{PEI})} = 25$ kDa) transfection (Fig. 3.12). Both, pDNA/PEI600 and pDNA/PEI600/MNP complexes showed more than 80% of cell viability after transfection. Moreover, in both cases cytotoxicity was lower than after pDNA/PEI ($MW_{(\text{PEI})} = 25$ kDa)-mediated transfection [151].

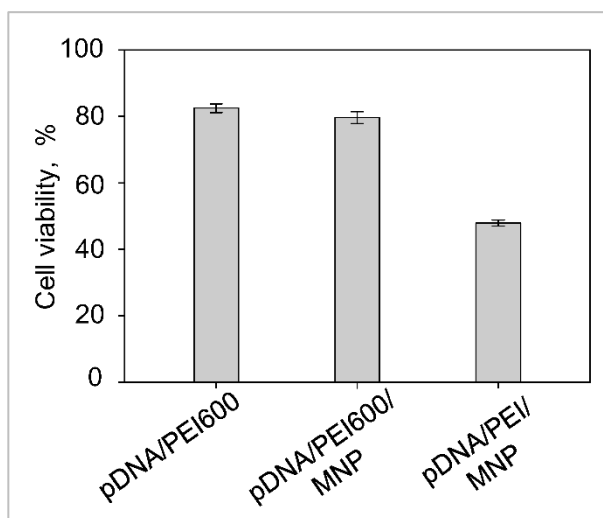


Figure 3.12: Cytotoxicity of PEI600-mediated transfection. COS-7 cells were transfected with pDNA/PEI600 (3 μg pDNA/well, NP ratio 100) or pDNA/PEI600/MNP (3 μg pDNA/well, NP ratio 100, 10 μg MNP per well) complexes. 48 h after transfection, MTT – assay was performed in order to evaluate the cell viability. The data were compared with DNA/PEI/MNP ($MW_{(\text{PEI})} = 25$ kDa, 3 μg pDNA/well, NP ratio 5)-mediated transfection. Results are representative of 3 independent experiments, each involved 8 replicates ($n=8$). The values are shown as mean \pm SEM. Adapted from [151].

In order to confirm the obtained data, a representative pEGFP transfection with pDNA/PEI600/MNP complexes at NP ratio of 100 and 10 μg of MNP per well is shown in Figure 3.11c.

4 Discussion

Initially, the MNP-based gene delivery system, studied in this work, was introduced by our group in 2008 [144]. As pilot *in vitro* and *in vivo* studies had been very promising, subsequent optimization of the carrier was performed by Anna Schade later on [149, 150]. The results showed that at certain conditions magnetic polyplexes were 100 – 1000 fold more efficient than pDNA/PEI complexes even without application of magnetic field. As a result of thorough optimization experiments in COS-7 we developed a transfection strategy, where low NP ratio, low MNP amount and optimal pDNA quantity may be of use for genetic modifications of “difficult-to-transfect” cells (i.e. stem cells) [150]. It is commonly known that such cell types are usually available in low amounts and are very sensitive to any toxic agents and procedures. Therefore, they strongly require a non-toxic and efficient approach for gene delivery.

Recent advances in stem cell research have brought new light to the use of stem cells for regenerative medicine and tissue engineering. Due to self – renewal and differentiation capacity, stem cells are of great interest for cell transplantation therapies, including regenerative medicine, cancer therapy and gene therapy. Genetic modifications of both, embryonic and adult stem cells could be performed to promote their differentiation *ex vivo* or to enhance their survival, selectivity and therapeutic effect *in vivo* [152].

One of the most promising and investigated adult stem cell types are hMSC. They have been discovered in various tissues and are often isolated from bone marrow. As these cells are widely used in biomedicine, The International Society for Cellular Therapy in 2006 proposed the minimal criteria to define hMSC. They include obligatory plastic adherence, expression of certain surface markers (CD105, CD73, CD29 and CD90), lack of expression of CD11b, CD14, CD19, CD34, CD45, CD79 α , CD117, HLA-antigen D-related. Moreover, the cells must be able to differentiate into adipocytes, osteocytes and chondrocytes under specific culture conditions [153]. Transplantation of hMSC was already shown to support cardiac regeneration, as these cells express matrix-mediating, antiapoptotic and angiogenic factors [154]. Moreover, their genetic modification before transplantation can improve cell survival and regenerative capacity, thus facilitating the recovery of infarcted tissue [155, 156].

Due to low toxicity and high efficiency, the transfection strategy described by our group previously [144, 150] could serve as a mild approach for genetic modifications of hMSC *in vitro*. Magnetic properties of pDNA/PEI/MNP complexes might allow subsequent *in vivo*

monitoring of modified cells after their transplantation by MRI, as well as selective targeting to the desired tissue by an external magnetic field.

4.1 Transfection in hMSC

4.1.1 Characterization of transfection complexes ($MW_{(PEI)} = 25$ kDa)

Characterization of pDNA/PEI and pDNA/PEI/MNP transfection complexes by PALS revealed that both systems have a well detectable positive surface charge exceeding +20 mV (Table 3.1). This confirms the stability of the complexes and their potential for successful interaction with negatively charged cell membrane. The DLS demonstrated that the hydrodynamic diameters of both systems were below 120 nm, though magnetic polyplexes were slightly bigger than polyplexes. Interestingly, the detected effective diameter of MNP alone was bigger than those of transfection complexes, probably due to tight binding of pDNA/PEI complexes on the surface of MNP via biotin – streptavidine linker. This fact may provide evidence, that transfection systems possess better colloidal properties and spherical stability than pure MNP.

Condensation assays for NP ratios ranging from 0.5 to 5 demonstrated that pDNA in polyplexes was completely retarded by PEI already at NP ratio 1.5 (Fig. 3.1).

4.1.2 Optimization of transfection in hMSC

The extensive optimization experiments in the COS-7 cell line, described previously [149, 150], provided reproducible and reliable data. This allowed the direct application of the optimized parameters for transfection in hMSC, thus saving human patient material for other experiments. However, the transfection rates with $1 \mu\text{g}/\text{cm}^2$ of pDNA were not high enough, therefore the pDNA amount was increased (Fig. 3.2a), that led to a significant decrease in cell viability (Fig. 3.2b). Another difficulty regarding hMSC transfection was a remarkably varying transfection efficiency among cells from different patients. This fact corresponds to previous findings of our group [157]. Nonetheless, magnetic polyplexes performed always better than polyplexes, demonstrating higher transfection rates even in the absence of a magnetic field (Fig. 3.2a, c, d). Thus, the mean transfection efficiency of pDNA/PEI/MNP was about 10%, while pDNA/PEI reached only 1.6% (Fig. 3.2c).

According to the International Society for Cellular Therapy, hMSC are characterized by the expression of specific surface markers and multilineage differentiation [153]. Therefore, it is of importance for future clinical applications, to maintain these characteristics after genetic

modifications. Therefore, in this work, immunophenotyping and differentiation assays were performed before and after transfection. Neither pDNA/PEI, nor magnetic polyplexes demonstrated any influence on surface markers expression (Table 3.2) and differentiation capacity (Fig. 3.3) of hMSC. These important results indicate the relative safety of both transfection methods.

4.1.3 Monitoring of transfection overtime

In order to better understand the transfection process, reporter gene expression in hMSC was monitored overtime for 48 h after transfection with either pDNA/PEI or pDNA/PEI/MNP complexes. Low levels of luciferase expression were observed as early as at 2 h and 6 h time points for both types of transfection. These results were confirmed by CLSM, where several complexes were observed inside the cells 2 h after transfection (data are not shown). According to the protocol for hMSC transfection, used in this work, changing of cell culture medium was always performed 4 h after transfection. That was done, aiming to discard the complexes, which had not been internalized by the cells, thus improving culture conditions. Hence, all the further measurements of reporter gene expression reflected the pDNA within the cells at 4 h time point post-transfection, similar to all other experiments, performed in this work. At 12 h time point a significant difference in luciferase activity after pDNA/PEI- and magnetic polyplexes-mediated transfection was observed (Fig. 3.4). Though reporter gene expression slightly increased at subsequent time points between 12 and 48 h, the majority of the cells was most probably transfected already at 12 h time point post-transfection.

4.2 Mechanism of MNP-mediated transfection

4.2.1 Insights the mechanism of transfection

The monitoring of luciferase reporter gene activity overtime after transfection with pDNA/PEI or magnetic polyplexes showed that both carriers provide a rapid gene delivery in hMSC. However, transfection with pDNA/PEI/MNP complexes was more efficient, than with polyplexes even in the absence of a magnetic field (Fig. 3.4). In order to understand the reasons for this effect, the transfection mechanism will be discussed and investigated below.

It has been previously shown that size, charge and structure of transfection complexes have a significant influence on their internalization route and intracellular kinetics [158-160]. The effective diameters of transfection complexes, used in this work, were significantly different,

but still less than 120 nm (see section 4.1.1 and Table 3.1). Hence, their cellular uptake and further processing should follow similar routes with comparable speed [160].

The next step after cellular entry is the transportation of transfection complexes towards the nucleus in endosomes. This process has undergone extensive investigation on different PEI-based polymers, used for transfection [161-164]. Due to a “proton sponge” effect of PEI, polyplexes can efficiently escape lysosomal degradation and easily release pDNA in the cytoplasm [165-167]. Many research groups, studying this process, stated that PEI is able to “buffer” lysosomes by increasing their pH value [168, 169]. However, this hypothesis has recently been challenged, as no PEI – induced changes in lysosomal pH were observed [112, 170]. Nevertheless, it is evident, that polyplexes reach lysosomes to a high extent and still provide efficient gene delivery, although the exact mechanism of lysosomal escape and pDNA release remain unclear.

At the last stage of the intracellular route of transfection complexes, the released pDNA enters the nucleus via various mechanisms, which are still extensively discussed. Under consideration are the entry via the nuclear pore complex, passive transfer during mitosis and undefined pathways, occurring in non-dividing cells [171].

While the mechanism of polyplex-mediated transfection has been in focus since decades, MNP-mediated transfection processes were not studied in details. The mechanism of magnetofection was reported by Huth et al. in 2004 [143]. However, their studies focused on the cellular entry of transfection complexes and the influence of an external magnetic field on this process. In general, they assumed that the mechanism of MNP-mediated transfection was similar to that of pDNA/PEI complexes and therefore was not studied in detail. They claimed that magnetic field, involved in magnetofection, had no influence on cellular entry and further processing of transfection complexes [143]. Thus, the efficiency of magnetically-assisted transfection was enhanced due to more rapid sedimentation of transfection complexes on the cell surface [143].

All transfection experiments in current work were performed in the absence of a magnetic field, clearly indicating that MNP are able to positively affect transfection efficiency of polyplexes without external magnetic exposure. The expected mechanism of magnetic polyplex-mediated transfection in comparison to polyplexes is shown in Figure 4.1 [124].

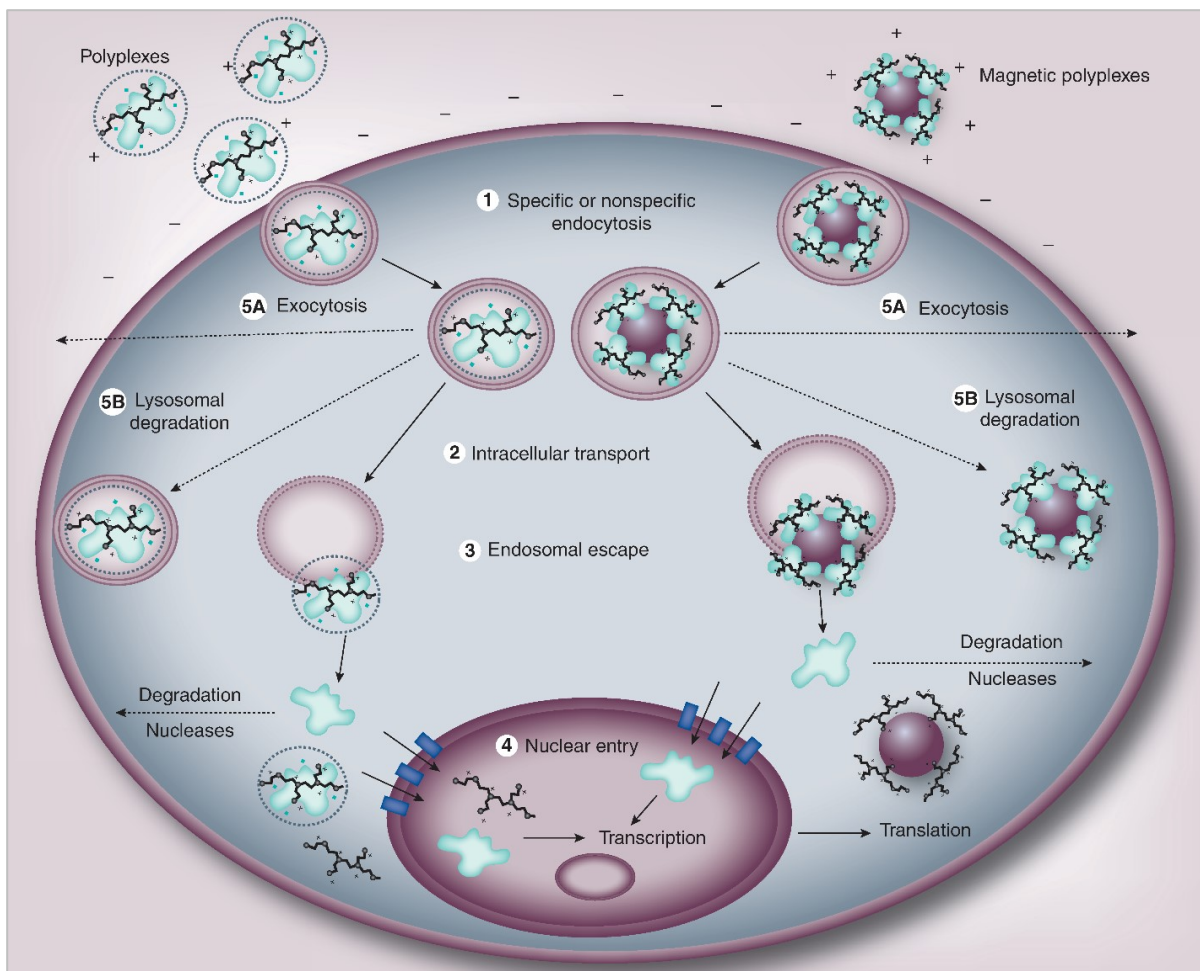


Figure 4.1: Expected mechanism of magnetic polyplex-mediated transfection in comparison to polyplexes. After cellular entry via endocytosis (1) both types of transfection complexes are transported along the cytoskeleton towards the nucleus (2). Next, pDNA alone or the whole complexes should be released from endosomes to perinuclear region (3), thus avoiding their exocytosis (5A) or lysosomal degradation (5B). The final step of successful transfection process is the nuclear entry of pDNA (4) followed by transcription or translation. In case of polyplexes, cationic polymer can also enter the nucleus. In case of MNP-based transfection, cationic polymer is expected to remain in the cytoplasm. Retrieved and adapted from <http://www.futuremedicine.com/> [124].

To better understand the mechanism of MNP-based transfection and prove the hypothesis in this work, transfection complexes were visualized and observed inside the cells at different time points after transfection.

4.2.2 Visualization of transfection complexes

The choice of appropriate methods is a crucial step in any research work, dedicated to study intracellular mechanisms, processes or pathways. It very much depends on the study objectives and investigated material. Different methodologies were previously successfully employed in order to reveal the mechanism of transfection (e.g. cellular uptake studies [158], electron

microscopy [143], confocal microscopy [158, 172], single particle tracking [173], labelling with quantum dots [174], Förster Resonance Energy Transfer (FRET) [175]).

To investigate the transfection mechanism, in this study confocal microscopy was used. For that, transfection complexes were visualized via fluorescent labelling techniques. This method is wide spread due to relative simplicity, wide selection of labelling reagents, broad application spectrum and universality. It may allow to obtain both, qualitative and quantitative data about intracellular trafficking of transfection complexes.

For the first time, in this work all three components of magnetic polyplexes (pDNA, PEI and MNP) were fluorescently labelled and visualized at once.

Fluorescent labelling protocols were initially optimized in order to maintain the functionality and the safety of transfection agents in COS-7 cells. These data were described in details by Anna Schade [150]. In current work, the performance of both, single-labelled and three-color labelled complexes, was tested in hMSC (Fig. 3.5). Additionally, the influence of labelling on size and surface charge of transfection complexes was evaluated by DLS and PALS methods (Table 3.3). Despite the slight increase in size of magnetic polyplexes, labelled transfection complexes provided high transfection efficiency and high cell viability in hMSC. The values were not significantly different from those, obtained for unlabelled complexes (Fig. 3.5). Thus, the labelling protocol was confirmed to be optimal also for hMSC, which allowed the correlation of microscopy data with *in vitro* transfection data in the following experiments.

SIM is a modern high – resolution technique with maximum resolution of 50-110 nm, which was employed in this work for the visualization of magnetic polyplexes without the cell environment [176, 177]. All three fluorescent signals (representing pDNA, PEI and MNP) had a good signal-to-noise ratio and were visually colocalized. Magnetic polyplexes had a spherical shape and size ranging from 200 nm to 300 nm. Furthermore, no single or two-color signals were detected, that can indicate that all pDNA was condensed in pDNA/PEI complexes, and all pDNA/PEI complexes were bound to MNP (Fig. 3.5).

However, close localization of the fluorophores inside the transfection complex, as well as their close emission/excitation spectra may trigger certain undesired interactions. An example of such interactions is FRET – a transfer of energy with subsequent false detection of one fluorophore in a wrong channel. It mostly occurs between fluorophores with close excitation and emission spectra, when the distance between them does not exceed 10 nm [178]. The presence of FRET between pairs of OG488/A565 and A565/Cy5 in labelled transfection complexes was studied in photobleaching experiments (Fig. 3.6). Importantly, no FRET was detected for magnetic polyplexes in this work, indicating that labelling procedures and

microscopic acquisition set up were optimal. These points were extremely important for reliable colocalization studies later on.

4.2.3 Intracellular localization of transfection complexes

Fluorescently labelled transfection complexes were observed in hMSC by means of CLSM at different time points after transfection. Already at 2 h time point both, pDNA/PEI and pDNA/PEI/MNP have entered the cell and were randomly distributed inside (data are not shown). However, this work was focused on the perinuclear region, as pDNA release process and its further nuclei entry are the most crucial steps of transfection [179]. Pollard et al. showed that only 1/1000 of cytosolically injected pDNA could be delivered to the cell nucleus and successfully expressed [180]. However, knowledge of the processes taking place in the perinuclear region during transfection is still insufficient.

Therefore, we performed an optical sectioning of transfected cells, focusing on the nucleus and perinuclear region. This revealed that in case of pDNA/PEI-mediated transfection pDNA delivered into the nuclei was still condensed by PEI (Fig. 3.7a and 3.8b, b'). In 2008, our group had already detected similar events [144], yet in COS-7 cells. These findings are in agreement with other reports, published earlier [181-183]. It is generally considered that most of the polyplexes enter the nucleus via temporary opening of the nuclear membrane during mitosis [171]. This hypothesis corresponds well to the studies where transfection efficiency was shown to be a cell cycle dependent process [184, 185]. Nevertheless, polyplex-mediated transfection was also successfully performed in non-dividing cells [186], thus indicating that pDNA is able to enter the nucleus of those cells in either free or condensed form [171]. However, the mechanism of this import remains unclear.

On the contrary, in cells which underwent magnetic polyplex-mediated transfection, pDNA signals inside the nuclei were colocalized neither with PEI - , nor with MNP – signals (Fig. 3.8a''). Moreover, it was possible for the first time to observe three different events in one visual field: the condensed magnetic polyplexes, complexes releasing pDNA in the perinuclear region and pDNA inside the nucleus (Fig. 3.8a'').

In 2008 it was already hypothesized, that pDNA/PEI and pDNA/PEI/MNP complexes follow different transfection mechanisms in terms of nuclear entry of pDNA [144]. The results described in this work, allow to confirm the hypothesis of Li et al. via demonstration of free intranuclear pDNA. Furthermore, morphological changes in composition of transfection complexes, presented in Figure 3.8a'' (2), can be explained by the process of pDNA release, which has not been reported previously. Importantly, in cells transfected by means of

pDNA/PEI complexes no similar processes were found, thus these events were exclusive for magnetic polyplex-mediated gene delivery. Hence, magnetic polyplexes may provide a more efficient pDNA release than polyplexes. In order to prove this hypothesis and provide quantitative data, the following pDNA release studies were performed.

4.2.4 Monitoring of pDNA release from transfection complexes

For monitoring of intracellular pDNA release process, colocalization of pDNA-Cy5/PEI-OG488 and PEI-OG488/MNP-A565 signals was evaluated using CLSM at different time points after transfection (Fig. 3.9). At the initial time point (2 h post transfection) pDNA was significantly more condensed inside magnetic polyplexes, than in pDNA/PEI complexes. This fact might be of benefit for transfection due to better protection of pDNA from degradation in the cytoplasm. Overall, in 24 h the values of measured C_{coef} indicated the release of pDNA from both, pDNA/PEI and pDNA/PEI/MNP complexes, though this process was twice more efficient in the case of magnetic polyplexes (26.8% vs. 58.3%) (Fig. 3.9a). These data were supported by the microscopic observations (see Section 4.2.3), where pDNA release events could only be found in the perinuclear region of cells, transfected with pDNA/PEI/MNP complexes. However, due to the fast degradation of free pDNA by nucleases, the location of this process becomes a crucial factor for successful transfection. Another important result of colocalization studies was a strong colocalization of PEI with MNP within magnetic polyplexes at all investigated time points (Fig. 3.9b). This indicated that pDNA release was related only to the pDNA/PEI decondensation process. The strong MNP-PEI connection is feasible due to the robust streptavidin-biotin interaction, which lies in the basis of magnetic polyplex-structure (see Section 1.5 and Fig. 1.4). As streptavidin – biotin interaction is one of the strongest noncovalent bindings in nature, it might retain PEI better than physical interactions and therefore allow an easy and efficient process of pDNA release. Moreover, due to the size of streptavidin – coated MNP, they are not able to enter the nucleus, thus retaining PEI in the perinuclear region. Some studies previously reported that efficiency of transfection depends on the number of plasmids, delivered to the nuclei [179, 187]. Moreover, Glover et al. assumed that the transcriptional activity of delivered pDNA can be affected by the carrier. For instance, polyplexes dissociating from the pDNA in the nucleus [180], interact with nuclear proteins and interfere with transcriptional machinery, resulting to cytotoxicity and limited transfection efficiency [179, 182]. Therefore, a system, which can efficiently release pDNA in the cytoplasm and does not allow the entrance of other reagents into the nucleus, may indeed provide better transfection rates, which has been demonstrated in this study.

4.3 Transfection with LMW PEI-based magnetic complexes

In the last decades PEI has been widely used alone or in combination with other reagents as an efficient transfection system both, *in vitro* and *in vivo* [111]. Due to its beneficial properties (see Section 1.4.2.2) PEI remains in the focus of nonviral gene delivery research. However, its cytotoxicity and inability to biodegrade are not favorable for *in vivo* applications and limit further clinical translation of PEI-based transfection systems. PEI, most successfully used for transfection experiments has a MW of 25 kDa. However, it has been demonstrated that PEI with lower MW (600 – 2000 Da) possesses much lower cytotoxicity, though not providing the desired transfection efficiency [116].

This part of the work aimed to perform a pilot investigation of magnetic polyplexes containing PEI with MW of 600 Da instead of a high molecular weight (HMW) PEI (MW = 25 kDa). It was assumed that the efficiency of LMW PEI may increase due to combination with MNP, while magnetic polyplexes may improve their safety profile. For that pDNA/PEI600/MNP transfection complexes were constructed in a similar manner as HMW PEI-based complexes using a streptavidin – biotin connection. At first, the size and surface charge of pDNA/PEI600 complexes with different NP ratios were evaluated. Notably, the NP ratios applicable for PEI600-based complexes were higher than those for HMW PEI due to a low amount of aminogroups in the first case. This was in accordance with other reports, where LMW PEI required high NP ratios for sufficient transfection [116, 188]. At NP ratios of 40 – 140 polyplexes had a size distribution of 160 - 230 nm and had a stable positive charge (Fig. 3.10), indicating the sufficient condensation of pDNA by LMW PEI. Furthermore, this range of NP ratios was used for gene reporter transfection experiments. Optimization of pDNA/PEI600-mediated transfection in COS-7 cells revealed that NP 100 provided the highest reporter gene expression (Fig. 3.11a). In the next step, the optimization of MNP amounts within the magnetic polyplexes was performed. Similar to the transfection experiments with HMW PEI, described above, no external magnetic field was employed. Interestingly, even a small amount of MNP led to an increase in transfection efficiency in comparison to pDNA/PEI600 complexes. However, magnetic polyplexes with 10 μg of MNP, NP ratio of 100 and 3 $\mu\text{g}/\text{cm}^2$ of pDNA provided the highest transfection rates (10-fold increase compared with pDNA/PEI600) and were considered as optimal conditions for LMW PEI-based transfection. These results were confirmed by EGFP transfection experiments, showed in Fig. 3.11c. The cytotoxicity tests showed that both, pDNA/PEI600 and pDNA/PEI600/MNP complexes are relatively safe and provide more than 80% of cell viability (Fig. 3.12), that was significantly

higher than cell viability after transfection with HMW PEI-containing polyplexes at similar conditions. Nevertheless, the efficiency of PEI600-based transfection complexes, even in combination with MNP, still could not outperform HMW PEI-containing polyplexes.

These pilot results underlined the need for further development of different strategies for improvement of MNP-based transfection. Although LMW PEI in combination with MNP was able to provide relatively safe transfection in the COS-7 cell line, its application in “difficult – to transfect” cells or further *in vivo* studies are limited by low efficiency. Many modification strategies have been already introduced and tested aiming to improve the performance of LMW PEI. For instance, hydrophobic modifications [189, 190], appending to polyesters [191], cross – linking with biodegradable linkages [188], citric acid [192] or targeting ligands[193] were used for creating efficient and safe LMW PEI-based gene delivery carriers *in vitro* and *in vivo*. However, for further clinical translation, these and other modifications should still undergo extensive investigations, and their targeting abilities should be improved.

4.4 Future perspectives of MNP-based gene delivery

Due to broad investigations on MNP-based gene delivery systems, including current work, this promising approach is able under certain conditions to outperform other nonviral transfection methods in terms of safety and efficiency. However, several drawbacks still limit its “bench-to-bedside” translation. Table 4.1 summarizes the most important properties and knowledge, which have to be considered before successful clinical translation of MNP-based transfection systems in the future. The table also shows the compliance of both, magnetic polyplexes, studied in this work and magnetofection complexes, with the listed requirements.

Table 4.1: Properties of MNP-based gene delivery systems, relevant for their future clinical translation.

	Transfection method		Comments / References
	pDNA/PEI/MNP	Magnetofection	
Easy production and reproducibility	+	+	[128, 136, 144, 149]
High load of genetic material	+	+	[128, 136, 144, 149]
Ability to load different genetic material	+	+	[129, 194, 195]
Protection of genetic material	+	+	[128, 136, 144, 149]
Efficient release of genetic material	+	+	[143, 149]

	Transfection method		Comments / References
	pDNA/PEI/MNP	Magnetofection	
Ability for controlled release of genetic material	-	-	Shown for similar structures only
Efficient translocation of genetic material to the nucleus	+/-	+/-	Possible with modified genetic material [196, 197]
Targeting potential	+	+	By external magnetic field or targeting ligands [144]
High efficiency <i>in vitro</i>	+/-	+/-	Still not comparable with viral vectors
High efficiency <i>in vivo</i>	-	-	More studies are required
Reproducibility of results	+	+	[128, 136, 144, 149]
High safety	+/-	+/-	More studies are required
Non immunogenicity	+/-	+/-	Extensive studies are required
Biocompatibility	-	-	PEI is not biocompatible
Biodegradability	-	-	PEI is not biodegradable
Well studied intracellular mechanism	+	+	[143, 149, 158]
Well studied <i>in vivo</i> pathway and biodistribution	-	-	No information
Broad preclinical studies	-	-	Not information

According to Table 4.1, both, magnetic polyplexes presented in the current study and commercially available magnetofection systems, already possess many features, beneficial for further clinical translation. In both cases MNP facilitate the transfection process and allow the targeting of transfection complexes by external magnetic fields *in vivo*. Moreover, due to the magnetite core, MNP possess good biocompatibility. PEI provides efficient condensation of nucleic acids, their protection and further release in the cytoplasm. However, PEI used for the construction of both transfection systems is not biodegradable and not biocompatible because of its toxicity. This fact reduces biocompatibility of the whole transfection system, even though its overall safety is rather high. The development of more appropriate *in vitro* and *in vivo* techniques to study biocompatibility and cytotoxicity of the transfection systems is also necessary, as well as extensive investigations on behavior of nanocarriers in relevant biological

fluids [198, 199]. Transfection efficiency of both systems is another parameter, which still requires improvement, as performance of the carriers depends on the cell type and still cannot outperform viral gene delivery.

The strategies to improve MNP – gene delivery include modifications of the carrier compounds (MNP and/or PEI) and variations of genetic material. With a focus on the recent advances in this field, both groups will be discussed below.

4.4.1 Modifications of the MNP-based carrier

The most widely used strategies to improve MNP-based gene delivery techniques include adjustment of transfection parameters, functionalization of MNP and modifications of a polymeric compound.

Thus, biocompatibility of PEI can be improved by means of the following strategies, recently described by Wang et al. [111]:

- Formation of polymeric micelles by grafting with copolymers (PEG, poly(L-lactide-co-glycolic acid) (PLGA), poly(lactic) acid (PLA), polycaprolactone, etc.);
- Formation of synthetic polymer nanoparticles (by use of poly(methyl methacrylate));
- Formation of biodegradable polymers (e.g. by use of tetraethylenpentamine (TEPA));
- Formation of biopolymer nanoparticles (by use of chitosan, cyclodextrin, gelatin).

For instance, Bansal et al. synthesized novel biodegradable polymers based on linear or branched LMW PEI [200]. Due to the Michael reaction (treatment with an excess of methyl acrylate), followed by amidation with TEPA they obtained two versatile carriers: TLP (TEPA@linear PEI) and TBP (TEPA@branched PEI), which were able to efficiently transfect mammalian cell cultures with no cytotoxicity. Moreover, the obtained transfection rates were higher, than those after commercially available transfection reagents (Lipofectamine[®], Superfect[®] and branched PEI with MW of 25 kDa) [200].

Wu et al. have recently presented another biodegradable modification of LMW PEI by means of the amphiphilic polymer Pluronic. After combination with a tumor targeting - multifunctional peptide, the polymer demonstrated efficient and safe reporter gene delivery in different cell lines (HeLa, HepG2, and NIH 3T3) [201]. Similar poly(ester amines) built on the basis of LMW PEI and Pluronic were reported by Wang et al. [202] They also showed higher

transfection rates in comparison with HMW PEI *in vitro* and *in vivo*, though were not tested for therapeutic gene delivery.

Although, these polymers should still undergo *in vivo* testing and mechanism studies, their combination with MNP might result in efficient, biocompatible and safe transfection systems.

Due to chemical stability under physiological conditions, high magnetic moments and low toxicity iron oxide MNP have good biocompatibility and therefore are already widely used in biomedical applications [199]. By combining them with different functional molecules (enzymes, antibodies, etc.) the biocompatibility of MNP can be further improved. Coating with other materials (PEG, chitosan, lipids, proteins) can enhance their stability and allow additional chemical modifications [199]. Moreover, due to modifications of the physical parameters (size, shape, composition, and shell-core architecture), their magnetic properties can be adjusted in order to improve their *in vivo* targeting capacity [203].

Nevertheless, any functional modification of the carrier elevates its complexity (e.g. multistep synthesis, additional purification and characterization studies) and production costs, while multicomponent, heterogeneous composition rises the regulatory barriers [204]. On the contrary, manipulations with genetic material, might improve the performance of MNP-based transfection systems without challenging modifications of the carrier.

4.4.2 Modifications of genetic material

Despite the progress in the construction of the carrier and its compounds, the process of translocation of genetic material into the nucleus remains one of the main barriers for successful gene delivery [196]. It has been demonstrated that only a small part of pDNA (1 to 10%), delivered into the cytoplasm reaches the nucleus and promotes gene expression [179, 187], which becomes a serious “bottleneck” for transfection in non-dividing cells. The nuclear import of delivered pDNA can be improved by including nuclear localization sequences or transcription factor –binding sites in the structure of a plasmid, as well as by introducing small molecule ligands [196].

For example, Vernon et al. have recently used a modified plasmid for the improvement of MNP-based transfection (Polymag Neo, nTMag and Neuromag) in the presence of an oscillating magnetic field. They showed that introduction of a DNA targeting sequence leads to enhanced transfection rates in model primary neurons (in comparison with Lipofectamine) [197].

Another advanced strategy for efficient nonviral gene delivery was developed on the basis of transposable elements, which compose 45% of the human genome [205]. Transposable elements-based transfection systems combine the advantages of viruses and naked DNA, providing efficient and sustained modification of the genome [206]. These systems usually include a transposon with gene expression cassette and a source of a transposase enzyme. Both structures can be harbored either on the same or on different plasmids, which are usually delivered to the cells by means of electroporation or hydrodynamic injection [206, 207]. PiggyBac and Sleeping Beauty are the most successful transposon systems that have already been widely applied for stem cell engineering, including generation of induced pluripotent stem cells [207-210]. Although Sleeping Beauty has already entered the clinical trials [24], much research is still aiming to improve the efficiency and safety of transposable elements-based systems. To this end, combination with MNP may improve the delivery process *in vitro* and enhance selectivity of this approach *in vivo*.

To date, the majority of gene delivery studies have been using plasmid DNA. However, the success of transfection with this approach strongly depends on the nuclear entry of genetic material [179]. Moreover, DNA-based gene therapies may lead to mutational insertions in the host genome, increasing the risk of tumorigenesis [211].

Therefore, many alternative RNA-based genetic constructs are currently in the focus of gene therapy. They include protein coding mRNAs and noncoding RNAs (ncRNAs). Short and long ncRNAs are expressed in response to the environmental stimuli and stress in the course of development. They were shown to have a great influence on gene expression by controlling the transcription process, posttranscriptional targeting and epigenetic modifications [212]. For instance, siRNAs represent short ncRNAs (21-23 oligonucleotides), which are able to cleave target mRNA, leading to a reduction in the levels of target protein. They can be designed to silence any gene of known sequence, thus their therapeutic potential is high. Importantly, siRNAs are involved just in posttranscriptional processes, which reduce possible adverse gene alterations [213]. Several studies have recently demonstrated successful delivery of different siRNA to cancer cells *in vitro* and *in vivo* by means of MNP of different structure (e.g. MNP including iron oxide, PEI, PEG, chitosan, silica) [214-218]. Moreover, some of those delivery systems were also successfully visualized and traced by MRI [215-217]. As a nonviral gene therapy approach siRNA has already entered clinical trials, although a number of these studies is less than 10. It has been applied for treatment of ocular and respiratory diseases, as well as for pancreas and breast cancer [24]. For instance, siRNA against vascular endothelial growth factor receptor-1 (Sirna-27) as intraocular injections has undergone Phase I and II clinical trials

in patients with age-related macular degeneration. Another siRNA for intranasal administration was tested for the treatment of Respiratory Syncytial Virus (RSV) infection [24].

Another important group of short ncRNAs includes miRNAs. These genetic constructs are able to control the gene expression by regulating the majority of mammalian protein - coding mRNAs on the posttranscriptional level [219]. Our group has recently utilized magnetic transfection complexes for efficient delivery of miRNA to both, expanded and freshly isolated hMSC aiming to improve their therapeutic potential for cardiac regeneration [194, 195, 220]. It was shown that magnetic transfection complexes were able to successfully deliver miRNA constructs to both types of hMSC. In case of expanded hMSC MNP-based carriers provided a prolonged functionality of delivered miRNA as compared with polyplexes. Moreover, it was shown *in vitro* that transfected cells could be manipulated by an external magnetic field, that might be of benefit for potential *in vivo* applications [220]. The group of Yin et al. has recently demonstrated a combined application of MNP-based miRNA delivery and hyperthermia induce apoptosis in cancer cells. They used magnetic zink-doped iron oxide nanoparticles ($ZnFe_2O_4$) to deliver a lethal-7a miRNA, that inhibits malignant growth by simultaneous targeting of several pathways. Glioblastoma multiforme brain cancer cells were used as a model in that study. The effect was further improved by magnetic hyperthermia performed after transfection. Though further *in vivo* studies are still pending, the method might become a promising approach for brain cancer treatment.

The first miRNA mimic-based drug has entered clinical trials in 2015. MRX34 (produced by Mirna Therapeutics, TX, USA) is a double-stranded RNA mimic of the tumor suppressor miRNA-34, encapsulated in a liposomal nanoparticle formulation. To date, the ongoing Phase I study has already involved more than 100 patients and demonstrated the very first clinical proof of concept in treatment of renal cell carcinoma, acral melanoma and hepatocellular carcinoma [89, 221].

The knowledge on the diversity of miRNAs and their broad regulation potential is rapidly growing. Many preclinical studies are currently underway and further clinical trials will follow. In combination with efficient and safe nonviral gene delivery systems, these genetic constructs might be a successful approach for both, direct and indirect gene therapy.

5 Conclusion

The results of this work showed that the MNP-based gene delivery system, introduced previously by our group, could efficiently and safely transfect hMSC, outperforming polyplexes alone even in the absence of a magnetic field. Furthermore, this work provided important insights to the mechanism of this process. This was feasible due to successful visualization of transfection complexes on the intracellular level and extensive studies of the pDNA release process, performed in the course of the project. Importantly, a method where all three components of the transfection system (pDNA, PEI and MNP) were selectively labelled and observed inside cells was introduced here for the first time. The findings of this work suggested that MNP-based transfection complexes provide better transfection efficiency due to more efficient release of pDNA in comparison to polyplexes. This underlined a strong influence of the carrier composition on transfection processes and its efficacy.

This work also included pilot tests of a magnetic transfection system, where HMW PEI was replaced by LMW PEI, aiming to improve the biocompatibility of the system. Although the safety of pDNA/PEI600/MNP complexes was rather high, the efficiency was not significantly improved in comparison to pDNA/PEI/MNP complexes. These results emphasized the necessity to further develop strategies for improvement of MNP-based transfection in order to proceed with the clinical translation of this approach.

In conclusion, the MNP-based gene delivery system, investigated in this work, already possesses certain properties, which could be beneficial for nucleic acid based modification of “difficult – to – transfect” cells and subsequent clinical applications. However, this carrier still requires an improvement of its biocompatibility properties and safety profile, which could be obtained by modifications of the carrier itself and/or the carried genetic material. An overview of the recent development of MNP-based gene delivery methods revealed great progress in this field. However, extensive preclinical studies, including thorough investigations of the *in vivo* pathways as well as biodistribution of transfection systems and all their components, will be required prior to clinical use.

6 Bibliography

1. Kotterman Ma, Chalberg Tw, Schaffer Dv. Viral Vectors for Gene Therapy: Translational and Clinical Outlook. *Annu Rev Biomed Eng* 17 63-89 (2015).
2. Griffith F. The Significance of Pneumococcal Types. *J Hyg (Lond)* 27(2), 113-159 (1928).
3. Alloway JI. The Transformation in Vitro of R Pneumococci into S Forms of Different Specific Types by the Use of Filtered Pneumococcus Extracts. *J Exp Med* 55(1), 91-99 (1932).
4. Avery Ot, Macleod Cm, Mccarty M. Studies on the Chemical Nature of the Substance Inducing Transformation of Pneumococcal Types : Induction of Transformation by a Desoxyribonucleic Acid Fraction Isolated from Pneumococcus Type Iii. *J Exp Med* 79(2), 137-158 (1944).
5. Zinder Nd, Lederberg J. Genetic exchange in Salmonella. *J Bacteriol* 64(5), 679-699 (1952).
6. Tatum El, Lederberg J. Gene Recombination in the Bacterium Escherichia coli. *J Bacteriol* 53(6), 673-684 (1947).
7. Watson Jd, Crick Fh. Genetical implications of the structure of deoxyribonucleic acid. *Nature* 171(4361), 964-967 (1953).
8. Wirth T, Parker N, Yla-Herttuala S. History of gene therapy. *Gene* 525(2), 162-169 (2013).
9. Cohen Sn, Chang Ac, Boyer Hw, Helling Rb. Construction of biologically functional bacterial plasmids in vitro. *Proc Natl Acad Sci U S A* 70(11), 3240-3244 (1973).
10. Genentech corporate website; <http://www.gene.com/>.
11. American Society of Gene & Cell Therapy; <http://www.asgct.org/>.
12. Rogers S, Pfuderer P. Use of viruses as carriers of added genetic information. *Nature* 219(5155), 749-751 (1968).
13. Fox Ms, Littlefield Jw. Reservations concerning gene therapy. *Science* 173(3993), 195 (1971).
14. Rosenberg Sa, Aebersold P, Cornetta K *et al*. Gene transfer into humans--immunotherapy of patients with advanced melanoma, using tumor-infiltrating lymphocytes modified by retroviral gene transduction. *N Engl J Med* 323(9), 570-578 (1990).
15. Blaese Rm, Culver Kw, Miller Ad *et al*. T lymphocyte-directed gene therapy for ADA-SCID: initial trial results after 4 years. *Science* 270(5235), 475-480 (1995).
16. Bordignon C, Notarangelo Ld, Nobili N *et al*. Gene therapy in peripheral blood lymphocytes and bone marrow for ADA- immunodeficient patients. *Science* 270(5235), 470-475 (1995).
17. Cavazzana-Calvo M, Hacein-Bey S, De Saint Basile G *et al*. Gene therapy of human severe combined immunodeficiency (SCID)-X1 disease. *Science* 288(5466), 669-672 (2000).
18. Stolberg Sg. The biotech death of Jesse Gelsinger. *N Y Times Mag* 136-140, 149-150 (1999).
19. Raper Se, Chirmule N, Lee Fs *et al*. Fatal systemic inflammatory response syndrome in a ornithine transcarbamylase deficient patient following adenoviral gene transfer. *Mol Genet Metab* 80(1-2), 148-158 (2003).
20. European Medicines Agency website; <http://www.ema.europa.eu/ema/>.

21. GlaxoSmithKline corporate website; Press release from 01 Apr 2016; <https://www.gsk.com/>.
22. Yla-Herttuala S. Endgame: glybera finally recommended for approval as the first gene therapy drug in the European union. *Mol Ther* 20(10), 1831-1832 (2012).
23. Yla-Herttuala S. The need for increased clarity and transparency in the regulatory pathway for gene medicines in the European Union. *Mol Ther* 20(3), 471-472 (2012).
24. Gene Therapy Clinical Trials Worldwide (by the Journal of Gene Medicine); <http://www.abedia.com/wiley/>.
25. Husain Sr, Han J, Au P, Shannon K, Puri Rk. Gene therapy for cancer: regulatory considerations for approval. *Cancer Gene Ther* 22(12), 554-563 (2015).
26. Collins M, Thrasher A. Gene therapy: progress and predictions. *Proc Biol Sci* 282(1821), (2015).
27. Kaestner L, Scholz A, Lipp P. Conceptual and technical aspects of transfection and gene delivery. *Bioorg Med Chem Lett* 25(6), 1171-1176 (2015).
28. Aiuti A, Cattaneo F, Galimberti S *et al*. Gene therapy for immunodeficiency due to adenosine deaminase deficiency. *N Engl J Med* 360(5), 447-458 (2009).
29. Cavazzana-Calvo M, Payen E, Negre O *et al*. Transfusion independence and HMGA2 activation after gene therapy of human beta-thalassaemia. *Nature* 467(7313), 318-322 (2010).
30. Cartier N, Aubourg P. Hematopoietic stem cell transplantation and hematopoietic stem cell gene therapy in X-linked adrenoleukodystrophy. *Brain Pathol* 20(4), 857-862 (2010).
31. Biffi A, Montini E, Lorioli L *et al*. Lentiviral hematopoietic stem cell gene therapy benefits metachromatic leukodystrophy. *Science* 341(6148), 1233158 (2013).
32. Aiuti A, Biasco L, Scaramuzza S *et al*. Lentiviral hematopoietic stem cell gene therapy in patients with Wiskott-Aldrich syndrome. *Science* 341(6148), 1233151 (2013).
33. Kalos M, Levine BI, Porter DI *et al*. T cells with chimeric antigen receptors have potent antitumor effects and can establish memory in patients with advanced leukemia. *Sci Transl Med* 3(95), 95ra73 (2011).
34. Brentjens Rj, Davila MI, Riviere I *et al*. CD19-targeted T cells rapidly induce molecular remissions in adults with chemotherapy-refractory acute lymphoblastic leukemia. *Sci Transl Med* 5(177), 177ra138 (2013).
35. Brentjens Rj, Riviere I, Park Jh *et al*. Safety and persistence of adoptively transferred autologous CD19-targeted T cells in patients with relapsed or chemotherapy refractory B-cell leukemias. *Blood* 118(18), 4817-4828 (2011).
36. Mcelrath Mj, De Rosa Sc, Moodie Z *et al*. HIV-1 vaccine-induced immunity in the test-of-concept Step Study: a case-cohort analysis. *Lancet* 372(9653), 1894-1905 (2008).
37. Buchbinder Sp, Mehrotra Dv, Duerr A *et al*. Efficacy assessment of a cell-mediated immunity HIV-1 vaccine (the Step Study): a double-blind, randomised, placebo-controlled, test-of-concept trial. *Lancet* 372(9653), 1881-1893 (2008).
38. Harro Cd, Robertson Mn, Lally Ma *et al*. Safety and immunogenicity of adenovirus-vectored near-consensus HIV type 1 clade B gag vaccines in healthy adults. *AIDS Res Hum Retroviruses* 25(1), 103-114 (2009).
39. Peters W, Brandl Jr, Lindbloom Jd *et al*. Oral administration of an adenovirus vector encoding both an avian influenza A hemagglutinin and a TLR3 ligand induces antigen specific granzyme B and IFN-gamma T cell responses in humans. *Vaccine* 31(13), 1752-1758 (2013).
40. Hill Av, Reyes-Sandoval A, O'hara G *et al*. Prime-boost vectored malaria vaccines: progress and prospects. *Hum Vaccin* 6(1), 78-83 (2010).

41. Smaill F, Jeyanathan M, Smieja M *et al.* A human type 5 adenovirus-based tuberculosis vaccine induces robust T cell responses in humans despite preexisting anti-adenovirus immunity. *Sci Transl Med* 5(205), 205ra134 (2013).
42. Rosengart Tk, Bishawi Mm, Halbreiner Ms *et al.* Long-term follow-up assessment of a phase I trial of angiogenic gene therapy using direct intramyocardial administration of an adenoviral vector expressing the VEGF121 cDNA for the treatment of diffuse coronary artery disease. *Hum Gene Ther* 24(2), 203-208 (2013).
43. Westphal M, Yla-Herttuala S, Martin J *et al.* Adenovirus-mediated gene therapy with sitimagene ceradenovec followed by intravenous ganciclovir for patients with operable high-grade glioma (ASPECT): a randomised, open-label, phase 3 trial. *Lancet Oncol* 14(9), 823-833 (2013).
44. Dreno B, Urosevic-Maiwald M, Kim Y *et al.* TG1042 (Adenovirus-interferon-gamma) in primary cutaneous B-cell lymphomas: a phase II clinical trial. *PLoS One* 9(2), e83670 (2014).
45. Manno Cs, Pierce Gf, Arruda Vr *et al.* Successful transduction of liver in hemophilia by AAV-Factor IX and limitations imposed by the host immune response. *Nat Med* 12(3), 342-347 (2006).
46. Nathwani Ac, Tuddenham Eg, Rangarajan S *et al.* Adenovirus-associated virus vector-mediated gene transfer in hemophilia B. *N Engl J Med* 365(25), 2357-2365 (2011).
47. Mease Pj, Wei N, Fudman Ej *et al.* Safety, tolerability, and clinical outcomes after intraarticular injection of a recombinant adeno-associated vector containing a tumor necrosis factor antagonist gene: results of a phase 1/2 Study. *J Rheumatol* 37(4), 692-703 (2009).
48. Moss Rb, Milla C, Colombo J *et al.* Repeated aerosolized AAV-CFTR for treatment of cystic fibrosis: a randomized placebo-controlled phase 2B trial. *Hum Gene Ther* 18(8), 726-732 (2007).
49. Stroes Es, Nierman Mc, Meulenberg Jj *et al.* Intramuscular administration of AAV1-lipoprotein lipase S447X lowers triglycerides in lipoprotein lipase-deficient patients. *Arterioscler Thromb Vasc Biol* 28(12), 2303-2304 (2008).
50. Carpentier Ac, Frisch F, Labbe Sm *et al.* Effect of alipogene tiparvovec (AAV1-LPL(S447X)) on postprandial chylomicron metabolism in lipoprotein lipase-deficient patients. *J Clin Endocrinol Metab* 97(5), 1635-1644 (2012).
51. Gaudet D, Methot J, Dery S *et al.* Efficacy and long-term safety of alipogene tiparvovec (AAV1-LPLS447X) gene therapy for lipoprotein lipase deficiency: an open-label trial. *Gene Ther* 20(4), 361-369 (2012).
52. Bainbridge Jw, Smith Aj, Barker Ss *et al.* Effect of gene therapy on visual function in Leber's congenital amaurosis. *N Engl J Med* 358(21), 2231-2239 (2008).
53. Simonelli F, Maguire Am, Testa F *et al.* Gene therapy for Leber's congenital amaurosis is safe and effective through 1.5 years after vector administration. *Mol Ther* 18(3), 643-650 (2009).
54. Jacobson Sg, Cideciyan Av, Ratnakaram R *et al.* Gene therapy for leber congenital amaurosis caused by RPE65 mutations: safety and efficacy in 15 children and adults followed up to 3 years. *Arch Ophthalmol* 130(1), 9-24 (2011).
55. Maclaren Re, Groppe M, Barnard Ar *et al.* Retinal gene therapy in patients with choroideremia: initial findings from a phase 1/2 clinical trial. *Lancet* 383(9923), 1129-1137 (2014).
56. Bowles De, Mcphee Sw, Li C *et al.* Phase I gene therapy for Duchenne muscular dystrophy using a translational optimized AAV vector. *Mol Ther* 20(2), 443-455 (2012).

57. Mendell Jr, Rodino-Klapac Lr, Rosales Xq *et al.* Sustained alpha-sarcoglycan gene expression after gene transfer in limb-girdle muscular dystrophy, type 2D. *Ann Neurol* 68(5), 629-638 (2010).
58. Zsebo K, Yaroshinsky A, Rudy Jj *et al.* Long-term effects of AAV1/SERCA2a gene transfer in patients with severe heart failure: analysis of recurrent cardiovascular events and mortality. *Circ Res* 114(1), 101-108 (2014).
59. Brantly Ml, Spencer Lt, Humphries M *et al.* Phase I trial of intramuscular injection of a recombinant adeno-associated virus serotype 2 alpha1-antitrypsin (AAT) vector in AAT-deficient adults. *Hum Gene Ther* 17(12), 1177-1186 (2006).
60. Flotte Tr, Trapnell Bc, Humphries M *et al.* Phase 2 clinical trial of a recombinant adeno-associated viral vector expressing alpha1-antitrypsin: interim results. *Hum Gene Ther* 22(10), 1239-1247 (2011).
61. Lewitt Pa, Rezaei Ar, Leehey Ma *et al.* AAV2-GAD gene therapy for advanced Parkinson's disease: a double-blind, sham-surgery controlled, randomised trial. *Lancet Neurol* 10(4), 309-319 (2011).
62. Marks Wj, Jr., Ostrem JI, Verhagen L *et al.* Safety and tolerability of intraputamenal delivery of CERE-120 (adeno-associated virus serotype 2-neurturin) to patients with idiopathic Parkinson's disease: an open-label, phase I trial. *Lancet Neurol* 7(5), 400-408 (2008).
63. Christine Cw, Starr Pa, Larson Ps *et al.* Safety and tolerability of putamenal AADC gene therapy for Parkinson disease. *Neurology* 73(20), 1662-1669 (2009).
64. Andtbacka Rh, Kaufman HI, Collichio F *et al.* Talimogene Laherparepvec Improves Durable Response Rate in Patients With Advanced Melanoma. *J Clin Oncol* 33(25), 2780-2788 (2015).
65. Park Bh, Hwang T, Liu Tc *et al.* Use of a targeted oncolytic poxvirus, JX-594, in patients with refractory primary or metastatic liver cancer: a phase I trial. *Lancet Oncol* 9(6), 533-542 (2008).
66. Breitbach Cj, Burke J, Jonker D *et al.* Intravenous delivery of a multi-mechanistic cancer-targeted oncolytic poxvirus in humans. *Nature* 477(7362), 99-102 (2011).
67. Heo J, Reid T, Ruo L *et al.* Randomized dose-finding clinical trial of oncolytic immunotherapeutic vaccinia JX-594 in liver cancer. *Nat Med* 19(3), 329-336 (2013).
68. Crystal Rg. Adenovirus: the first effective in vivo gene delivery vector. *Hum Gene Ther* 25(1), 3-11 (2014).
69. Al-Dosari Ms, Gao X. Nonviral gene delivery: principle, limitations, and recent progress. *AAPS J* 11(4), 671-681 (2009).
70. Wang W, Li W, Ma N, Steinhoff G. Non-viral gene delivery methods. *Curr Pharm Biotechnol* 14(1), 46-60 (2013).
71. Schlenk F, Grund S, Fischer D. Recent developments and perspectives on gene therapy using synthetic vectors. *Ther Deliv* 4(1), 95-113 (2013).
72. Jin L, Zeng X, Liu M, Deng Y, He N. Current progress in gene delivery technology based on chemical methods and nano-carriers. *Theranostics* 4(3), 240-255 (2014).
73. Powell Rj. Update on clinical trials evaluating the effect of biologic therapy in patients with critical limb ischemia. *J Vasc Surg* 56(1), 264-266 (2012).
74. Mitchell Ms, Abrams J, Thompson Ja *et al.* Randomized trial of an allogeneic melanoma lysate vaccine with low-dose interferon Alfa-2b compared with high-dose interferon Alfa-2b for Resected stage III cutaneous melanoma. *J Clin Oncol* 25(15), 2078-2085 (2007).
75. Daud Ai, Deconti Rc, Andrews S *et al.* Phase I trial of interleukin-12 plasmid electroporation in patients with metastatic melanoma. *J Clin Oncol* 26(36), 5896-5903 (2008).

76. Khorsandi Se, Bachellier P, Weber Jc *et al.* Minimally invasive and selective hydrodynamic gene therapy of liver segments in the pig and human. *Cancer Gene Ther* 15(4), 225-230 (2008).
77. Bedikian Ay, Richards J, Kharkevitch D, Atkins Mb, Whitman E, Gonzalez R. A phase 2 study of high-dose Allovectin-7 in patients with advanced metastatic melanoma. *Melanoma Res* 20(3), 218-226 (2010).
78. Gonzalez R, Hutchins L, Nemunaitis J, Atkins M, Schwarzenberger Po. Phase 2 trial of Allovectin-7 in advanced metastatic melanoma. *Melanoma Res* 16(6), 521-526 (2006).
79. Alton Ew, Baker A, Baker E *et al.* The safety profile of a cationic lipid-mediated cystic fibrosis gene transfer agent following repeated monthly aerosol administration to sheep. *Biomaterials* 34(38), 10267-10277 (2013).
80. Angell C, Xie S, Zhang L, Chen Y. DNA Nanotechnology for Precise Control over Drug Delivery and Gene Therapy. *Small* 12(9), 1117-1132 (2016).
81. Zhang Y, Yu Lc. Single-cell microinjection technology in cell biology. *Bioessays* 30(6), 606-610 (2008).
82. Villemejjane J, Mir Lm. Physical methods of nucleic acid transfer: general concepts and applications. *Br J Pharmacol* 157(2), 207-219 (2009).
83. Sun Y, Jurgovsky K, Moller P *et al.* Vaccination with IL-12 gene-modified autologous melanoma cells: preclinical results and a first clinical phase I study. *Gene Ther* 5(4), 481-490 (1998).
84. Mahvi Dm, Sondel Pm, Yang Ns *et al.* Phase I/IB study of immunization with autologous tumor cells transfected with the GM-CSF gene by particle-mediated transfer in patients with melanoma or sarcoma. *Hum Gene Ther* 8(7), 875-891 (1997).
85. Comerota Aj, Throm Rc, Miller Ka *et al.* Naked plasmid DNA encoding fibroblast growth factor type 1 for the treatment of end-stage unreconstructible lower extremity ischemia: preliminary results of a phase I trial. *J Vasc Surg* 35(5), 930-936 (2002).
86. Simovic D, Isner Jm, Ropper Ah, Pieczek A, Weinberg Dh. Improvement in chronic ischemic neuropathy after intramuscular phVEGF165 gene transfer in patients with critical limb ischemia. *Arch Neurol* 58(5), 761-768 (2001).
87. Newman Cm, Bettinger T. Gene therapy progress and prospects: ultrasound for gene transfer. *Gene Ther* 14(6), 465-475 (2007).
88. Antkowiak M, Torres-Mapa Ml, Stevenson Dj, Dholakia K, Gunn-Moore Fj. Femtosecond optical transfection of individual mammalian cells. *Nat Protoc* 8(6), 1216-1233 (2013).
89. Clinical trials database (by US National Institutes of Health); <https://clinicaltrials.gov/>.
90. Martin B, Sainlos M, Aissaoui A *et al.* The design of cationic lipids for gene delivery. *Curr Pharm Des* 11(3), 375-394 (2005).
91. Byk G. Cationic lipid-based gene delivery. In: *Pharmaceutical Perspectives of Nucleic Acid-Based Therapy*, Mahato Ri, Kim Sw (Ed.^(Eds). CRC Press 273-304 (2003).
92. Thermo Fischer Scientific corporate website; <https://www.thermofisher.com/>.
93. Nabel Gj, Gordon D, Bishop Dk *et al.* Immune response in human melanoma after transfer of an allogeneic class I major histocompatibility complex gene with DNA-liposome complexes. *Proc Natl Acad Sci U S A* 93(26), 15388-15393 (1996).
94. Nabel Gj, Nabel Eg, Yang Zy *et al.* Direct gene transfer with DNA-liposome complexes in melanoma: expression, biologic activity, and lack of toxicity in humans. *Proc Natl Acad Sci U S A* 90(23), 11307-11311 (1993).
95. Vical Inc. corporate website. Press release from 12 Aug 2013; <http://www.vical.com/>.
96. Alton Ew, Stern M, Farley R *et al.* Cationic lipid-mediated CFTR gene transfer to the lungs and nose of patients with cystic fibrosis: a double-blind placebo-controlled trial. *Lancet* 353(9157), 947-954 (1999).

97. Caplen Nj, Alton Ew, Middleton Pg *et al.* Liposome-mediated CFTR gene transfer to the nasal epithelium of patients with cystic fibrosis. *Nat Med* 1(1), 39-46 (1995).
98. Gill Dr, Southern Kw, Mofford Ka *et al.* A placebo-controlled study of liposome-mediated gene transfer to the nasal epithelium of patients with cystic fibrosis. *Gene Ther* 4(3), 199-209 (1997).
99. Noone Pg, Hohneker Kw, Zhou Z *et al.* Safety and biological efficacy of a lipid-CFTR complex for gene transfer in the nasal epithelium of adult patients with cystic fibrosis. *Mol Ther* 1(1), 105-114 (2000).
100. Porteous Dj, Dorin Jr, Mclachlan G *et al.* Evidence for safety and efficacy of DOTAP cationic liposome mediated CFTR gene transfer to the nasal epithelium of patients with cystic fibrosis. *Gene Ther* 4(3), 210-218 (1997).
101. Hyde Sc, Southern Kw, Gileadi U *et al.* Repeat administration of DNA/liposomes to the nasal epithelium of patients with cystic fibrosis. *Gene Ther* 7(13), 1156-1165 (2000).
102. Lv H, Zhang S, Wang B, Cui S, Yan J. Toxicity of cationic lipids and cationic polymers in gene delivery. *J Control Release* 114(1), 100-109 (2006).
103. Nguyen Lt, Atobe K, Barichello Jm, Ishida T, Kiwada H. Complex formation with plasmid DNA increases the cytotoxicity of cationic liposomes. *Biol Pharm Bull* 30(4), 751-757 (2007).
104. Ruiz Fe, Clancy Jp, Perricone Ma *et al.* A clinical inflammatory syndrome attributable to aerosolized lipid-DNA administration in cystic fibrosis. *Hum Gene Ther* 12(7), 751-761 (2001).
105. Grigsby Cl, Leong Kw. Balancing protection and release of DNA: tools to address a bottleneck of non-viral gene delivery. *J R Soc Interface* 7 Suppl 1 S67-82 (2009).
106. Behr Jp, Demeneix B, Loeffler Jp, Perez-Mutul J. Efficient gene transfer into mammalian primary endocrine cells with lipopolyamine-coated DNA. *Proc Natl Acad Sci U S A* 86(18), 6982-6986 (1989).
107. Cotten M, Wagner E. Non-viral approaches to gene therapy. *Curr Opin Biotechnol* 4(6), 705-710 (1993).
108. Haensler J, Szoka Fc, Jr. Polyamidoamine cascade polymers mediate efficient transfection of cells in culture. *Bioconj Chem* 4(5), 372-379 (1993).
109. Eliyahu H, Barenholz Y, Domb Aj. Polymers for DNA delivery. *Molecules* 10(1), 34-64 (2005).
110. Boussif O, Lezoualc'h F, Zanta Ma *et al.* A versatile vector for gene and oligonucleotide transfer into cells in culture and in vivo: polyethylenimine. *Proc Natl Acad Sci U S A* 92(16), 7297-7301 (1995).
111. Xia W, Dechao N, Chen H, Pei L. Polyethyleneimine-Based Nanocarriers for Gene Delivery. *Current Pharmaceutical Design* 21(42), 6140-6156 (2015).
112. Benjaminsen Rv, Matthebjerg Ma, Henriksen Jr, Moghimi Sm, Andresen Tl. The possible "proton sponge" effect of polyethylenimine (PEI) does not include change in lysosomal pH. *Mol Ther* 21(1), 149-157 (2013).
113. Varga Cm, Tedford Nc, Thomas M, Klibanov Am, Griffith Lg, Lauffenburger Da. Quantitative comparison of polyethylenimine formulations and adenoviral vectors in terms of intracellular gene delivery processes. *Gene Ther* 12(13), 1023-1032 (2005).
114. Moghimi Sm, Symonds P, Murray Jc, Hunter Ac, Debska G, Szewczyk A. A two-stage poly(ethylenimine)-mediated cytotoxicity: implications for gene transfer/therapy. *Mol Ther* 11(6), 990-995 (2005).
115. Beyerle A, Irmeler M, Beckers J, Kissel T, Stoeger T. Toxicity pathway focused gene expression profiling of PEI-based polymers for pulmonary applications. *Mol Pharm* 7(3), 727-737 (2010).

116. Godbey Wt, Wu Kk, Mikos Ag. Size matters: molecular weight affects the efficiency of poly(ethylenimine) as a gene delivery vehicle. *J Biomed Mater Res* 45(3), 268-275 (1999).
117. Xu Q, Wang Ch, Pack Dw. Polymeric carriers for gene delivery: chitosan and poly(amidoamine) dendrimers. *Curr Pharm Des* 16(21), 2350-2368 (2010).
118. Tang Mx, Redemann Ct, Szoka Fc, Jr. In vitro gene delivery by degraded polyamidoamine dendrimers. *Bioconjug Chem* 7(6), 703-714 (1996).
119. Merdan T, Kunath K, Petersen H *et al.* PEGylation of poly(ethylene imine) affects stability of complexes with plasmid DNA under in vivo conditions in a dose-dependent manner after intravenous injection into mice. *Bioconjug Chem* 16(4), 785-792 (2005).
120. Navarro G, Pan J, Torchilin Vp. Micelle-like nanoparticles as carriers for DNA and siRNA. *Mol Pharm* 12(2), 301-313 (2015).
121. Alhakamy Na, Nigatu As, Berklund Cj, Ramsey Jd. Noncovalently associated cell-penetrating peptides for gene delivery applications. *Ther Deliv* 4(6), 741-757 (2013).
122. Vives E. Present and future of cell-penetrating peptide mediated delivery systems: "is the Trojan horse too wild to go only to Troy?" *J Control Release* 109(1-3), 77-85 (2005).
123. Voronina N, Delyagina E, David R, Steinhoff G. Inorganic nanoparticles for gene delivery. In: *Advances and Challenges in the Delivery of Nucleic Acid Therapeutics (Volume 1)*, Merkel O, Amiji M (Ed.^(Eds). Future Medicine Ltd 108-123 (2015).
124. Delyagina E, Li W, Ma N, Steinhoff G. Magnetic targeting strategies in gene delivery. *Nanomedicine (Lond)* 6(9), 1593-1604 (2011).
125. Gupta Pk, Hung Ct. Magnetically controlled targeted micro-carrier systems. *Life Sci* 44(3), 175-186 (1989).
126. Hassan Ee, Gallo Jm. Targeting anticancer drugs to the brain. I: Enhanced brain delivery of oxantrazole following administration in magnetic cationic microspheres. *J Drug Target* 1(1), 7-14 (1993).
127. Mah C, Fraites Tj, Jr., Zolotukhin I *et al.* Improved method of recombinant AAV2 delivery for systemic targeted gene therapy. *Mol Ther* 6(1), 106-112 (2002).
128. Scherer F, Anton M, Schillinger U *et al.* Magnetofection: enhancing and targeting gene delivery by magnetic force in vitro and in vivo. *Gene Ther* 9(2), 102-109 (2002).
129. OZ Biosciences corporate website; <http://www.ozbiosciences.com/content/13-magnetofection>.
130. Mcbain Sc, Griesenbach U, Xenariou S *et al.* Magnetic nanoparticles as gene delivery agents: enhanced transfection in the presence of oscillating magnet arrays. *Nanotechnology* 19(40), 405102 (2008).
131. Fouriki A, Farrow N, Clements Ma, Dobson J. Evaluation of the magnetic field requirements for nanomagnetic gene transfection. *Nano Rev* 1 1:5167 (2010).
132. nanoTherics corporate website; <http://www.nanotherics.com/magnetofect.htm>.
133. Subramanian M, Lim J, Dobson J. Enhanced nanomagnetic gene transfection of human prenatal cardiac progenitor cells and adult cardiomyocytes. *PLoS One* 8(7), e69812 (2013).
134. Fouriki A, Clements Ma, Farrow N, Dobson J. Efficient transfection of MG-63 osteoblasts using magnetic nanoparticles and oscillating magnetic fields. *J Tissue Eng Regen Med* 8(3), 169-175 (2014).
135. Fouriki A, Dobson J. Oscillating magnet array-based nanomagnetic gene transfection of human mesenchymal stem cells. *Nanomedicine (Lond)* 9(7), 989-997 (2013).
136. Plank C, Zelphati O, Mykhaylyk O. Magnetically enhanced nucleic acid delivery. Ten years of magnetofection-progress and prospects. *Adv Drug Deliv Rev* 63(14-15), 1300-1331 (2011).

137. Estelrich J, Escribano E, Queralt J, Busquets Ma. Iron oxide nanoparticles for magnetically-guided and magnetically-responsive drug delivery. *Int J Mol Sci* 16(4), 8070-8101 (2015).
138. Xing R, Liu G, Zhu J, Hou Y, Chen X. Functional magnetic nanoparticles for non-viral gene delivery and MR imaging. *Pharm Res* 31(6), 1377-1389 (2013).
139. Sosnovik De, Nahrendorf M, Weissleder R. Magnetic nanoparticles for MR imaging: agents, techniques and cardiovascular applications. *Basic Res Cardiol* 103(2), 122-130 (2008).
140. Weissleder R, Stark Dd, Engelstad Bl *et al.* Superparamagnetic iron oxide: pharmacokinetics and toxicity. *AJR Am J Roentgenol* 152(1), 167-173 (1989).
141. Chemicell corporate website; <http://www.chemicell.com/>.
142. Muthana M, Kennerley Aj, Hughes R *et al.* Directing cell therapy to anatomic target sites in vivo with magnetic resonance targeting. *Nat Commun* 6 8009 (2015).
143. Huth S, Lausier J, Gersting Sw *et al.* Insights into the mechanism of magnetofection using PEI-based magnetofectins for gene transfer. *J Gene Med* 6(8), 923-936 (2004).
144. Li W, Ma N, Ong Ll *et al.* Enhanced thoracic gene delivery by magnetic nanobead-mediated vector. *J Gene Med* 10(8), 897-909 (2008).
145. Chertok B, David Ae, Yang Vc. Polyethyleneimine-modified iron oxide nanoparticles for brain tumor drug delivery using magnetic targeting and intra-carotid administration. *Biomaterials* 31(24), 6317-6324 (2010).
146. Zhang Y, Li W, Ou L *et al.* Targeted delivery of human VEGF gene via complexes of magnetic nanoparticle-adenoviral vectors enhanced cardiac regeneration. *PLoS One* 7(7), e39490 (2012).
147. Gaebel R, Furlani D, Sorg H *et al.* Cell origin of human mesenchymal stem cells determines a different healing performance in cardiac regeneration. *PLoS One* 6(2), e15652 (2011).
148. Manders Emm, Verbeek Fj, Aten Ja. Measurement of Colocalization of Objects in Dual-Color Confocal Images. *Journal of Microscopy-Oxford* 169 375-382 (1993).
149. Delyagina E, Schade A, Scharfenberg D *et al.* Improved transfection in human mesenchymal stem cells: effective intracellular release of pDNA by magnetic polyplexes. *Nanomedicine (Lond)* 9(7), 999-1017 (2014).
150. Schade A. Intracellular Visualization of Nanoparticle-based Gene Delivery via Selective Fluorescent Labeling. *University of Rostock, Medical Faculty* Master thesis 43 p. (2011).
151. Delyagina E, Li W, Schade A, Kuhlo a-L, Ma N, Steinhoff G. Low Molecular Weight Polyethyleneimine Conjugated to Magnetic Nanoparticles as a Vector for Gene Delivery. *AIP Conference Proceedings* 1311(1), 479-484 (2010).
152. Yin Pt, Han E, Lee Kb. Engineering Stem Cells for Biomedical Applications. *Adv Healthc Mater* 5(1), 10-55 (2015).
153. Dominici M, Le Blanc K, Mueller I *et al.* Minimal criteria for defining multipotent mesenchymal stromal cells. The International Society for Cellular Therapy position statement. *Cytotherapy* 8(4), 315-317 (2006).
154. Nesselmann C, Li W, Ma N, Steinhoff G. Stem cell-mediated neovascularization in heart repair. *Ther Adv Cardiovasc Dis* 4(1), 27-42 (2010).
155. Li W, Ma N, Ong Ll *et al.* Bcl-2 engineered MSCs inhibited apoptosis and improved heart function. *Stem Cells* 25(8), 2118-2127 (2007).
156. Mangi Aa, Noiseux N, Kong D *et al.* Mesenchymal stem cells modified with Akt prevent remodeling and restore performance of infarcted hearts. *Nat Med* 9(9), 1195-1201 (2003).

157. Wang W, Li W, Ou L *et al.* Polyethylenimine-mediated gene delivery into human bone marrow mesenchymal stem cells from patients. *J Cell Mol Med* 15(9), 1989-1998 (2010).
158. Arsianti M, Lim M, Marquis Cp, Amal R. Polyethylenimine based magnetic iron-oxide vector: the effect of vector component assembly on cellular entry mechanism, intracellular localization, and cellular viability. *Biomacromolecules* 11(9), 2521-2531 (2010).
159. Arsianti M, Lim M, Marquis Cp, Amal R. Assembly of polyethylenimine-based magnetic iron oxide vectors: insights into gene delivery. *Langmuir* 26(10), 7314-7326 (2010).
160. Rejman J, Oberle V, Zuhorn Is, Hoekstra D. Size-dependent internalization of particles via the pathways of clathrin- and caveolae-mediated endocytosis. *Biochem J* 377(Pt 1), 159-169 (2004).
161. Drake Dm, Pack Dw. Biochemical investigation of active intracellular transport of polymeric gene-delivery vectors. *J Pharm Sci* 97(4), 1399-1413 (2008).
162. Suh J, Wirtz D, Hanes J. Efficient active transport of gene nanocarriers to the cell nucleus. *Proc Natl Acad Sci U S A* 100(7), 3878-3882 (2003).
163. Grosse S, Aron Y, Thevenot G, Monsigny M, Fajac I. Cytoskeletal involvement in the cellular trafficking of plasmid/PEI derivative complexes. *J Control Release* 122(1), 111-117 (2007).
164. Doyle Sr, Chan Ck. Differential intracellular distribution of DNA complexed with polyethylenimine (PEI) and PEI-polyarginine PTD influences exogenous gene expression within live COS-7 cells. *Genet Vaccines Ther* 5 11 (2007).
165. Behr Jp. The proton sponge: A trick to enter cells the viruses did not exploit. *CHIMIA International Journal for Chemistry* 51(1-2), 34-36 (1997).
166. Akinc A, Thomas M, Klibanov Am, Langer R. Exploring polyethylenimine-mediated DNA transfection and the proton sponge hypothesis. *J Gene Med* 7(5), 657-663 (2005).
167. Yang S, May S. Release of cationic polymer-DNA complexes from the endosome: A theoretical investigation of the proton sponge hypothesis. *J Chem Phys* 129(18), 185105 (2008).
168. Forrest Ml, Pack Dw. On the kinetics of polyplex endocytic trafficking: implications for gene delivery vector design. *Mol Ther* 6(1), 57-66 (2002).
169. Godbey Wt, Barry Ma, Saggau P, Wu Kk, Mikos Ag. Poly(ethylenimine)-mediated transfection: a new paradigm for gene delivery. *J Biomed Mater Res* 51(3), 321-328 (2000).
170. Won Yy, Sharma R, Konieczny Sf. Missing pieces in understanding the intracellular trafficking of polycation/DNA complexes. *J Control Release* 139(2), 88-93 (2009).
171. Grosse S, Thevenot G, Monsigny M, Fajac I. Which mechanism for nuclear import of plasmid DNA complexed with polyethylenimine derivatives? *J Gene Med* 8(7), 845-851 (2006).
172. Peng L, Liu M, Xue Yn, Huang Sw, Zhuo Rx. Transfection and intracellular trafficking characteristics for poly(amidoamine)s with pendant primary amine in the delivery of plasmid DNA to bone marrow stromal cells. *Biomaterials* 30(29), 5825-5833 (2009).
173. Sauer Am, De Bruin Kg, Ruthardt N, Mykhaylyk O, Plank C, Brauchle C. Dynamics of magnetic lipoplexes studied by single particle tracking in living cells. *J Control Release* 137(2), 136-145 (2009).
174. Chen Hh, Ho Yp, Jiang X, Mao Hq, Wang Th, Leong Kw. Quantitative comparison of intracellular unpacking kinetics of polyplexes by a model constructed from quantum dot-FRET. *Mol Ther* 16(2), 324-332 (2008).

175. Matsumoto Y, Itaka K, Yamasoba T, Kataoka K. Intranuclear fluorescence resonance energy transfer analysis of plasmid DNA decondensation from nonviral gene carriers. *J Gene Med* 11(7), 615-623 (2009).
176. Gustafsson Mg. Surpassing the lateral resolution limit by a factor of two using structured illumination microscopy. *J Microsc* 198(Pt 2), 82-87 (2000).
177. Gustafsson Mg. Nonlinear structured-illumination microscopy: wide-field fluorescence imaging with theoretically unlimited resolution. *Proc Natl Acad Sci U S A* 102(37), 13081-13086 (2005).
178. Jares-Erijman Ea, Jovin Tm. FRET imaging. *Nat Biotechnol* 21(11), 1387-1395 (2003).
179. Glover Dj, Leyton Dl, Moseley Gw, Jans Da. The efficiency of nuclear plasmid DNA delivery is a critical determinant of transgene expression at the single cell level. *J Gene Med* 12(1), 77-85 (2010).
180. Pollard H, Remy Js, Loussouarn G, Demolombe S, Behr Jp, Escande D. Polyethylenimine but not cationic lipids promotes transgene delivery to the nucleus in mammalian cells. *J Biol Chem* 273(13), 7507-7511 (1998).
181. Godbey Wt, Wu Kk, Mikos Ag. Tracking the intracellular path of poly(ethylenimine)/DNA complexes for gene delivery. *Proc Natl Acad Sci U S A* 96(9), 5177-5181 (1999).
182. Clamme Jp, Krishnamoorthy G, Mely Y. Intracellular dynamics of the gene delivery vehicle polyethylenimine during transfection: investigation by two-photon fluorescence correlation spectroscopy. *Biochim Biophys Acta* 1617(1-2), 52-61 (2003).
183. Oh Yk, Suh D, Kim Jm, Choi Hg, Shin K, Ko Jj. Polyethylenimine-mediated cellular uptake, nucleus trafficking and expression of cytokine plasmid DNA. *Gene Ther* 9(23), 1627-1632 (2002).
184. Mannisto M, Ronkko S, Matto M *et al.* The role of cell cycle on polyplex-mediated gene transfer into a retinal pigment epithelial cell line. *J Gene Med* 7(4), 466-476 (2005).
185. Brunner S, Sauer T, Carotta S, Cotten M, Saltik M, Wagner E. Cell cycle dependence of gene transfer by lipoplex, polyplex and recombinant adenovirus. *Gene Ther* 7(5), 401-407 (2000).
186. Abdallah B, Hassan A, Benoist C, Goula D, Behr Jp, Demeneix Ba. A powerful nonviral vector for in vivo gene transfer into the adult mammalian brain: polyethylenimine. *Hum Gene Ther* 7(16), 1947-1954 (1996).
187. Cohen Rn, Van Der Aa Ma, Macaraeg N, Lee Ap, Szoka Fc, Jr. Quantification of plasmid DNA copies in the nucleus after lipoplex and polyplex transfection. *J Control Release* 135(2), 166-174 (2009).
188. Thomas M, Ge Q, Lu Jj, Chen J, Klibanov A. Cross-linked Small Polyethylenimines: While Still Nontoxic, Deliver DNA Efficiently to Mammalian Cells in Vitro and in Vivo. *Pharmaceutical Research* 22(3), 373-380 (2005).
189. Teo Py, Yang C, Hedrick JI *et al.* Hydrophobic modification of low molecular weight polyethylenimine for improved gene transfection. *Biomaterials* 34(32), 7971-7979 (2013).
190. He P, Hagiwara K, Chong H, Yu Hh, Ito Y. Low-Molecular-Weight Polyethyleneimine Grafted Polythiophene for Efficient siRNA Delivery. *Biomed Res Int* 2015 406389 (2015).
191. Xun Mm, Liu Yh, Guo Q *et al.* Low molecular weight PEI-appended polyesters as non-viral gene delivery vectors. *Eur J Med Chem* 78 118-125 (2014).
192. Giron-Gonzalez Md, Salto-Gonzalez R, Lopez-Jaramillo Fj *et al.* Polyelectrolyte Complexes of Low Molecular Weight PEI and Citric Acid as Efficient and Nontoxic

- Vectors for in Vitro and in Vivo Gene Delivery. *Bioconjug Chem* 27(3), 549-561 (2016).
193. Li D, Kong Y, Yu H *et al.* The construction of a novel kind of non-viral gene delivery vector based on protein as core backbone. *Vox Sang* 94(3), 234-241 (2008).
 194. Schade A, Muller P, Delyagina E *et al.* Magnetic Nanoparticle Based Nonviral MicroRNA Delivery into Freshly Isolated CD105(+) hMSCs. *Stem Cells Int* 2014 197154 (2014).
 195. Schade A, Delyagina E, Scharfenberg D *et al.* Innovative Strategy for MicroRNA Delivery in Human Mesenchymal Stem Cells via Magnetic Nanoparticles. *International Journal of Molecular Sciences* 14(6), 10710 (2013).
 196. Lam Ap, Dean Da. Progress and prospects: nuclear import of nonviral vectors. *Gene Ther* 17(4), 439-447 (2010).
 197. Vernon Mm, Dean Da, Dobson J. DNA Targeting Sequence Improves Magnetic Nanoparticle-Based Plasmid DNA Transfection Efficiency in Model Neurons. *Int J Mol Sci* 16(8), 19369-19386 (2015).
 198. Fortier C, Durocher Y, De Crescenzo G. Surface modification of nonviral nanocarriers for enhanced gene delivery. *Nanomedicine (Lond)* 9(1), 135-151 (2014).
 199. Li X, Wei J, Aifantis Ke *et al.* Current investigations into magnetic nanoparticles for biomedical applications. *J Biomed Mater Res A* 104(5), 1285-1296 (2016).
 200. Bansal R, Gupta Kc, Kumar P. Biodegradable and versatile polyethylenimine derivatives efficiently transfer DNA and siRNA into mammalian cells. *Colloids Surf B Biointerfaces* 135 661-668 (2015).
 201. Wu Z, Zhan S, Fan W *et al.* Peptide-Mediated Tumor Targeting by a Degradable Nano Gene Delivery Vector Based on Pluronic-Modified Polyethylenimine. *Nanoscale Research Letters* 11(1), 1-13 (2016).
 202. Wang M, Wu B, Tucker Jd, Lu P, Lu Q. Poly(ester amine) constructed from polyethylenimine and pluronic for gene delivery in vitro and in vivo. *Drug Delivery* 1-10 (2016).
 203. Kolhatkar Ag, Jamison Ac, Litvinov D, Willson Rc, Lee Tr. Tuning the magnetic properties of nanoparticles. *Int J Mol Sci* 14(8), 15977-16009 (2013).
 204. Cheng Z, Al Zaki A, Hui Jz, Muzykantov Vr, Tsourkas A. Multifunctional nanoparticles: cost versus benefit of adding targeting and imaging capabilities. *Science* 338(6109), 903-910 (2012).
 205. Vand Rajabpour F, Raoofian R, Habibi L, Akrami Sm, Tabrizi M. Novel trends in genetics: transposable elements and their application in medicine. *Arch Iran Med* 17(10), 702-712 (2014).
 206. Aronovich El, Mcivor Rs, Hackett Pb. The Sleeping Beauty transposon system: a non-viral vector for gene therapy. *Hum Mol Genet* 20(R1), R14-20 (2011).
 207. Izsvak Z, Hackett Pb, Cooper Lj, Ivics Z. Translating Sleeping Beauty transposition into cellular therapies: victories and challenges. *Bioessays* 32(9), 756-767 (2010).
 208. Belay E, Matrai J, Acosta-Sanchez A *et al.* Novel hyperactive transposons for genetic modification of induced pluripotent and adult stem cells: a nonviral paradigm for coaxed differentiation. *Stem Cells* 28(10), 1760-1771 (2010).
 209. Woltjen K, Michael Ip, Mohseni P *et al.* piggyBac transposition reprograms fibroblasts to induced pluripotent stem cells. *Nature* 458(7239), 766-770 (2009).
 210. Voigt F, Wiedemann L, Zuliani C *et al.* Sleeping Beauty transposase structure allows rational design of hyperactive variants for genetic engineering. *Nat Commun* 7 11126 (2016).
 211. Moore Ps, Chang Y. Why do viruses cause cancer? Highlights of the first century of human tumour virology. *Nat Rev Cancer* 10(12), 878-889 (2010).

212. Ounzain S, Crippa S, Pedrazzini T. Small and long non-coding RNAs in cardiac homeostasis and regeneration. *Biochim Biophys Acta* 1833(4), 923-933 (2013).
213. Zhao J, Mi Y, Feng Ss. siRNA-based nanomedicine. *Nanomedicine (Lond)* 8(6), 859-862 (2013).
214. Xiong L, Bi J, Tang Y, Qiao Sz. Magnetic Core-Shell Silica Nanoparticles with Large Radial Mesopores for siRNA Delivery. *Small* (2016).
215. Medarova Z, Balcioglu M, Yigit Mv. Controlling RNA Expression in Cancer Using Iron Oxide Nanoparticles Detectable by MRI and In Vivo Optical Imaging. *Methods Mol Biol* 1372 163-179 (2016).
216. Li T, Shen X, Chen Y *et al.* Polyetherimide-grafted Fe(3)O(4)@SiO2(2) nanoparticles as theranostic agents for simultaneous VEGF siRNA delivery and magnetic resonance cell imaging. *Int J Nanomedicine* 10 4279-4291 (2015).
217. Chen Y, Wang X, Liu T *et al.* Highly effective antiangiogenesis via magnetic mesoporous silica-based siRNA vehicle targeting the VEGF gene for orthotopic ovarian cancer therapy. *Int J Nanomedicine* 10 2579-2594 (2015).
218. Arami S, Rashidi Mr, Mahdavi M, Fathi M, Entezami Aa. Synthesis and characterization of Fe3O4-PEG-LAC-chitosan-PEI nanoparticle as a survivin siRNA delivery system. *Hum Exp Toxicol* (2016).
219. Liu N, Olson En. MicroRNA regulatory networks in cardiovascular development. *Dev Cell* 18(4), 510-525 (2010).
220. Schade A. MicroRNA-based Stem Cell Modifications using Magnetic Transfection Complexes – A Non-Viral Approach towards Cardiac Regeneration. *University of Rostock, Medical Faculty* PhD thesis 119 p. (2016).
221. Mirna Therapeutics corporate website; <http://www.mirnarx.com/pipeline/mirna-MRX34.html>.

7 Appendix

List of abbreviations

μg	microgram (1*10 ⁻⁶ gram)
μl	microliter (1*10 ⁻⁶ liter)
A565	Atto 565
AAV	adeno – associated virus
ADA	adenosine deaminase
BCA	bicinchoninic acid
bp	base pairs
BSA	bovine serum albumin
CCFM	cell culture freezing medium
C_{coef}	colocalization coefficient
CD	cluster of differentiation
cDNA	complementary deoxyribonucleic acid
CFTR	cystic fibrosis transmembrane regulator
CLSM	confocal laser scanning microscopy
cm ²	square centimeters
CMV	cytomegalovirus
CO ₂	carbon dioxide
COS-7	african green monkey kidney fibroblast-like cell line
CPPs	cell penetrating peptides
Da	dalton
DAPI	4',6-diamidino-2-phenylindole
DLS	dynamic light scattering
DMEM	Dulbecco`s Modified Eagle Medium
DMRIE	1,2-dimyristyloxypropyl-3-dimethyl-hydroxy ethyl ammonium bromide
DMSO	dimethyl sulfoxide
DNA	deoxyribonucleic acid
DOL	degree of labelling
DOPE	dioleolyphosphatidylethanolamine
DOTAP	N-[1-(2,3-dioleoyloxy)propyl]-N,N,N-trimethylammonium chloride
DOTMA	N-[1-(2, 3-dioleoyloxy)propyl]-N,N,N-trimethylammonium chloride
dsRNA	double-stranded ribonucleic acid
e.g.	<i>Exempli gratia</i> (Latin)
EDTA	ethylenediaminetetraacetic acid

EGFP	enhanced green fluorescent protein
EMA	European Medicines Agency
EM-CCD	electron multiplying charge coupled device
et al.	<i>et alia</i> (Latin)
etc.	<i>et cetera</i> (Latin)
FABP-4	fatty acid binding protein-
FBS	fetal bovine serum
FDA	Food and Drug Administration
Fe ₃ O ₄	Iron (II,III) oxide or magnetite
Fig.	figure
FRET	Förster resonance energy transfer
g	gram
g	standard gravity
GNE	Glucosamine [UDP-N-acetyl]-2-epimerase/N-acetylmannosamine kinase
h	hours
HCl	Hydrochloric acid
HEK 293	human embryonic kidney 293 cell line
HeLa	human cervical cancer cell line
HepG2	human liver cancer cell line
HIV	human immunodeficiency virus
HLA-B7	human leukocyte antigen serotype B7
hMSC	human mesenchymal stem cells
HUVEC	human umbilical vein endothelial cells
i.e.	<i>id est</i> (Latin)
IgG	immunoglobulin G
InNP	inorganic nanoparticles
kDa	kilodalton
l	liter
LMW	low molecular weight
LPL	lipoprotein lipase
M	molar
mg	milligram
MHC	major histocompatibility complex
min	minutes
miRNA	micro ribonucleic acid
ml	milliliter
mM	millimolar
MNC	mononuclear cells

MNP	magnetic nanoparticles
MNP-A565	magnetic nanoparticles, labelled with Atto 565
MRI	magnetic resonance imaging
mRNA	messenger ribonucleic acid
MSCGM	mesenchymal stem cell growth medium
MTT	3-(4,5-Dimethylthiazol-2-yl)-2,5-diphenyltetrazolium bromide
mV	millivolt
MW	molecular weight
NA	numerical aperture
NaCl	Sodium chloride
ncRNA	noncoding ribonucleic acid
ng	nanogram
NIH 3T3	mouse embryonic fibroblast cell line
nm	nanometer
NP	nitrogen/phosphate ratio
OD	optical density
OG488	oregon green 488
PALS	phase analysis light scattering
PAMAM	poly(amidoamines)
PBS	phosphate-buffered saline
pDNA	plasmid deoxyribonucleic acid
pDNA-Cy5	plasmid deoxyribonucleic acid labelled with Cyan 5
PEG	polyethylene glycol
pEGFP	plasmid encoding enhanced green fluorescent protein
PEI	polyethylenimine
PEI600	polyethylenimine with molecular weight of 600 dalton
PEI-OG488	polyethylenimine labelled with oregon green 488
PFA	paraformaldehyde
pH	molar concentration of hydrogen ions
PLA	poly(lactic) acid
PLGA	poly(L-lactide-co-glycolic acid)
PLL	poly(L-lysine)
pmol	picomol
PVDF	polyvinylidene difluoride
RLU	relative light units
RNA	ribonucleic acid
RPMI	Roswell Park Memorial Institute
RT	room temperature

SCID	severe combined immunodeficiency
SD	standard deviation
SEM	standard error of the mean
shRNA	small hairpin ribonucleic acid
siRNA	small interfering ribonucleic acid
SR-SIM	superresolution – structured illumination microscopy
TBE	Tris-borate-EDTA
TEPA	tetraethylenpentamine
Tris	trisaminomethane
U	units
UK	United Kingdom
USA	United States of America
UV-Vis	ultraviolet-visible
VEGF	vascular endothelial growth factor
vs.	versus
w/v	weight to volume
w/w	weight to weight
α MEM	Minimum essential medium alpha

List of figures

- Figure 1.1:** Overview of the methods, utilized in gene therapy clinical trials worldwide.
- Figure 1.2:** Chemical structures of cationic polymers and dendrimers mostly used as gene delivery carriers.
- Figure 1.3:** Different strategies used for the construction of MNP-based gene carriers, by means of molecular linkers (a) or physical interactions (b).
- Figure 1.4:** Schematic structure of pDNA/PEI/MNP transfection complex.
- Figure 2.1:** The principle of biotinylation of PEI using Sulfo-NHS-LC-Biotin linker.
- Figure 2.2:** Determination of iron concentration.
- Figure 2.3:** Set up for fluorescent labelling of transfection complexes.
- Figure 3.1:** Gel electrophoresis of pDNA/PEI transfection complexes at different NP ratios (from 0.25 to 3.0) in comparison to pDNA alone.
- Figure 3.2:** Optimization of transfection conditions with pDNA/PEI/MNP complexes in comparison to pDNA/PEI complexes ($MW_{(PEI)} = 25$ kDa) in hMSC.
- Figure 3.3:** Characterization of hMSC.
- Figure 3.4:** Monitoring of transfection efficiency in hMSC over time.
- Figure 3.5:** Characterization and visualization of fluorescently labelled transfection complexes.
- Figure 3.6:** Photobleaching experiments.
- Figure 3.7:** Intracellular localization of transfection complexes in hMSC 24 h after transfection.
- Figure 3.8:** Intracellular localization of transfection complexes in hMSC 24 h after transfection, including possible pDNA release events.
- Figure 3.9:** Monitoring of pDNA release from transfection complexes in hMSC.
- Figure 3.10:** Characterization of pDNA/PEI600 transfection complexes.
- Figure 3.11:** Optimization of transfection conditions with PEI600-containing complexes in COS-7 cells.
- Figure 3.12:** Cytotoxicity of PEI600-mediated transfection.
- Figure 4.1:** Expected mechanism of magnetic polyplex-mediated transfection in comparison to polyplexes.

List of tables

- Table 1.1:** Viral vectors most recently used in gene therapy clinical trials worldwide (Phase I/II) and their clinical applications (years 2005-2015).
- Table 1.2:** Nonviral vectors, most recently used in gene therapy clinical trials worldwide (Phase I/II/III) and their clinical applications (years 2005-2015).
- Table 1.3:** Examples of chemical carriers for transfection, currently available on the market.
- Table 2.1:** Cell seeding numbers for Luciferase Reporter Gene Assay, EGFP expression assay and laser scanning microscopy.
- Table 2.2:** List of fluorochromes and laser lines (incl. main beam splitters (MBS) used for their excitation).
- Table 3.1:** Particle size and surface charge of magnetic nanoparticles alone and transfection complexes (NP ratio 2.5, 1 $\mu\text{g}/\text{ml}$ iron) determined by DLS and PALS, respectively.
- Table 3.2:** Characterization of hMSC
- Table 3.3:** Particle size and surface charge of single-labelled and three-color labelled magnetic transfection complexes (NP ratio 2.5, 1 $\mu\text{g}/\text{ml}$ iron) determined by DLS and PALS, respectively.
- Table 4.1:** Properties of MNP-based gene delivery systems, relevant for their future clinical translation.

Acknowledgement

First and foremost I would like to express my greatest appreciation and thanks to Prof. Dr. med. Gustav Steinhoff. In 2009, he gave me a great opportunity to join his team at the Reference and Translation Center for Cardiac Stem Cell Therapy, which had a strong impact on my life and career. I am truly grateful for that chance, as well as for his supervision and guidance throughout the course of this work, for his motivation and support that made the completion of this dissertation possible.

I express my special appreciation to Prof. Dr. rer. nat. Robert David for critical scientific discussions, valuable advices and proofreading of my dissertation.

My great appreciation and thanks go to Prof. Olga Kudritskaya for providing me the initial contact with Prof. Dr. med. Gustav Steinhoff and continuous support and encouragement through all these years.

Special thanks go to Dr. Nan Ma and Dr. Wenzhong Li for their scientific mentoring, professional advices and inspiration.

My special appreciation goes to my colleague and a very good friend Dr. Anna Schade, for her understanding, team working, support, motivation and great time within the “nanogroup”. I would also like to thank Dr. Dario Furlani, Dr. Nana-Maria Wagner, Dr. Kyriaki Chatzivasileiou, Julia Reetz-Bäder and Erik Pittermann - nice colleagues and great friends, who filled these years up with energy, joy and fun.

I want to extend my thanks to all the members of FKGO team: Dr. Cornelia Lux, Dr. Anna Skorska, Dr. Ralf Gäbel, Dr. Marion Ludwig, Dr. Christian Rimmbach, Dr. Koji Hirano, Dr. Weiwei Wang, Dr. Yue Zhang, Peter Mark, Julia Jung, Natalia Voronina, Frauke Hausburg, Paula Müller, Dorothee Scharfenberg and Margit Schwarz. Many thanks to the great technicians, Margit Fritsche, Madeleine Bartsch and Anita Tölk, who have always been supportive, professional and very helpful. Thank you all for your collaboration, team spirit and the great time spent in the lab.

Moreover, I would like to thank the members of Translation Management team: Dr. Gudrun Tiedemann, Dr. Frauke Stähler, Dr. Ulrike Ruch, Dr. Sandra Kurzawski and Dr. Jana Große. My special appreciation goes to project assistants, Jana Gabriel and Katrin Höfer. Thank you for your professionalism, support and care in all work- and life-related issues.

I am truly thankful to my parents, Natalia Delyagina and Mikhail Delyagin, for all their love, support and encouragement. I am grateful for all their efforts to provide me with outstanding education for the sake of my future career.

Many thanks to my husband, Artem Zharkov and my children, Diana and Roman, for their endless love, patience and belief. You gave me power and inspiration essential for the completion of this work. Thank you.

Curriculum Vitae

First name / Surname

Evgenya Delyagina



Nationality

Russian

Date of birth

August 14, 1986

Family

Married, two children

Work experience

Dates

January 2009 – July 2014

Organization

Reference and Translation Center for Cardiac Stem Cell Therapies, Department of Cardiac Surgery, University of Rostock, Rostock, Germany

Position held

Research fellow

Dates

August 2008 – December 2008

Organization

Quintiles Transnational, St. Petersburg, Russia

Position held

Clinical Trials Assistant

Education and training

Dates

January 2009 – July 2014

Degree / Educational institution

Post-graduate student (PhD) Medical Science, Medical faculty, University of Rostock, Rostock, Germany

Dissertation: “Magnetic nanoparticle-based gene delivery: mechanisms and clinical perspectives”

Supervisor: Prof. Dr.med. Gustav Steinhoff

Dates

September 2003 – June 2008

Degree / Educational institution

Master of Pharmacy, Pharmaceutical faculty, St.Petersburg State Chemical Pharmaceutical Academy, St.Petersburg, Russia

Master thesis: “Premises and facilities of drugstores”

Supervisor: Dr. Natalia Zolotareva

Dates	October 2006 – May 2007
Educational institution	Scientific training, Department of Molecular Genetics, Institute of Experimental Medicine, St. Petersburg, Russia Main focus: Gene delivery to mice' embryos Supervisor: Prof. Dr. Vadim Vasilyev
Dates	June 2006 – August 2006
Educational institution	Scientific training, The Institute of Regenerative Medicine, Department of Cardiac Surgery, University of Rostock, Rostock, Germany Main focus: Non-viral gene delivery to mammalian cells. Supervisor: PD Dr. Nan Ma
Dates	September 2005 – May 2006
Educational institution	Medical English, Faculty of Philology, Saint-Petersburg State University, St. Petersburg, Russia
Dates	June 2003
Educational institution	Graduate, School of General Education N258 specialized in Chemistry and Physics, St. Petersburg, Russia
Languages	English - working proficiency German - working proficiency (B2) French - elementary proficiency Russian - mother tongue

Publication List

1. **E. Delyagina**, N. Ma, W. Wang, Y. Zhang, A. Kuhlo, E. Flick, H. Gatzten, G. Steinhoff, W. Li „Magnetically guided transfection in suspension cells with PEI 25kDa conjugated to magnetic nanoparticles“. *Biomedizinische Technik/Biomedical Engineering* 2010; 55 (Issue s1), 37-39. (*Impact Factor* 1.65)
2. **E. Delyagina**, N. Ma, W. Wang, Y. Zhang, A. Kuhlo, E. Flick, H. Gatzten, G. Steinhoff, W. Li „PEI 600 Da conjugated to magnetic nanobeads as a non-viral vector for gene delivery“. *Biomedizinische Technik/Biomedical Engineering* 2010; 55 (Issue s1), 116-117. (*Impact Factor* 1.65)
3. **E. Delyagina**, N. Ma, W. Wang, Y. Zhang, A. Kuhlo, E. Flick, H. Gatzten, F. Zhang, E. Burkel, G. Steinhoff, W. Li „Carbon nanotube – mediated polyethylenimine for gene delivery“. *Biomedizinische Technik/Biomedical Engineering* 2010; 55 (Issue s1), 40-41. (*Impact Factor* 1.65)
4. **E. Delyagina**, W. Li, A. Schade, A. Kuhlo, N. Ma, G. Steinhoff: “Low Molecular Weight Polyethyleimine conjugated to magnetic nanoparticles as a vector for gene delivery“. *AIP Conference Proceedings* 1311, 2010: 479-484.
5. **E. Delyagina**, W. Li, N. Ma, G. Steinhoff: „Magnetic targeting strategies in gene delivery“. *Nanomedicine (Lond)* 2011 Nov; 6(9): 1593-1604. (*Impact Factor* 4.889)
6. Y. Zhang, W. Li, L. Ou, W. Wang, **E. Delyagina**, C. Lux, H. Sorg, K. Riehemann, G. Steinhoff, N. Ma. „Targeted delivery of human VEGF gene via complexes of magnetic nanoparticle-adenoviral vectors enhanced cardiac regeneration“. *PLoS One* 2012; 7(7): e39490. (*Impact Factor* 3.057)
7. P. Donndorf, D. Useini, CA. Lux, B. Vollmar, **E. Delyagina**, M. Laupheimer, A. Kaminski, G. Steinhoff. „Analysing migratory properties of human CD 133⁺ stem cells in vivo after intraoperative sternal bone marrow isolation“. *Cell Transplantation* 2013; 22(9): 1627-35. (*Impact Factor* 2.54)
8. C. Klopsch, R. Gäbel, A. Kaminski, P. Mark, W. Wang, A. Toelk, **E. Delyagina**, G. Kleiner, L. Koch, B. Chichkov, P. Mela, S. Jockenhoevel, N. Ma, G. Steinhoff. „Spray- and laser-assisted biomaterial processing for fast and efficient autologous cell-plus-matrix tissue engineering“. *Journal of Tissue Engineering and Regenerative Medicine* 2015 Dec;9(12):E177-90. (*Impact Factor* 4.71)
9. E. Grambow, F. Mueller-Graf, **E. Delyagina**, M. Frank, A. Kuhla, B. Vollmar. “Effect of the hydrogen sulfide donor GYY4137 on platelet activation and microvascular thrombus formation in mice”. *Platelets*. 2014; 25(3): 166-74. (*Impact Factor* 1.42)
10. A. Schade, **E. Delyagina**, D. Scharfenberg, A. Skorska, C. Lux, R. David, G. Steinhoff. “Innovative strategy for microRNA delivery in human mesenchymal stem cells via Magnetic Nanoparticles”. *International Journal of Molecular Sciences* 2013 May 23; 14(6): 10710-26. (*Impact Factor* 3.257)
11. **E. Delyagina**, A. Schade, D. Scharfenberg, A. Skorska, C. Lux, W. Li, G. Steinhoff. „Improved transfection in human mesenchymal stem cells: effective intracellular release of

- pDNA by magnetic polyplexes“. *Nanomedicine (Lond)* 2014 May; 9(7): 999-1017. (*Impact Factor 4.889*)
12. A. Schade, P. Müller, **E. Delyagina**, N. Voronina, A. Skorska, C. Lux, G. Steinhoff, R. David, G. Steinhoff. „Magnetic Nanoparticle Based Nonviral MicroRNA Delivery into Freshly Isolated CD105(+) hMSCs“. *Stem Cells International* 2014; 2014:197154. (*Impact Factor 3.687*)
 13. N. Voronina, **E. Delyagina**, R. David, G. Steinhoff. „Inorganic nanoparticles for gene delivery“. *Advances and Challenges in the Delivery of Nucleic Acid Therapeutics* (E-book). 2015 October. Volume 1: 108-123.

Conference Presentation List

1. **E. Delyagina**, N. Ma, W. Wang, A. Kuhlo, Y. Zhang, E. Flick, H. Gatzen, G. Steinhoff, W. Li “PEI 600 Da conjugated to magnetic nanobeads as a non-viral vector for gene delivery”, 8th international Conference on the Scientific and Clinical Applications of magnetic carriers, May 25-29, 2010, Rostock, Germany (**poster presentation**)
2. **E. Delyagina**, N. Ma, W. Wang, Y. Zhang, A. Kuhlo, E. Flick, H. Gatzen, G. Steinhoff, W. Li „Magnetically guided transfection in suspension cells with PEI 25 kDa conjugated to magnetic nanoparticles” BMT 2010 44. DGBMT Jahrestagung, October 05-08, 2010, Rostock, Germany (**oral presentation**)
3. **E. Delyagina** “Gene and drug delivery nanotechnology”. St. Petersburg State Chemical Pharmaceutical Academy, May 24-25, 2011, St. Petersburg, Russia (**invited lecture**)
4. **E. Delyagina**, A. Schade, D. Scharfenberg, A. Skorska, C.A. Lux, W. Li, G. Steinhoff. “Nonviral transfection in human mesenchymal stem cells via magnetic nanoparticles: efficient DNA release in the perinuclear region”. 3rd EACTS Meeting on Cardiac and Pulmonary Regeneration, December 14-15, 2012, Berlin, Germany (**oral presentation**)
5. A. Schade, **E. Delyagina**, D. Scharfenberg, G. Steinhoff. “An innovative non-viral strategy for efficient microRNA delivery in human mesenchymal stem cells for regenerative medicine”. 3rd EACTS Meeting on Cardiac and Pulmonary Regeneration, December 14-15, 2012, Berlin, Germany (**poster presentation**)
6. A. Schade, **E. Delyagina**, A. Skorska, C.A. Lux, R. David, G. Steinhoff. „Efficient modifications of human mesenchymal stem cells using novel non-viral gene carriers for regenerative medicine”. 8th annual conference of the German Society for Stem Cell Research (GSZ), September 6, 2013, Rostock, Germany (**oral presentation**)